IEC 62396-1

Edition 1.0 2012-05

INTERNATIONAL STANDARD

colour inside

Process management for avionics – Atmospheric radiation effects – Part 1: Accommodation of atmospheric radiation effects via single event effects within avionics electronic equipment

IEC Central Office
3, rue de Varembé
CH-1211 Geneva 20
Switzerland

Tel.: +41 22 919 02 11
Fax: +41 22 919 03 00
info@iec.ch
www.iec.ch

About the IEC

The International Electrotechnical Commission (IEC) is the leading global organization that prepares and publishes International Standards for all electrical, electronic and related technologies.

About IEC publications

The technical content of IEC publications is kept under constant review by the IEC. Please make sure that you have the latest edition, a corrigenda or an amendment might have been published.

Useful links:

IEC publications search - www.iec.ch/searchpub

The advanced search enables you to find IEC publications by a variety of criteria (reference number, text, technical committee,…).
It also gives information on projects, replaced and withdrawn publications.

IEC Just Published - webstore.iec.ch/justpublished

Stay up to date on all new IEC publications. Just Published details all new publications released. Available on-line and also once a month by email.

Electropedia - www.electropedia.org

The world's leading online dictionary of electronic and electrical terms containing more than 30 000 terms and definitions in English and French, with equivalent terms in additional languages. Also known as the International Electrotechnical Vocabulary (IEV) on-line.

Customer Service Centre - webstore.iec.ch/csc

If you wish to give us your feedback on this publication or need further assistance, please contact the Customer Service Centre: csc@iec.ch.

IEC 62396-1

Edition 1.0 2012-05

INTERNATIONAL STANDARD

Process management for avionics – Atmospheric radiation effects – Part 1: Accommodation of atmospheric radiation effects via single event effects within avionics electronic equipment

INTERNATIONAL ELECTROTECHNICAL COMMISSION

PRICE CODE XD

ICS 03.100.50; 31.020; 49.060

ISBN 978-2-83220-099-5

CONTENTS

INTERNATIONAL ELECTROTECHNICAL COMMISSION

PROCESS MANAGEMENT FOR AVIONICS – ATMOSPHERIC RADIATION EFFECTS –

Part 1: Accommodation of atmospheric radiation effects via single event effects within avionics electronic equipment

FOREWORD

1) The International Electrotechnical Commission (IEC) is a worldwide organization for standardization comprising all national electrotechnical committees (IEC National Committees). The object of IEC is to promote international co-operation on all questions concerning standardization in the electrical and electronic fields. To this end and in addition to other activities, IEC publishes International Standards, Technical Specifications, Technical Reports, Publicly Available Specifications (PAS) and Guides (hereafter referred to as "IEC Publication(s)"). Their preparation is entrusted to technical committees; any IEC National Committee interested in the subject dealt with may participate in this preparatory work. International, governmental and non-governmental organizations liaising with the IEC also participate in this preparation. IEC collaborates closely with the International Organization for Standardization (ISO) in accordance with conditions determined by agreement between the two organizations.
2) The formal decisions or agreements of IEC on technical matters express, as nearly as possible, an international consensus of opinion on the relevant subjects since each technical committee has representation from all interested IEC National Committees.
3) IEC Publications have the form of recommendations for international use and are accepted by IEC National Committees in that sense. While all reasonable efforts are made to ensure that the technical content of IEC Publications is accurate, IEC cannot be held responsible for the way in which they are used or for any misinterpretation by any end user.
4) In order to promote international uniformity, IEC National Committees undertake to apply IEC Publications transparently to the maximum extent possible in their national and regional publications. Any divergence between any IEC Publication and the corresponding national or regional publication shall be clearly indicated in the latter.
5) IEC itself does not provide any attestation of conformity. Independent certification bodies provide conformity assessment services and, in some areas, access to IEC marks of conformity. IEC is not responsible for any services carried out by independent certification bodies.
6) All users should ensure that they have the latest edition of this publication.
7) No liability shall attach to IEC or its directors, employees, servants or agents including individual experts and members of its technical committees and IEC National Committees for any personal injury, property damage or other damage of any nature whatsoever, whether direct or indirect, or for costs (including legal fees) and expenses arising out of the publication, use of, or reliance upon, this IEC Publication or any other IEC Publications.
8) Attention is drawn to the Normative references cited in this publication. Use of the referenced publications is indispensable for the correct application of this publication.
9) Attention is drawn to the possibility that some of the elements of this IEC Publication may be the subject of patent rights. IEC shall not be held responsible for identifying any or all such patent rights.

IEC 62396-1 has been prepared by IEC technical committee 107: Process management for avionics.

IEC 62396-1 cancels and replaces IEC/TS 62396-1 published in 2006.

This International Standard includes the following technical changes with respect to the Technical Specification:

a) Guidance has been provided on the environment for altitudes above 60 000 feet (18,3 km) and the effects on electronics are documented in Annex E and F;
b) Annex G has been added to provide late news as of 2011 on SEE cross-sections applicable to the atmospheric neutron environment.

The text of this international standard is based on the following documents:

FDIS	Report on voting
107/176/FDIS	107/182/RVD

Full information on the voting for the approval of this international standard can be found in the report on voting indicated in the above table.

This publication has been drafted in accordance with the ISO/IEC Directives, Part 2.

A list of all the parts in the IEC 62396 series, published under the general title *Process management for avionics – Atmospheric radiation effects*, can be found on the IEC website.

The committee has decided that the contents of this publication will remain unchanged until the stability date indicated on the IEC web site under "http://webstore.iec.ch" in the data related to the specific publication. At this date, the publication will be

- reconfirmed,
- withdrawn,
- replaced by a revised edition, or
- amended.

A bilingual version of this publication may be issued at a later date.

IMPORTANT – The 'colour inside' logo on the cover page of this publication indicates that it contains colours which are considered to be useful for the correct understanding of its contents. Users should therefore print this document using a colour printer.

INTRODUCTION

This industry-wide technical specification informs avionics systems designers, electronic equipment, component manufacturers and their customers of the kind of ionising radiation environment that their devices will be subjected to in aircraft, the potential effects this radiation environment can have on those devices, and some general approaches for dealing with these effects.

The same atmospheric radiation (neutrons and protons) that is responsible for the radiation exposure that crew and passengers acquire while flying is also responsible for causing the single event effects (SEE) in the avionics electronic equipment. There has been much work carried out over the last few years related to the radiation exposure of aircraft passengers and crew. A standardised industry approach on the effect of the atmospheric neutrons on electronics should be viewed as consistent with and an extension of the on-going activities related to the radiation exposure of aircraft passengers and crew.

Atmospheric radiation effects are one factor that could contribute to equipment hard and soft fault rates. From a system safety perspective, using derived fault rate values, the existing methodology described in ARP4754 (accommodation of hard and soft fault rates in general) will also accommodate atmospheric radiation effect rates.

In addition, this International Standard refers to the JEDEC Standard JESD89A, which relates to soft errors in electronics by atmospheric radiation at ground level (at altitudes less than 10 000 feet (3 040 m)).

PROCESS MANAGEMENT FOR AVIONICS – ATMOSPHERIC RADIATION EFFECTS –

Part 1: Accommodation of atmospheric radiation effects via single event effects within avionics electronic equipment

1 Scope

This part of IEC 62396 is intended to provide guidance on atmospheric radiation effects on avionics electronics used in aircraft operating at altitudes up to 60 000 feet (18,3 km). It defines the radiation environment, the effects of that environment on electronics and provides design considerations for the accommodation of those effects within avionics systems.

This International Standard is intended to help aerospace equipment manufacturers and designers to standardise their approach to single event effects in avionics by providing guidance, leading to a standard methodology.

Details of the radiation environment are provided together with identification of potential problems caused as a result of the atmospheric radiation received. Appropriate methods are given for quantifying single event effect (SEE) rates in electronic components. The overall system safety methodology should be expanded to accommodate the single event effects rates and to demonstrate the suitability of the electronics for the application at the component and system level.

2 Normative references

The following documents, in whole or in part, are normatively referenced in this document and are indispensable for its application. For dated references, only the edition cited applies. For undated references, the latest edition of the referenced document (including any amendments) applies.

IEC/TS 62239:2008, *Process management for avionics – Preparation of an electronic components management plan*

NOTE IEC/TS 62239-1, *Process management for avionics – Management plan – Part 1: Preparation and maintenance of an electronic components management plan* is under study and will supersede IEC/TS 62239.

IEC/TS 62396-2:2008, *Process management for avionics – Atmospheric radiation effects – Part 2: Guidelines for single event effects testing for avionics systems*

IEC/TS 62396-3, *Process management for avionics – Atmospheric radiation effects – Part 3: Optimising system design to accommodate the single event effects (SEE) of atmospheric radiation*

IEC/TS 62396-4:2008, *Process management for avionics – Atmospheric radiation effects – Part 4: Guidelines for designing with high voltage aircraft electronics and potential single event effects*

IEC/TS 62396-5, *Process management for avionics – Atmospheric radiation effects – Part 5: Guidelines for assessing thermal neutron fluxes and effects in avionics systems*

3 Terms and definitions

For the purposes of this document, the following terms and definitions apply.

NOTE Users of this international standard may use alternative definitions consistent with convention within their companies.

3.1
aerospace recommended practice
documents relating to avionics which are published by the Society of Automotive Engineers (SAE)

3.2
analogue single event transient
ASET
spurious signal or voltage produced at the output of an analogue device by the deposition of charge by a single particle

3.3
availability
probability that a system is working at instant *t*, regardless of the number of times it may have previously failed and been repaired

Note 1 to entry: For equipment, the fraction of time the equipment is functional divided by the total time the equipment is expected to be operational, i.e. the time the equipment is functional plus any repair time.

3.4
avionics equipment environment
for aeronautical equipment, the applicable environmental conditions (as described per the equipment specification) that the equipment is able to withstand without loss or degradation in equipment performance during all of its manufacturing cycle and maintenance life

Note 1 to entry: The length of the maintenance life is defined by the equipment manufacturer in conjunction with customers.

3.5
capable
ability of a component to be used successfully in the intended application

3.6
certified
assessment and compliance to an applicable third party standard and maintenance of a certificate and registration (i.e. JAN, IECQ)

3.7
characterisation
process of testing a sample of components to determine the key electrical parameter values that can be expected of all produced components of the type tested

3.8
component application
process that assures that the component meets the design requirements of the equipment in which it is used

3.9
component manufacturer
organisation responsible for the component specification and its production

3.10
critical charge
smallest charge that will cause a SEE if injected or deposited in the sensitive volume

Note 1 to entry: For many devices, the unit applied was the picocoulomb (pC); however, for small geometry devices, this parameter is measured in femtocoulomb (fC).

3.11
cross-section
σ
in radiation terms for proton and neutron interactions, combination of sensitive area and probability of an interaction depositing the critical charge for a SEE

Note 1 to entry: The cross-section may be calculated using the following formula:
σ = number *of errors/particle fluence*

Note 2 to entry: The units for cross-section are cm^2 per device or per bit.

3.12
digital single event transient
DSET
spurious digital signal or voltage, induced by the deposition of charge by a single particle that can propagate through the circuit path during one clock cycle

Note 1 to entry: See 6.2.4 of this document.

3.13
electron
elementary particle having a mass of approximately 1/1 840 atomic mass units, and negative charge of $1{,}602 \times 10^{-19}$ C

3.14
electronic components management plan
ECMP
equipment manufacturer's document that defines the processes and practices for applying components to an equipment or range of equipment

Note 1 to entry: Generally, it addresses all relevant aspects of controlling components during system design, development, production, and post-production support.

3.15
electronic components
electrical or electronic devices that are not subject to disassembly without destruction or impairment of design use

Note 1 to entry: They are sometimes called electronic parts, or piece parts.

EXAMPLE Resistors, capacitors, diodes, integrated circuits, hybrids, application specific integrated circuits, wound components and relays.

3.16
electronic equipment
item produced by the equipment manufacturer, which incorporates electronic components

EXAMPLE End items, sub-assemblies, line-replaceable units and shop-replaceable units.

3.17
electronic flight instrumentation system
EFIS
example of an avionics electronic system requiring system development assurance level A type II and for which the pilot will be within the loop through pilot/system information exchange

3.18
expert
person who has demonstrated competence to apply knowledge and skill to the specific subject

3.19
firm fault
term used at the aircraft function level. It is a failure that cannot be reset other than by rebooting the system or by cycling the power to the relevant functional element

Note 1 to entry: Such a fault could impact the value for the MTBF of the LRU and provide no fault found during subsequent test.

3.20
fly by wire
FBW
example of avionics electronic system requiring system development assurance level A type I and for which the pilot will not be within the aircraft stability control loop

3.21
functional hazard analysis
FHA
assessment of all hazards against a set of defined hazard classes

3.22
giga electron volt
GeV
radiation particle energy giga electron volts (thousand million electron volts)

Note 1 to entry: The SI equivalent energy is 160,2 picojoules.

3.23
gray
Gy
SI unit of ionising radiation dose and the energy deposited as ionization and excitation (J) per unit mass (kg)

Note 1 to entry: Related units are centigray (cGy) and rad. 1 cGy is equal to 1 rad.

3.24
hard error
permanent or semi-permanent damage of a cell by atmospheric radiation that is not recoverable even by cycling the power off and on

3.25
hard fault
term used at the aircraft function level which refers to the permanent failure of a component within an LRU

Note 1 to entry: A hard fault results in the removal of the LRU affected and the replacement of the permanently damaged component before a system/system architecture can be restored to full functionality. Such a fault could impact the value for the MTBF of the LRU repaired.

3.26
heavy ions
positively charged nuclei of the elements heavier than hydrogen and helium

3.27
in-the-loop
test methodology where an LRU is placed within a radiation beam that provides a simulation of the atmospheric neutron environment and where the inputs to the LRU would be from an electronic fixture external to the beam to enable a closed loop system

Note 1 to entry: The electronic fixture would contain a host computer for the aircraft simulation model. The electronic fixture would also contain appropriate signal conditioning for compatibility with the LRU. In the case of an automatic control function, the outputs from the LRU could be, in turn, sent to an actuation means or directly to the host computer. The host computer would automatically close a stability loop (as in the case of a fly-by-wire control system). In the case of a navigation function, the outputs from the LRU could be sent to a display system where the pilot could then close the navigation loop.

3.28
integrated modular avionics
IMA
implementation of aircraft functions in a multitask computing environment where the computations for each specific system implementing a particular function are confined to a partition that is executed by a common computing resource (a single digital electronic circuit)

3.29
latch-up
triggering of a parasitic pnpn circuit in bulk CMOS, resulting in a state where the parasitic latched current exceeds the holding current. This state is maintained while power is applied

3.30
linear energy transfer
LET
energy deposited per unit path length in a semiconductor along the path of the radiation

Note 1 to entry: The units applicable are MeV·cm^2/mg.

3.31
linear energy transfer threshold
LETth
for a given component, the minimum LET to cause an effect at a particle fluence of 1×10^7 ions/cm^2

3.32
line replaceable unit
LRU
piece of avionics electronic equipment that may be replaced during the maintenance cycle of the system

3.33
mega electron volt
MeV
radiation particle energy mega electron volts (million electron volts)

Note 1 to entry: The SI equivalent energy is 160,2 femtojoule.

3.34
mean time between failure
MTBF
measure of reliability requirements and is the mean time between failure of equipment or a system in service

3.35
mean time between unscheduled removals
MTBUR
measure of reliability requirements and is the mean time between unscheduled removal of equipment or a system in service

3.36
multiple bit upset
MBU
the energy deposited in the silicon of an electronic component by a single ionising particle causes upset to more than one bit in the same word

Note 1 to entry: The definition of MBU has been updated due to the introduction of the definition of MCU.

3.37
multiple cell upset
MCU
the energy deposited in the silicon of an electronic component by a single ionising particle induces several bits in an integrated circuit (IC) to upset at one time

3.38
neutron
elementary particle with atomic mass number of one and which carries no charge

Note 1 to entry: It is a constituent of every atomic nucleus except hydrogen.

3.39
particle fluence
for a unidirectional beam of particles, this is the number of particles crossing unit surface area at right angles to the beam

Note 1 to entry: For isotropic flux, this is the number entering sphere of unit cross-sectional area.

Note 2 to entry: The units applicable are particles/cm^2.

3.40
particle flux
fluence rate per unit time

Note 1 to entry: The units applicable are particles/cm^2·s.

3.41
pion or pi-meson
sub-atomic particle

Note 1 to entry: The charge possibilities are (+1, –1, 0) and they are produced by energetic nuclear interactions.

3.42
preliminary system safety assessment
PSSA
systematic evaluation of a proposed system architecture and implementation based on the Functional Hazard Assessment and failure condition classification to determine safety

Note 1 to entry: See section 2.2 ARP4761 [118].

3.43
proton
elementary particle with atomic mass number of one and positive electric charge and which is a constituent of all atomic nuclei

3.44
reliability
***R*(*t*)**
for a system with constant failure rate, the conditional probability that a system will remain operational over the time interval 0 to *t* given by:

$$R(t) = e^{-\lambda t} \quad \text{and } \lambda = 1/\text{MTBF}$$

3.45
risk
measure of the potential inability to achieve overall program objectives within defined cost, schedule, and technical constraints

3.46
single bit upset
SBU
in a semiconductor device when the radiation absorbed by the device is sufficient to change a single cell's logic state

Note 1 to entry: After a new write cycle, the original state can be recovered.

3.47
single event burnout
SEB
burn out of a powered electronic component or part thereof as a result of the energy absorption triggered by an individual radiation event

3.48
single event effect
SEE
response of a component caused by the impact of a single particle (for example galactic cosmic rays, solar energetic particles, energetic neutrons and protons)

Note 1 to entry: The range of responses can include both non-destructive (for example upset) and destructive (for example latch-up or gate rupture) phenomena.

3.49
single event functional interrupt
SEFI
occurrence of an upset, usually in a complex device (e.g. a microprocessor), such that a control path is corrupted, leading the part to cease to function properly

Note 1 to entry: This effect has sometimes been referred to as lockup, indicating that sometimes the part can be put into a "frozen" state (see 6.2.6).

3.50
single event gate rupture
SEGR
in the gate of a powered insulated gate component when the radiation charge absorbed by the device is sufficient to cause gate rupture, which is destructive

3.51
single event latch-up
SEL
in a four layer semiconductor device when the radiation absorbed by the device is sufficient to cause a node within the powered semiconductor device to be held in a fixed state whatever input is applied until the device is de-powered, such latch up may be destructive or non-destructive

3.52
single event transient
SET
spurious signal or voltage, induced by the deposition of charge by a single particle that can propagate through the circuit path during one clock cycle

Note 1 to entry: See 6.2.4 of this document.

3.53
single event upset
SEU
in a semiconductor device when the radiation absorbed by the device is sufficient to change a cell's logic state

Note 1 to entry: After a new write cycle, the original state can be recovered.

3.54
single hard error
SHE
single event induced hard error
in a single event the radiation absorbed by the device is sufficient to cause permanent stuck-bit in the device, and a hard error within the equipment

3.55
soft error
change of state of a latched logic state from one to zero or vice-versa

Note 1 to entry: It is also known as a single event upset.

Note 2 to entry: It is non-destructive and can be rewritten or reset.

3.56
soft fault
term used at the aircraft function level that refers to the characteristic of invalid digital logic cell(s) state changes within digital hardware electronic circuitry

Note 1 to entry: It is a fault that does not involve replacement of a permanently damaged component within an LRU but it does involve restoring the logic cells to valid states before a system/system architecture can be restored to full functionality. Such a fault condition has been suspected in the "no fault found" syndrome for functions implemented with digital technology and it would probably impact the value for the MTBUR of the involved LRU. If a soft fault results in the mistaken replacement of a component within the LRU, the replacement could impact the value for the MTBF of the LRU repaired.

3.57
solar energetic particle (SEP) events
during these periods there is enhancement of solar particles (protons, ions and some neutrons) caused by solar flare activity or coronal mass ejections

Note 1 to entry: The enhancement can last from a few hours to several days. A small fraction has sufficiently energetic spectra to produce significantly enhanced secondary neutron fluxes in the atmosphere.

3.58
substitute component
component used as a replacement in equipment after the equipment design has been approved

Note 1 to entry: In some contexts, the term "alternate component" is used to describe a substitute component that is "equal to or better than" the original component.

3.59
system safety assessment
SSA
assessment performed to verify compliance with the safety requirements

3.60
system
collection of hardware and software elements that implement a specific aircraft function or set of aircraft functions

3.61
total ionising dose
TID
cumulative radiation dose that goes into ionization that is received by a device during a specified period of time

3.62
validation
method of confirmation of component radiation tolerance by the equipment manufacturer, when there is no in-service data from prior use or radiation data from a test laboratory

4 Abbreviations and acronyms

AC	Advisory Circular
AIR	atmospheric ionizing radiation
ARP	aerospace recommended practices
ASET	analogue single event transient
ASIC	application specific integrated circuit
BIT	built-in test
BPSG	borophosphosilicate glass
CECC	CENELEC electronic components committee
CMOS	complimentary metal oxide semiconductor
COTS	commercial-off-the-shelf
D-D	deuterium-deuterium
DOE	Department Of Energy (USA)
DRAM	dynamic random access memory
DSET	digital single event transient
DSP	digital signal processor
D-T	deuterium-tritium
E	energy
ECMP	electronic components management plan
EDAC	error detection and correction
EFIS	Electronic Flight Instrumentation System
ESA	European Space Agency
eV	electron Volt
EXPACS	EXcel-based Program for calculating Atmospheric Cosmic-ray Spectrum
FBW	fly-by-wire
FHA	functional hazard analysis
FIT	failure in time
FPGA	field programmable gate array
GCR	galactic cosmic rays
GeV	giga electron volt
GLE	ground level event
GV	giga volt (rigidity unit)
HW	hardware
IBM	International Business Machines

IC	Integrated circuit
ICE	Irradiation of Chip and Electronics
IECQ	IEC Quality Assessment System for Electronic Components
IEEE	Institute of Electrical and Electronics Engineers
IEEE Trans. Nucl. Sci.	IEEE Transactions on Nuclear Science
IGBT	insulated gate bipolar transistor
IGRF	International Geomagnetic Reference Field
IMA	integrated modular avionics
IUCF	Indiana University Cyclotron Facility (USA)
JAN	Joint Army Navy (USA Department of Defence)
JEDEC	JEDEC Solid State Technology Association
JESD	JEDEC standard
JPL	Jet Propulsion Laboratory (USA)
LET	linear energy transfer
LETth	linear energy transfer threshold
LRU	line replaceable unit
MBU	multiple bit upset
MCU	multiple cell upset
MeV	mega electron volt
MOSFET	metal oxide semiconductor field effect transistor
MTBF	mean time between failure
MTBUR	mean time between unscheduled removals
NASA	National Aeronautical and Space Administration (USA)
PCN	product change notification
PSI	Paul Scherrer Institute (Switzerland)
PSSA	preliminary system safety assessment
PWM	pulse width modulator
QARM	QinetiQ Atmospheric Radiation Model
RADECS	RADiation Effects on Components and Systems
RAM	random access memory
SAFETI	Systems and Airframe Failure Emulation Testing and Integration
SBU	single bit upset
SC	stacked capacitance
SDRAM	synchronous dynamic random access memory
SEB	single event burnout
SECDED	single event correction double event detection
SEDR	single event dielectric rupture
SEE	single event effect
SEFI	single event functional interrupt
SEGR	single event gate rupture
SEL	single event latch-up
SEP	solar energetic particles
SER	soft error rate
SET	single event transient
SEU	single event upset
SHE	single event induced hard error
SRAM	static random access memory
SSA	system safety assessment
SSEEM	segmented secondary electron emission monitor

SW	software
TIC	trench internal capacitance
TID	total ionizing dose
TRIUMF	Tri-University Meson Facility (Canada)
TSL	Theodor Svedberg Laboratory (Sweden)
WNR	Weapons Neutron Research Los Alamos National laboratory (USA)

5 Radiation environment of the atmosphere

5.1 Radiation generation

The atmosphere is penetrated by a flux of various charged and neutral particles that in combination create a complex ionising radiation environment. These particles are created by the interaction of the continuous stream of primary cosmic ray particles with the atoms in the atmosphere (mainly nitrogen and oxygen), and so are called secondary cosmic rays. The primary cosmic rays are usually referred to as the galactic cosmic rays (GCR), indicating that their origins are beyond that of the solar system.

The galactic cosmic radiation is composed of atomic nuclei that have been completely ionised (fully stripped of their electrons) and subsequently accelerated to very high energies. GCR consist of about 83 % protons, 16 % alpha particles and 2 % heavy ions (particles with atomic number $Z > 2$). As the primary cosmic rays, mainly very high-energy protons, bombard the atmosphere, they create a cascade of secondary, tertiary, etc. particles from their interactions with the atoms of the atmosphere. Thus, for each primary cosmic ray entering, many more secondary particles are created. At a very approximate level, the flux of incoming primary cosmic rays at the top of the atmosphere is 3 particle/cm^2·s, and at aircraft altitudes, the flux of all secondary particles is about 10 particle/cm^2·s. The density of the lowest portion of atmosphere is so high, that most of the flux of particles is absorbed, so that at sea level the nominal flux of secondary particles is less than 0,1 particle/cm^2·s.

The flux of secondary particles is not uniform around the earth due to the effect of the earth's magnetic field that is at right angles to the particle direction at the equator. Particles cross field lines at right angles at the equator and are bent away while at the poles they travel parallel to the field and are not deflected. As a result the primary cosmic rays are able to penetrate into the atmosphere more readily near the magnetic poles and they interact with the atoms in the atmosphere creating larger numbers of cascade particles.

5.2 Effect of secondary particles on avionics

Some of the secondary particles can interact with microelectronic devices within aircraft avionics systems and cause single event effects (SEE) in the devices. These secondary particles deposit enough charge through the recoils they create within a sensitive portion of a device to result in a malfunction of the device. It has been found that neutrons, protons and pions are the main particles that can cause these effects.

5.3 Atmospheric neutrons

5.3.1 General

Neutrons are the secondary cosmic ray particles that have been shown to be mainly responsible for causing single event upsets (SEUs) in memories and other devices on aircraft since the early 1990s. This identification of the neutrons as the main cause of the SEUs was based on several different kinds of correlations:

a) the variations of the upset rates against altitude and geographic latitude followed the variation of the neutron flux with altitude and latitude,

b) neutron induced SEU rates calculated using SEU cross-sections measured in a laboratory and integrated with the neutron flux in the atmosphere agreed with measured in-flight SEU rates; and

c) upset rates at ground level, due to secondary neutrons are proportional to rates at aircraft altitudes. For the neutrons, as well as all of the secondary particles within the atmosphere, the variation of the particle flux with three parameters (energy, altitude and latitude) is most important for understanding the variation of the SEU rate.

5.3.2 Energy spectrum of atmospheric neutrons

The energy variation of the atmospheric neutrons is usually presented by plotting the differential flux (flux per unit energy interval) as a function of energy, which is often called the spectrum (see Figure 1). Monte Carlo generated spectra have produced the following fractions < 1 MeV 0,53; 1 MeV to 10 MeV 0,2; > 10 MeV 0,27. The fits quoted below may give slightly different values. Measurements of the energy spectrum of the cosmic ray neutrons have been made since the 1950s using a variety of techniques. In Figure 1 we plot four neutron spectra at an altitude of approximately 40 000 feet (12,2 km). These include the original measurements made by Hess in 1959 [1][1], a calculation by Armstrong in 1973 [2] a fit to measurements by Hewitt et al at NASA in 1977 [3] and the recent DOE measurements by a fit to measurement by Goldhagen in an ER-2 aircraft during 1997 [4].

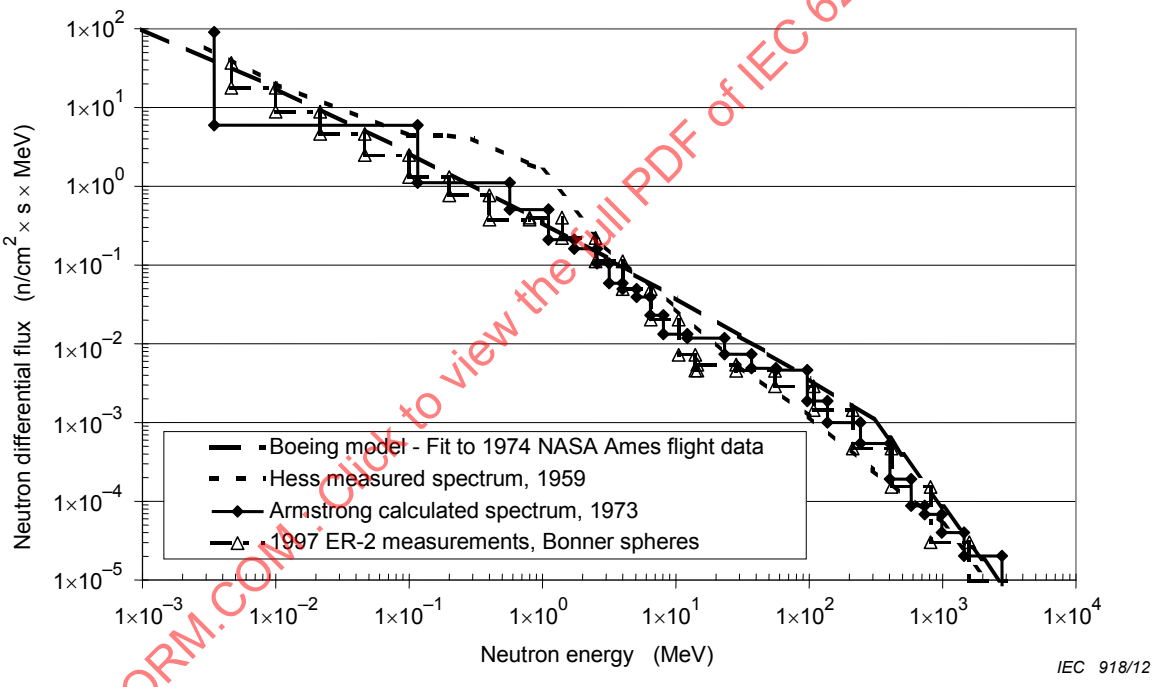

Figure 1 – Energy spectrum of atmospheric neutrons at 40 000 feet (12 160 m), latitude 45 degrees

A fit to the NASA Ames Research Center's 1974 flight data (energy (E) up to 300 MeV), that had been used in the past has been modified for energy > 300 MeV using the more recent measurements. The modified spectrum is given, with energy in MeV, as

$$\mathrm{d}N/\mathrm{d}E = \begin{cases} 0{,}346E^{-0{,}922} \times \exp\left(-0{,}0152(\ln E)^2\right) & E < 300 \text{ MeV} \\ 340E^{-2{,}2} & E > 300 \text{ MeV} \end{cases} \quad \text{n/cm}^2 \times \text{s} \times \text{MeV} \qquad (1)$$

It should be noted that when this differential flux is integrated for energy > 10 MeV, the integrated neutron flux is ~5 600 n/cm^2 per hour, which can be rounded up to 6 000 n/cm^2 per hour. This nominal high energy neutron flux 6 000 n/cm^2 per hour at 40 000 feet (12,2 km) and geographic latitude 45° may be treated as a typical in flight envelope and scaled for

[1] Figures in square brackets refer to the Bibliography.

different avionics applications (for example, for altitude variation per 5.3.3 and for latitude variation per 5.3.4). For lower energies, the model gives a flux of 3 200 n/cm^{2}h for 1 <E < 10 MeV, with 1 600 n/cm^{2}h in the range of 1 < E < 3 MeV and 1 600 n/cm^{2}h in the range of 3 < E < 10 MeV. This flux of 6 000 n/cm^2 per hour for E > 10 MeV is conservative by a factor of approximately 2 compared to the ER-2 aircraft measurement results. At ground level the flux is approximately a factor of 300 lower than at 40 000 feet (12,2 km), thus on the ground, the flux for energy > 10 MeV is 20 n/cm^2 per hour, [5] and this agrees with an independently derived calculation for New York City [6].

The greater than 10 MeV neutrons will be the dominant cause of SEE on sensitive devices with geometric feature size above 150 nanometres (nm), however for devices with feature size at and below 150 nm the contribution of neutrons with energy between 1 and 10 MeV may be significant. Although, for such devices, based on reference 7 the contribution from the 1 < E 10 MeV neutrons to the overall SEE rate is 10 %. Therefore when calculating the SEE contribution from parts having geometric feature size 150 nm and below to 90 nm the SEE rate from E > 1 MeV shall be calculated as 1,1 SEE rate E > 10 MeV. This neutron conversion factor has been derived using geometries between 150 nm and 90 nm and needs to be kept under review as further low energy neutron test data on small feature size devices (below 150 nm) become available. A greater than 1 MeV nominal neutron flux of 9 200 n/cm^2 per hour at 40 000 feet (12,2 km) and 45° latitude shall be used. This value can be scaled to other altitudes and latitudes, using the Tables D.1 and D.2.

5.3.3 Altitude variation of atmospheric neutrons

The altitude variation of the atmospheric neutron derives from the competition between the various production and removal processes that affect how the neutrons and the initiating cosmic rays interact with the atmosphere. The result is a maximum in the flux at about 60 000 feet (18,3 km), called the Pfotzer maximum that can be seen in Figure 2. The figure compares the altitude variation of the 1 MeV to 10 MeV neutron flux. A much more rigorous approach was taken by NASA-Langley in developing a model that is currently called AIR [10]. It utilised measurements made on aircraft during the 1960s and 1970s, and developed a model that gives the 1 MeV to 10 MeV neutron flux as a function of three parameters, the atmospheric depth (g/cm^2), vertical rigidity cut-off (GV) and solar weather conditions.

A still more rigorous model has been developed based extensive calculations incorporating three key steps, calculation of the initial cosmic ray spectrum, the rigidity cut-off calculation and a Monte Carlo code to generate and transport the secondary particle radiation through the atmosphere. This code package is called the QinetiQ Atmospheric Radiation Model, QARM [11] and it can be accessed and utilized via the Internet [12]. It can provide estimates of the secondary cosmic ray particle fluxes and spectra at all locations for all particles including neutrons and protons. A similar code package that is also available via the Internet is called EXPACS (Excel-based programme for calculating atmospheric cosmic-ray spectrum [13]), and is based on analytical functional fits to Monte Carlo-generated spectra [14]. QARM and EXPACS yield similar results for the atmospheric neutron spectrum [15]. Predicted SEU rates in the atmosphere based on using QARM for six different SRAMs are about a factor of 2 lower than rates calculated using the neutron spectrum (see 5.3.2) in this standard [15].

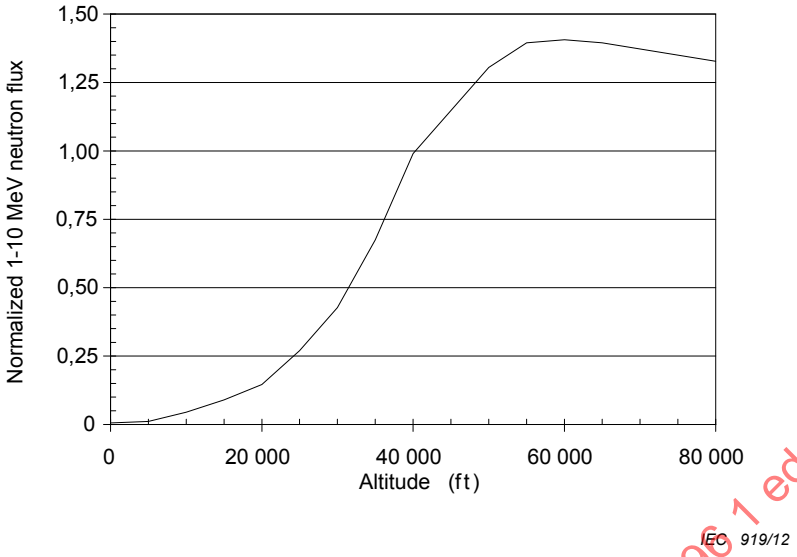

Figure 2 – Model of the atmospheric neutron flux variation with altitude (see Annex D)

A tabular description of the variation of atmospheric neutron flux with altitude and also with latitude as given by the Boeing model is provided in Annex D to enable calculation of neutron flux at various flight locations.

5.3.4 Latitude variation of atmospheric neutrons

The latitude variation is expressed in terms of the vertical rigidity cut-off (R), in units of GV. The rigidity cut-offs indicate the required rigidity (essentially the particle momentum divided by its charge) of primary cosmic ray particles needed to penetrate to a given location above the atmosphere. At the equator, where the magnetic field is at right angles to particle direction, it requires particles with the highest rigidity (R ~ 15 GV) to penetrate to this region, and where it is parallel to the particle direction, near the poles, particles with $R < 1$ GV can reach. The geographical distribution of the vertical rigidity cut-offs around the world at an altitude of 20 km [16] is shown in Figure 3.

Figure 3 shows the distribution of vertical rigidity cut-off curves across the globe based on the 1980 epoch that was developed in [16], combining measurements and calculations, with the rigidity cut-offs being averaged over geographical longitude for each 5° in geographical latitude. The reference [16] authors updated their rigidity cut-off model with a new set of data based on the 1995 epoch and it is tabulated in JESD-89A. This newer set of calculations and measurements produced a model with rigidity values within 1°×1° accuracy. These rigidity values were averaged over broader angular bins (5° in latitude × 15° in longitude) and these averaged values are tabulated in Annex A of JESD-89A. Based on a comparison of the updated rigidity values from JESD-89A (1995 epoch) to the older values in Figure 3 (1980 epoch), the rigidity cut-off values have decreased slightly. A comparison was carried out at a longitude of 0° and for latitudes ranging between 30° and 60°. In most cases the change was a decrease of ~0,15 to 0,2 in the overall vertical rigidity across all latitude levels. Since the change in rigidity was approximately constant, the percentage change was much higher at higher latitudes where the absolute value of the rigidity is smaller. Thus, for latitudes < 50°, the per cent decrease was < 5 %, for 50° to 55° it was between 5 % and 7 %, and for 60° it was ~15 %. These variations in the vertical rigidity cut-offs due to changes in the geomagnetic field over a 15 year period appear to be small enough to indicate that the corresponding change in the atmospheric neutron flux will be relatively small and Figure 3 is still useful. Fully up to date cut-off rigidities are available through the QARM code [12] using trajectory integrations in the latest IGRF magnetic field plus external source terms dependent on geomagnetic disturbance index (Kp) using the Tsyganenko 2001 model. These can be computed on-line for any selected location. For flight path calculations a set of 49 pre-calculated maps is used. Geomagnetic disturbances can significantly lower the cut-off rigidity (by about a factor 2 for Kp = 6 for a 1 Gv cut-off at zero disturbance). The influence on

particle fluxes can be about 10 % for galactic cosmic rays but factors of 5 or more during solar particle events.

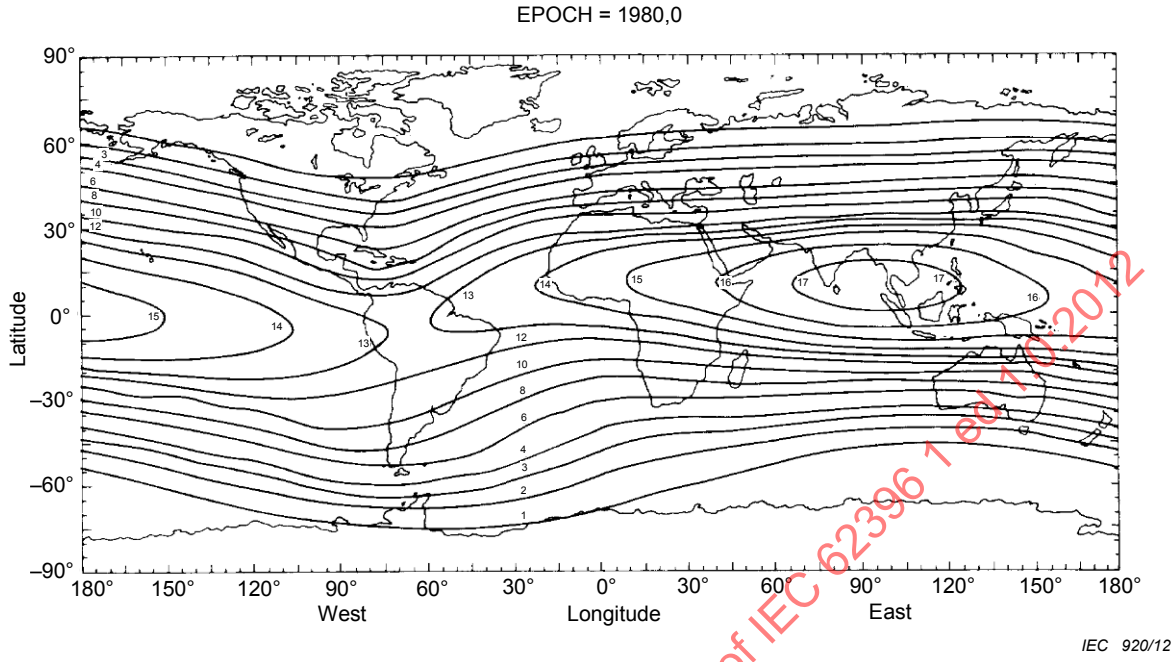

Figure 3 – Distribution of vertical rigidity cut-offs around the world

Two models are also available for the variation of the 1 MeV to 10 MeV neutron flux as a function of latitude, a simplified Boeing model and the NASA-Langley AIR model. The simplified Boeing model is based on measurements made in aircraft during the 1960s, in particular pole-pole latitude surveys aboard a Boeing 707 aircraft [17]. The initial data was given as the neutron flux as a function of the vertical rigidity cut off. Based on the observation in Figure 3 that the rigidity cut offs exhibit their main variation with latitude, the vertical cut-offs were averaged over geographical longitude for each 5° in geographical latitude. These contours are evolving with time due to the Earth's changing geomagnetic field. This allowed the measured 1 MeV to 10 MeV neutron flux, originally given as a function of rigidity cut off, to be converted to a curve of the 1 MeV to 10 MeV neutron flux as a function of latitude and this is shown in Figure 4.

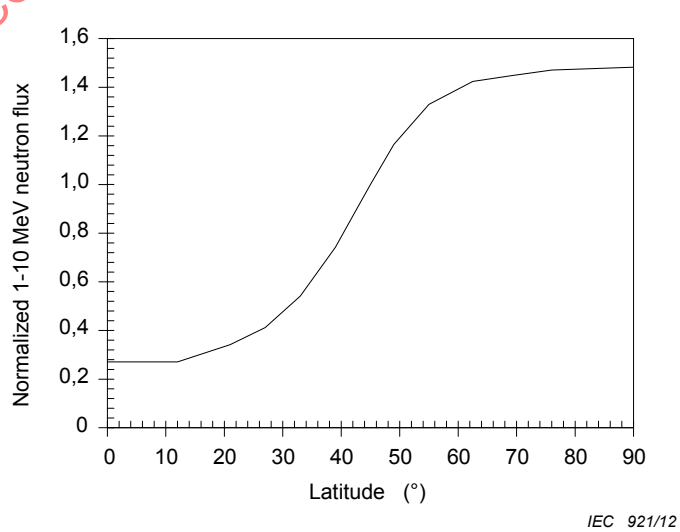

Figure 4 – Model of atmospheric neutron flux variation with latitude

The variation of the neutron flux with altitude shown in Figure 2 for energies 1 MeV to 10 MeV has also been shown to apply for neutrons with higher energies [9]. Therefore Figures 2 and 4 can be used to scale the greater than 10 MeV neutron flux of 6 000 n/cm^2 per hour which applies at 40 000 feet (12,2 km) and 45° latitude to other altitudes and latitudes. It should be noted that there is a strong dependence of cut-off rigidity and hence particle fluxes on longitude and this is available in the QARM model. For example at 45^o latitude there is a factor 5 variation in cut-off rigidity with longitude and this translates into a factor 3 variation in neutron fluxes from galactic cosmic rays.

The 1 MeV to 10 MeV neutrons have a significant SEE contribution for devices with geometries 150 nm and below (see 5.3.2).

5.3.5 Thermal neutrons within aircraft

Thermal neutrons are low energy neutrons that have scattered sufficiently to be in thermal equilibrium with their surroundings. At room temperatures this leads to an average energy of 0,025 eV. The majority of the thermal neutrons inside the aircraft are created by the interaction of the aircraft structure and all of its contents with the higher energy neutrons within the atmosphere. Thermal neutrons can be significant because they have a very high probability of interacting with certain isotopes, such as boron 10 (B10), and boron is present in microelectronics in two main areas, as a p dopant, and in some forms of the glassivation layer, for example borophosphosilicate glass. Thus, a 0,025 eV neutron interacting with a B10 atom leads to two charged particles in a device with a combined 2,3 MeV of energy; if this energy is deposited within the sensitive volume of a microelectronic device, it can lead to SEU.

To date, only one study has attempted to calculate the thermal neutron flux within an aeroplane [18]. The hydrogenous materials within an aeroplane, the fuel, the passengers and crew and the baggage, all serve to thermalise the higher energy neutrons. An entire large commercial airliner was modelled in terms of 20 sub-volumes, some extremely large. Even with this crude model the calculations were very useful, showing that at the several locations within the aeroplane that were reported upon, the thermal neutron flux was about a factor of 10 higher than it is just outside the aeroplane. The number of measurements of SEU cross-sections in devices induced by thermal neutrons is very limited (see 8.3.3), but more recent references significantly expand on this data [19, 20, 21, 22].

The subject of thermal neutron effects is covered in more detail in IEC/TS 62396-5.

5.4 Secondary protons

Charged particles have also been measured in the atmosphere, most of which are, like the neutrons, cosmic ray secondaries, from the interaction of the primary cosmic rays with the oxygen (O) and nitrogen (N) nuclei in the air. The secondary protons can cause single event effects in electronics in a manner very similar to that of the neutrons. The distribution of secondary protons is similar to that of neutrons, especially with respect to energy and altitude. The energy spectrum of the atmospheric protons is similar to that of the neutrons, as seen in Figure 5, which contains proton measurements at two mountain tops (US and Russia, [23, 24] and from one balloon experiment [24]. The mountain-top data indicate a peaking in the differential proton flux at about 200 to 300 MeV. Figure 5 shows that for energies up to about 500 MeV, the secondary protons in the atmosphere are about 20 to 30 % of the flux of the neutrons, but at higher energies the proton and neutron fluxes are comparable. Measurements have shown that for secondary protons in the energy range (100 MeV < energy < 750 MeV), the variation with altitude is very similar to that of the neutrons [25], i.e., there is a maximum at ~80 g/cm^2 (55 000 feet (16,8 km)), the Pfotzer maximum. With respect to the latitude variation there is a slight decrease in the total atmospheric proton flux of about a factor of 2 in traversing from the polar to equatorial regions, which is less pronounced than the latitude variation with neutrons. Therefore, for purposes of calculating SEE rates in the atmosphere, since the neutron flux dominates and the suggested flux of 6 000 n/cm^2 per hour (energy > 10 MeV) is conservative, the

contribution of the protons to the SEE rate can be considered as being included within the neutron-induced SEE rate.

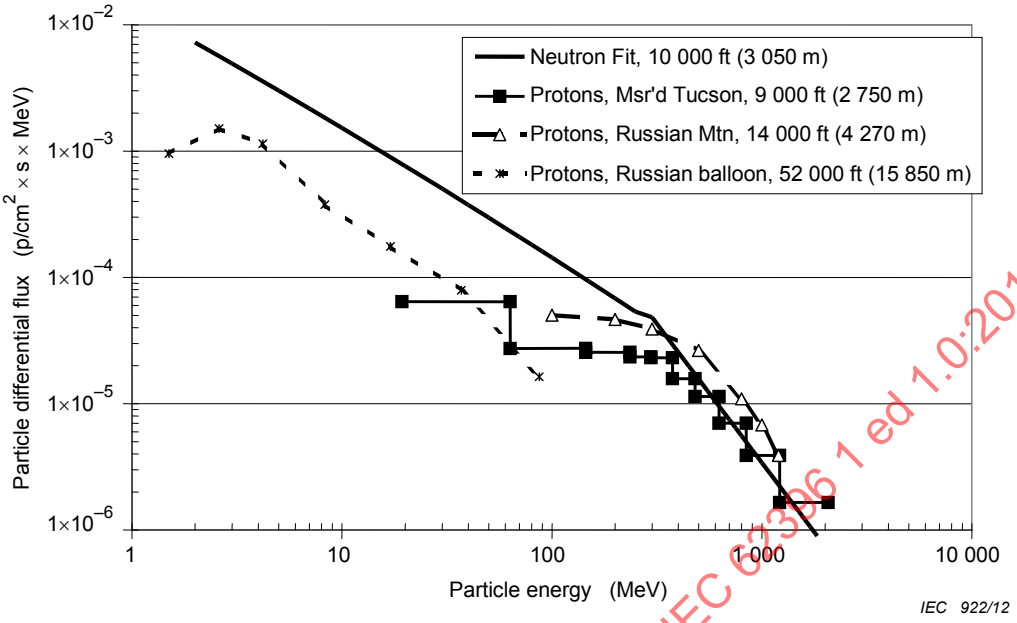

Figure 5 – Energy spectrum of protons within the atmosphere

5.5 Other particles

The other charged particle secondary cosmic ray within the atmosphere that can induce single event effects in electronics is the pion (there are both positively and negatively charged pions). However, in the atmosphere at aircraft altitudes, the pion flux is only a small fraction of the neutron and proton flux. For energies ≤ 1 GeV, the pion/proton (π/p) ratio is estimated to be ~0,1, and it applies at both aircraft altitudes, 500 g/cm^2 (20 000 feet (6,1 km)), as well as ground level [26]. At 40 000 feet (12,2 km) and at an energy of 1 GeV, the differential pion flux has been calculated to be ~1/30 that of the neutrons and protons (the differential neutron and proton fluxes are about equal), and at 100 MeV, the differential pion flux is ~1/100 that of the neutron flux [27]. Thus, the flux of pions in the atmosphere is so small (<1 %) compared to that of the neutrons, that they can be ignored for purposes of effects on electronics. The QARM model [12] can provide detailed flux and spectrum information within the atmosphere for these other cosmic ray secondary particles, including protons.

Electrons and gamma rays are also produced as secondary cosmic radiation in the atmosphere. Although these particles do not have a high enough dE/dx (energy deposition per path length) in silicon to cause single event effects in electronics, they do deposit ionising dose in the electronics. In general terms, the fluxes of high energy electrons and gamma rays are roughly comparable to those of the atmospheric neutrons.

There are also a very small percentage of heavy ions, i.e., primary cosmic rays and their secondary fragments, in the atmosphere that survive the passage through the hundreds of g/cm^2 of atmosphere. However their flux is very low. Therefore, heavy ions in the atmosphere can be generally ignored as a potential threat to electronics, although for the case of very high altitudes it is possible that some heavy ions may be encountered. Only for altitudes greater than 60 000 feet (18,3 km), may additional consideration need to be given for the effects of heavy ions [28, 29], for the effects from primary cosmic rays and their secondary fragments. At present, the QARM model [12] does not provide information on the reduced fluxes of primary cosmic ray heavy ions and their secondary fragments within the atmosphere although enhancements are in hand.

5.6 Solar enhancements

Solar activity follows an approximately 11 year cycle, during which time there are periods of heightened activity (approximately the middle 6 years) and lessened activity (approximately the first 2,5 years and last 2,5 years). During the entire period there is a finite probability of eruptions on the sun, such as solar flares or coronal mass ejections that result in energetic particles being emitted.

In general, these solar energetic particles have less energy than the galactic cosmic rays. The first particles reach the Earth in a matter of minutes but the enhancements last for several hours to days. They interact with the atmosphere to create secondary particles in a similar way to galactic cosmic rays but their lower energy means that they produce much steeper altitude and latitude profiles. For a few events the particle energies are sufficiently high to give enhanced secondary fluxes at aircraft altitudes and on the ground (so-called ground level events or GLEs).

The enhanced secondary cosmic rays during solar flares have been measured on the ground by the worldwide network of cosmic ray neutron detectors (continually tracking the variation of the cosmic ray environment) and occasionally by instruments aboard aircraft [30, 31]. The SEP enhancement in the atmospheric neutron flux, relative to the background flux (>10 MeV) of 6 000 n/cm^2 per hour in 5.3.2, has been calculated for a number of worst-case scenarios. These scenarios are dependent on the particle spectra from specific solar flare events, the altitude and the rigidity cut-off. For the September 1989 flare, the enhancement factors at 39 000 feet (12 km) are 41 and 1,6 for rigidities of 0 GV and 3 GV respectively, and at an altitude of 56 000 feet (17 km) the factors increase to 73 and 2,4 respectively. With the February 1956 flare, for which the incoming particle spectrum is less well characterized, the enhancement factor is 263 at 0 GV and 39 000 feet (12 km). Thus, extremely high SEE rates could occur in the high latitude regions ($R \leq 1$ GV) during worst case flares that could be enhanced by a factor as high as 300 at 39 000 feet (12 km).

These events are usually of short duration (several hours) and for worst case take-off times are contained within the duration of long haul flights. Hence although the worst case instantaneous rate enhancement is as high as a factor of 263 the increased SEE rate averaged over a high latitude flight would be more like 25 times the solar minimum quiet-time rate. The QARM model includes seven solar particle events which have been modelled in detail [32]. Five of these have been compared favourably with the limited available flight data on air crew dose. Use of these events in QARM enables the worst case flight scenarios with respect to take-off time to be determined. The February 1956 event is the worst case available and based on ground level data is the worst since such monitoring commenced in 1942. However, based on the indirect evidence of nitrate samples in ice cores, the first solar flare ever observed (the Carrington event of 1 September 1859) could have been four times worse [33, 34]. In addition analysis of events with respect to air crew dose [35] shows that four other events in the 1940s could have exceeded 10 times the normal flight-averaged dose or SEE rate at high latitude and 39 000 feet. With the more recent events of 29 September 1989 and 20 January 2005 (this fortunately only at high southern latitudes due to large anisotropy in arrival directions) also in this category the frequency of such worst case events should be taken as seven in 67 years. Some 23 other events (e.g. 15 April 2001) could have given route-averaged rates at high latitude ranging from 10 % to 200 % of quiet time over this time period.

5.7 High altitudes greater than 60 000 feet (18 290 m)

Although neutrons are the dominant cause of SEEs up to about 40 000 feet (12,2 km) other particles become increasingly important at higher altitudes. Protons contribute to the neutron rate at 60 000 feet (18,3 km) and above 60 000 feet (18,3 km), while above this altitude there is significant penetration of cosmic ray heavy ions and their secondary fragments. In addition the importance of solar particle events increases and the February 1956 event would have been six times worse at 60 000 feet (18,3 km) compared to 40 000 feet (12,2 km). Currently models such as QARM include neutrons and protons but not heavy ions.

Heavy ions produce SEE by direct ionization and techniques such as CREME96 [36, 37] are used for space systems. These are based on the characterisation of the environment by the spectrum of particles as a function of linear energy transfer (LET). This is usually plotted in integral form; i.e. the flux of particles having greater LET. The path length distribution through a parallelepiped representation of a device sensitive volume is then employed to give the spectrum of charge depositions and hence the number greater than a device threshold for SEE. Earlier work [28] has presented LET spectra for the upper atmosphere using semi-empirical cross-sections for heavy ion interactions and the generation of fragments. Modern Monte-Carlo radiation transport codes such as FLUKA [38] now contain physics modules to deal with ion-ion collisions and these are being applied to generate response functions for the atmosphere.

Annexes E and F give details of the high altitude environment and calculation of SEE rates produced by heavy ions as well as neutrons and protons. Figures E.6 and E.7 can be effectively used to estimate the SEU contribution from the three particles (neutrons, secondary protons and primary cosmic ray heavy ions) within the atmosphere as a function of altitude, based on the SEU response of a particular SRAM. From Figures E.6 and E.7 the neutron SEU contribution is seen to decrease at altitudes above 60 000 feet the proton contribution reaches a plateau at 60 000 feet and the heavy ion contribution increases significantly above 80 000 feet.

6 Effects of atmospheric radiation on avionics

6.1 Types of radiation effects

The ionising radiation environment in the atmosphere, and therefore within an aircraft, can cause a variety of effects on the electronics used in avionics. Three basic types of radiation effects on electronics are dealt with in this clause, single event effects, total ionising dose and displacement damage. It is shown that some single event effects have an impact on the avionics but that total ionising dose and displacement damage are not of concern. Thus, the main focus is on single event effects in avionics. "Single event effects" is a generic term and encompasses all of the potential effects on the electronics caused by the interaction of a single element of radiation; in the case of atmospheric radiation, this is secondary neutrons.

Out of the many types of particles resulting from cosmic rays cascading through the Earth's atmosphere reaching sea level, neutrons are the most significant in causing electronic circuit problems.

6.2 Single event effects (SEE)

6.2.1 General

All single event effects (SEE) are caused by the deposition of energy within a microelectronic device by a single particle that interacts with the device. The energy deposition, which occurs either directly or indirectly, leads to charge being collected. When the incoming particle is charged (for example, cosmic ray heavy ion), the ionization proceeds directly as the particle deposits its energy by ionising the surrounding silicon atoms. The greater the ability of the particle to release its energy, the greater the energy deposited by the particle (expressed as the LET (linear energy transfer), energy/path length), the more likely that the charge released is sufficient to cause an effect. When the single particle is neutral, such as a neutron, the particle first has to have a nuclear interaction with an atom within or near the active area of the device. This creates recoiling atoms, called recoils, which possess energy that is deposited (indirectly) into the surrounding silicon atoms.

A proton is charged but it has a low enough LET in silicon that it has not yet been shown to cause SEE by direct ionization. However, at high energies (> 5 MeV), it also has nuclear reactions with silicon in a manner similar to how a neutron of the same energy would interact. Thus to date, protons cause single event effects in devices only through nuclear reactions. Based on actual measurements, we assume that for energies > 100 MeV, protons and neutrons have the same ability to induce a single event upset (SEU), a flip in the logic state,

in electronic devices. This is called the SEU cross-section, and hence, atmospheric neutrons are assumed to have the same SEU cross-section as high energy protons.

In avionics, SEEs have been observed in electronic devices used in aircraft since the early 1990s [5, 8, 39, 40, 41]. In the existing literature, SEUs in memory devices have been recorded. Most if not all of the upsets have been attributed to the atmospheric neutrons. As the size of the total number of bits in an aircraft that are susceptible to SEU has increased geometrically over the last decade (more bits/device, greater functionality led to the need for more memory), the number of SEUs being induced has similarly increased. However, there is not a great deal of documented evidence of these in-flight SEUs for a variety of reasons:

a) the use of error detection and correction schemes is routinely used in avionics, but since the errors are corrected, there is little interest in recording the errors that are detected and corrected;

b) the occurrence of these errors is considered proprietary information, hence it is rarely collected, and even less often analysed; and

c) most error correction schemes look for errors only in memory that is being utilised, hence bit flips in unused memory will always be ignored.

6.2.2 Single event upset (SEU)

Single event upset (SEU) is the most common type of a single event effect. SEU is caused by the deposition of charge in a device by a single particle that is sufficient to change the logic state of a single bit from one binary state to the other. SEUs are sometimes called soft errors because they are readily corrected by reinitialising the bits. Devices susceptible to SEUs generally have been memory bits, register bits or latches. Random access memories are generally the most susceptible devices to SEU because they contain the largest number of memory bits. However due to the large number of volatile memory bits contained within microprocessor cached memories and registers, microcontrollers, ASICs and field programmable gate arrays (FPGAs) are also vulnerable. SEU susceptibility increases as the applied supply voltage decreases.

More recently the potential for SEU due to thermal neutrons has been observed in high density complex devices that have very small feature size and a low critical charge for upset. Thermal neutrons are produced when the high energy secondary neutrons interact with the aircraft structure, in particular the hydrogenous materials for example baggage, passengers and fuel. The thermal neutron flux within the aircraft may be about 2 times that of the high energy neutrons at some locations. A thermal neutron SEU cross-section comparable to that of the high energy secondary neutrons was observed during the SEU testing of SRAMs by several different groups (see 8.3.3). These devices have a thermal neutron cross-section because they contain boron 10. The comparatively high thermal neutron flux associated with the aircraft environment means that for devices that contain boron 10 in any percentage, consideration shall be given to the thermal neutron flux (for further details refer to Annex A).

6.2.3 Multiple bit upset (MBU) and multiple cell upset (MCU)

Multiple bit upset (MBU) refers to multiple bits (bits that are in the same logical word) being upset during the same SEE interaction,. MBU differs from multiple cell upset (MCU) in which two or more bits (cells) are upset, usually bits physically located near each other, but not necessarily in the same logical word. The multiple cell upset (MCU) fraction [probability of MCU/probability of SEU or MCU cross-section (multiplicity > 1)/SEU cross-section] is increasing with decreasing feature size and with more recent IC fabrication in a dramatic way. This is believed to be due to charge sharing, i.e., the charge deposited by the energetic neutron interacting with the SRAM is being shared by a number of adjacent memory bits.

With regard to SRAMs, those fabricated in ~2003 had a MCU fraction of ~3 % for 130 nm devices but ~6 % for 90 nm devices when tested in a spallation neutron beam in Japan [42]. However, based on a later compilation of such data [43] from eight different sources, including reference [42], the MCU fraction was definitely increasing with decreasing feature

size however there appear to be two separate trendlines. For one set of devices the MCU fraction starts relatively low, similar to reference [42] (~2 % for 150 nm devices), but increases by about a factor of 20 as the feature size decreases from 150 nm to 50 nm. For the other set of devices the MCU fraction starts much higher, e.g. ~40 % for 150 nm devices, but increases much more slowly, by about a factor of 2 as the feature size decreases from 150 nm to 50 nm. Further, more recent data have shown substantially wider variations, with data points falling in between the two trendlines. What is consistent with the two trendlines is that when extrapolating out to a feature size of ~35 nm, the MCU fraction will be 1.0, i.e. all SEUs will result in two or more bits being upset.

One of the recent papers [44] also investigated the effect of changing the angle of incidence of the neutron beam striking the device on the MCU fraction. The MCU fraction increased with the angle of incidence, it was lowest for normal incidence and highest for grazing incidence (90°), but the overall measured increase over normal incidence was at most ~80 % at 90° and ~30 % at 45°.

The variation of the MCU fraction with energy was examined [45] via testing with monoenergetic protons and the overall conclusion is that the MCU fraction decreased very slightly with decreasing energy. The variation with proton energy was not uniform, but the approximate decrease in the MCU fraction was from ~25 % for E = 200 MeV to 20 % for E = 46 MeV for the first device, and from ~18 % for E = 200 MeV to ~15 % for E =32 MeV for the second device.

Thus for SRAMs, the MCU rate as a fraction of the SEU rate primarily depends on the feature size (and more crudely the year of fabrication) of the device, with the neutron/proton energy having a very small effect and the angle of incidence having a larger effect. The large variation in the MCU fraction in the various SRAMs tested by different researchers cited above should be duly noted. As a result, only the conservative upper bounds summarized below can be provided for the MCU fraction in SRAMs, and even these are not the most conservative values that could be used. If these values are considered too high, individualized SEE testing would be required to measure the MCU fraction in actual devices.

For older devices, fabricated prior to 2003, the guidance in the original IEC/TS 62396-1 according to which a MCU fraction of 3 % should be used. For devices fabricated between 2003 and 2006, a MCU fraction of 10 % may be used. For devices fabricated after 2006 and in particular for feature sizes of < 100 nm, an upper bound of 30 % may be used.

For DRAMs the situation is much different, because DRAMs contain control logic in their periphery. Thus when this logic is upset, entire bitlines and rows can be upset, resulting in thousands of bits being in error due to a single neutron hit. Such thousand bit errors are called burst errors and can often be considered as a SEFI rather than a multiple cell upset.

The MBU / MCU fraction relative to SEU increases with incident particle energy and has been observed to be 7 % for 63 MeV protons on 16 Mega bit DRAMs. Multiplicities up to 4 have been observed for protons and nineteen for ions [46, 47].

Utilizing the data from [48], the situation regarding MCU in DRAMs can be generalized based on the feature size, similar to the crucial role played by feature size regarding MCU in SRAMs. At a feature size of 180 nm, the MCU fraction is about 5 %, and for devices with larger feature sizes, the guidance in the original IEC/TS 62396-1 according to which a MCU fraction of 3 % should be used. However, for the 180 nm devices, multi-thousand bit upsets are possible, but there is wide variation in the SEFI response of the two SDR DRAMs in which it was measured. The SEFI/SBU ration varied between 0,3 % to 24 % and the absolute cross-section varied between $3{,}5 \times 10^{-11}$ to $1{,}3 \times 10^{-10}$ cm²/device.

For 110 nm DRAMs, the fraction for classical MCU is very uncertain because of the tremendous variation in the MCU fraction, which is from 2 % to 100 % in the three different devices tested, all 512 Mbit DDR2 devices. However, in terms of absolute MCU cross-section the variation is much smaller, between ~1×10^{-11} to $3{,}5 \times 10^{-11}$ cm^2/device. For the SEFI

type of event that results in 1E3-1E4 erroneous bits, SEFI was much more likely than SBU. Thus, the SEFI/SBU ratio (per device basis) varied between ~1-20, with an average value of ≈ 5, and the absolute SEFI cross-section varied between 1×10^{-11} to 2×10^{-11} cm^2/device.

For 90 nm DRAMs, the situation is similar to that of the 110 nm DRAMs. However, only one of the four 90 nm DDR2 devices tested exhibited the classical MCU, and for this device, the MCU fraction was 14 %. All four DDR2 showed the SEFI type of response of thousands of errors, but in this case, SBU was more likely than SEFI, and for these four the SEFI/SBU ratio was ~15 %. The absolute SEFI cross-section varied between 4×10^{-12} to 4×10^{-11} cm^2/device. However, in a separate test of DDR and DDR2 DRAMs of 90-110 nm [49], devices from two vendors exhibited burst errors, while four separate devices from a third vendor showed no burst errors. Thus, the susceptibility to burst errors varies among DRAM vendors, some devices are immune.

In summary, it appears that the multi-thousand bit burst or SEFI events are more of a problem than the classical 2-bit or 3-bit MCU, but DRAMs from some vendors are susceptible to the burst errors, yet not from all vendors. For devices that are susceptible to burst errors, the overall trend in the absolute SEFI cross-section appears to be gradually decreasing with feature size, from ~1×10^{-10} cm^2/device for 180 nm to ≈1×10^{-11} cm^2/device for 90 nm.

6.2.4 Single effect transients (SET)

An SEU-related event in some devices that leads to the generation of a single event transient (SET) which a device may interpret as a new bit of information. These transients are spurious signals or voltages, induced by the deposition of charge by a single particle that propagates through the circuit path during one clock cycle. These signals may be harmful by propagating to a latch and becoming fixed, or striking an internal node and causing an unwanted response, or they can be effectively removed by the legitimate synchronous signals of the circuit. Initially, such transients were observed in linear analogue devices such as comparators and operational amplifiers, but they have also been recorded in digital devices. In analogue devices the SET may be manifested as a change in the timing of voltage or current signals, and is dependent on the magnitude of the driving differential voltage. Most SET tests have been performed using beams of heavy ions, but SET has also been induced in linear devices with high-energy proton beams [50, 51, 52], hence the atmospheric neutrons also cause this kind of effect.

A digital single event transient (DSET) is a spurious digital signal or voltage, induced by the deposition of charge by a single particle that can propagate through the circuit path during one clock cycle (see 6.2.4). As the frequency of digital electronics has risen above 100 MHz the potential for DSET has increased. A DSET that is clocked into a flip flop or register may appear as an SEU in that element.

An analogue single event transient (ASET) is a spurious signal or voltage produced at the output of an analogue device by the deposition of charge by a single particle. This erroneous output may persist long enough to provide false values to monitoring circuit elements e.g. analogue to digital converters effectively providing corrupt data.

6.2.5 Single event latch-up (SEL)

Single event latch-up (SEL) is a regenerative current flow condition in which a parasitic n-p-n-p pathway in a silicon device is turned on by the deposition of charge from a single particle. SEL has generally been a concern in bulk CMOS devices, but it has also been seen in CMOS devices with relatively thick (> 10 μm) epitaxial layers. The regenerative circuit provides a path for large current flow and can often lead to destructive breakdown. Even if the breakdown does not occur, the latched path will persist until power is removed from the device, so power shall be recycled to restore normal operation. Beginning in 1992, a small number of CMOS devices have been shown to be susceptible to proton and neutron-induced latch-up [53, 54]. SEL susceptibility decreases as the applied voltage decreases, and increases as the device temperature increases. In addition, on very rare occasions, other

single event induced mechanisms have been observed which can lead to a high current condition in a device that could lead to its destruction. One such example is a driver contention mechanism in one type of FPGA [55] and other specialized mechanisms have been observed to impact bipolar devices [56, 57].

6.2.6 Single event functional interrupt (SEFI)

Single event functional interrupt (SEFI) refers to a SEU in a device, usually a complex device, for example, a microprocessor, such that a control path is corrupted, leading the part to cease to function properly. This effect has sometimes been referred to as lockup, indicating that the part has been put into a "frozen" state. Generally, SEFI is brought about by a SEU in a critical bit, such as a bit that controls important downstream operations. Examples of such bits are program counters, special function registers, control, timing and mode registers in DRAMs and even built-in test (BIT) bits utilised by the device vendor only for pre-screen testing. In some devices such as DRAMs [58] and FPGAs [59], a SEFI can lead to an increase in the supply current which is similar to the effect of a single event latch-up, but proceeds via a different mechanism.

6.2.7 Single event burnout (SEB)

Devices such as N-channel power MOSFETs, insulated gate bipolar transistors (IGBTs) and bipolar power transistors and diodes, which have large applied voltage biases and high internal electric fields, are susceptible to single event induced burnout (SEB). The penetration of the source-body-drain region by the charge deposited by a heavy ion can forward bias the thin body region under the source. If the terminal bias applied to the drain exceeds the local breakdown voltage of the parasitic bipolar, the single event induced pulse initiates avalanching in the drain depletion region that eventually leads to destructive burnout. In commercial N-channel power MOSFETs, this effect can occur at values of the drain voltage, V_{DS}, lower than the rated voltage of the device. Based on the results from radiation testing in a heavy ion beam, a threshold V_{DS} is defined as the highest V_{DS} at which the MOSFET can be operated with no probability of SEB being induced by that heavy ion. Energetic neutrons and protons are also able to induce SEB in N-channel power MOSFETs [60]. In all cases, the threshold V_{DS} for neutrons and protons is higher than it is for heavy ions. SEB is precluded by operating the MOSFET below the V_{DS} threshold for neutrons and protons as determined by radiation testing. For high voltage devices, those with a rated V_{DS} of $\geq$ 400 V, tests at ground level (V_{DS} at $>$ 90 % of rated voltage) have experienced destructive failures that are consistent with rates due to SEB by the atmospheric neutrons [61]. Since the atmospheric neutron flux level at aircraft altitudes is more than 100 times greater than at ground level, the potential for SEB in high voltage devices in avionics is a potential concern. Laser testing may be used to determine susceptibility of high voltage devices to SEB (see B.5). The effects of atmospheric radiation on high voltage electronics and design mitigation are detailed in IEC/TS 62396-4.

6.2.8 Single event gate rupture (SEGR)

Both N-channel and P-channel power MOSFETs are subject to single event gate rupture (SEGR). This effect is explained via the transient plasma filament created by a heavy ion track when it strikes the MOSFET through the thin gate oxide region. As a result of this ion track filament, there is a localised increase in the oxide field which can cause oxide breakdown leading first to gate leakage and finally to gate rupture. With MOSFETs, ground level testing of high voltage devices [61] has shown that in some of the devices the failure was due to SEGR, rather than SEB. Thus the high energy atmospheric neutrons are able to induce SEGR in some high voltage MOSFETs.

A related effect that has been seen in devices such as field programmable gate arrays (FPGA) is single event dielectric rupture (SEDR) in which a thin dielectric is ruptured by heavy ions with very high LET. Testing to date has shown that the dielectrics are ruptured only by heavy ions with very high LETs, and not by energetic neutrons or protons.

6.2.9 Single event induced hard error (SHE)

It has long been known that heavy ions are able to cause "stuck bits" in SRAMs. These events are sometimes referred to as single hard errors (SHE). These hard errors are due to very localised total dose effects, caused by a few ions impinging on the gate oxide of sensitive transistors. Stuck bits are significant because they can invalidate the most common form of error detection and correction, EDAC, called SECDED, single error correct, double error detect. Stuck bits are not corrected by EDAC so they persist. If a word contains a stuck bit, a single SEU in another bit in that word at any time then produces an observable error. In the early occurrences of these hard errors, they were caused only by heavy ions with high LET. More recently the first occurrence of SHE by protons in a laboratory test was published, indicating that in newer devices (in this case a 64 Mbit DRAM, [62]), protons, and hence atmospheric neutrons, are capable of inducing stuck bits.

6.2.10 SEE potential risks based on future technology

As technology develops in the future the impact of atmospheric radiation on devices will increase and the following list highlights potential impact.

a) The effects MBU and MCU for future devices of ≤ 35nm, a MCU fraction of 100 % should be expected.

   The MCU rate for SRAM devices fabricated before 2003 with feature sizes 200 nm and above is typically a few per cent. As feature sizes of more recent SRAM devices have reduced to 150 nm, the MCU rate has increased to about 40 % and the expectation is that for feature sizes of 35 nm and below, an MCU fraction of 100 % will result.

b) Effects on small geometry Flash ROM

   Traditionally the non-volatile ROM memory has been very tolerant to the neutrons in atmospheric radiation. However at feature sizes approaching and lower than 100 nm the memories may become susceptible to various SEE, including SEFI.

c) Direct ionization by protons is significant for 65 nm and below

   Testing of SOI SRAMs at feature sizes of 90 nm and below shows that there is no threshold energy for proton-induced upsets in some devices and the cross-section in fact increases below 1 MeV [63, 64]. Direct ionization by protons at high LET values near the end of track, as opposed to nuclear reactions, is sufficient to give SEU in such devices. These low energy, or stopping, protons are generated in materials local to the device and will add to the SEU rates.

   For electronic devices used in large fielded systems such as aircraft, the greater the mass surrounding the electronics it is unlikely that the electronics within will be susceptible to SEU from direct ionization from external low energy protons. This is because the “end of track” distance within which the highest proton LET is achieved in silicon (required to produce a SEU) is 1 μm to 2 μm (~4-8 × 10^{-5} inches), compared to the centimetres of material that surround the IC devices, making energy deposition from the protons within the sensitive 1 μm to 2 μm unlikely. However the devices will be sensitive to secondary protons generated locally in materials surrounding the device.

d) Direct ionization by muons

   Muons behave like electrons but are 200 times heavier and come from pion decay. Pions are created just like neutrons during nuclear reactions between cosmic ray protons and the oxygen and nitrogen in the atmosphere. Because muons are weakly interacting they do not cause upsets by interacting with silicon and so can only cause upset through direct ionization. Muons are the most dominant particle in cosmic rays at ground level but most have energies of 1 000 MeV or higher. However some will be produced at lower energy or be degraded to lower energy. For SEE from direct ionization to take place the muons have to be 1 MeV or below.

6.3 Total ionising dose (TID)

Total ionising dose (TID) effects refer to the cumulative effect of ionization (charge build-up) in an IC device leading to a gradual degradation of electrical parameters. When a MOS (metal

oxide-semiconductor) device is exposed to ionising radiation, electron-hole pairs are created throughout the oxide that induces the build-up of charge which leads to device degradation. The main mechanisms are the build-up of positive oxide trap charge in the oxide, and of interface-trap charge in the interface between the silicon and the silicon dioxide. Large concentrations of oxide-trap charge cause increased leakage current in a device. Large concentrations of interface-trap charge increase the threshold voltage of transistors, degrading the timing parameters of a device. Similar effects are also caused in bipolar devices.

Based on previous total dose testing experience of microelectronics devices over the past 20 years, involving probably thousands of different devices, an effective lower bound on the minimum TID level that can cause a device to operate out of spec is 1 000 cGy(Si). For the vast majority of devices, including almost all commercial off the shelf (COTS) devices, the TID threshold level is much higher than 1 000 cGy. Nevertheless, using 1 000 cGy as the minimum threshold, and even including a factor of 2 for margin, this means that a worst case minimum total dose level that aircraft avionics would have to absorb is 500 cGy before TID effects could possibly be an issue of concern in the avionics.

Ionising dose is contributed by all of the major particles that constitute the radiation environment within the atmosphere, i.e., neutrons, protons, electrons, photons, etc. Based on measurements made in a commercial airliner [65], the maximum dose rate from all of the particles is ~70 nGy per minute (~0,4 millirad per hour or ~4 microgray per hour). For a nominal 100 000 flight hours, this results in ~40 cGy of dose over that lifetime, which is an order of magnitude lower than the worst case TID threshold of 500 cGy. For aircraft at higher altitudes, for example 55 000 feet (16,8 km), the dose rate doubles to 8 microgray per hour with a maximum dose over 100 000 flight hours of 80 cGy well below the TID threshold. However the total ionising dose is cumulative and any dose from other sources should also be considered for example mechanical X-ray testing.

An upper bound estimate on the maximum dose that an electronics device might receive from an x-ray inspection is 1 milligray. This is extrapolated from the maximum dose that objects may receive from x-ray machines used to inspect luggage (10 microgray), and is also consistent with the approximate range of doses known to be received from commercial x-ray inspection systems (200 microgray to 500 microgray). Thus, TID effects are not generally an issue for avionics.

Mechanical X-ray and gamma ray inspection is carried out on certain parts of the airframe to demonstrate structural integrity. The radiation doses delivered by this type of inspection may be higher than that from the luggage inspection machines. Where such inspections are carried out if the cumulative dose received by any localised avionics electronic equipment over its lifetime in service potentially exceeds 50 cGy then consideration shall be given to removing the electronic equipment before the radiation inspection is carried out. Examples of such equipment include wing and engine mounted electronics.

6.4 Displacement damage

Still another kind of effect that ionising radiation can induce in microelectronic devices is displacement damage. This is also a cumulative effect, but in this case it refers to atoms that are displaced out of their lattice. When a sufficient number of atoms are displaced, the device no longer functions normally. This effect is primarily due to the heavier particles, neutrons and protons, since lighter particles, such as electrons and gamma rays, are much less effective in knocking atoms out of their lattice.

Based on previous experience of testing dozens of parts for displacement damage, an effective lower bound on the minimum neutron fluence that causes a device to operate out of spec is 1×10^{10} n/cm^2. The 1×10^{10} n/cm^2 value is based on displacement damage in sensitive optocouplers [66]. For microelectronic devices, the neutron fluence threshold for damage is higher. The basis for this testing was a fluence of 1 MeV equivalent neutrons. A large fraction of the neutrons at aircraft altitudes are at higher energies than 1 MeV, and their potential for causing displacement damage in devices is greater than that of 1 MeV neutrons.

The NIEL (non-ionising energy loss) function has been calculated for semiconductor materials such as silicon and gallium arsenide (GaAs) as a function of energy, and the NIEL is accepted as the best measure for the potential of a material to undergo displacement damage. Based on the NIEL for silicon by neutrons as a function of energy, it is conservative to assume that the higher energy neutrons have at the most a factor of 3 greater effectiveness in causing displacement damage compared to 1 MeV neutrons.

At aircraft altitudes, a useful estimate of the flux of high-energy neutrons (1 MeV to 1 000 MeV) is 8×10^3 n/cm^2 per hour. Thus assuming the electronics are exposed for 1×10^5 flight hours, this results in a neutron fluence of 8×10^8 n/cm^2. Using the factor of 3 as an upper bound equivalence between the higher energy neutrons and the 1 MeV neutrons for purposes of displacement damage, this fluence converts to a 1 MeV equivalent neutron fluence of $2{,}4 \times 10^9$ n/cm^2. This upper bound 1 MeV neutron equivalent fluence for avionics is still a factor of 4 below the minimum level to cause displacement damage to the most sensitive devices. Hence displacement damage is not a problem for avionics devices, based on a minimum 1 MeV neutron fluence of 1×10^{10} n/cm^2.

7 Guidance for system designs

7.1 Overview

Methodology and practices associated with safety aspects of system design can result in the accommodation of component and equipment soft and hard fault rates. If avionics electronic components that can experience atmospheric radiation induced upset and failure effects which have the potential to adversely affect aircraft safety are identified, the method of assessing the safety impact of such effects is identical to that used to assess other potential hazards associated with an electronic avionics product. Figure 6 contains a flow chart showing an outline of this process. The flowchart is consistent with the aerospace recommended practices (ARP) contained in ARP4754 (Certification Considerations for Highly-Integrated or Complex Aircraft Systems) and ARP4761 (Guidelines and Methods for Conducting the Safety Assessment Process on Civil Airborne Systems and Equipment). In addition to the ARPs, quantitative requirements for the availability of aircraft functions are provided in AC23.1309-1C and AC25.1309-1A. Additional guidance for system designers is provided in IEC/TS 62396-3.

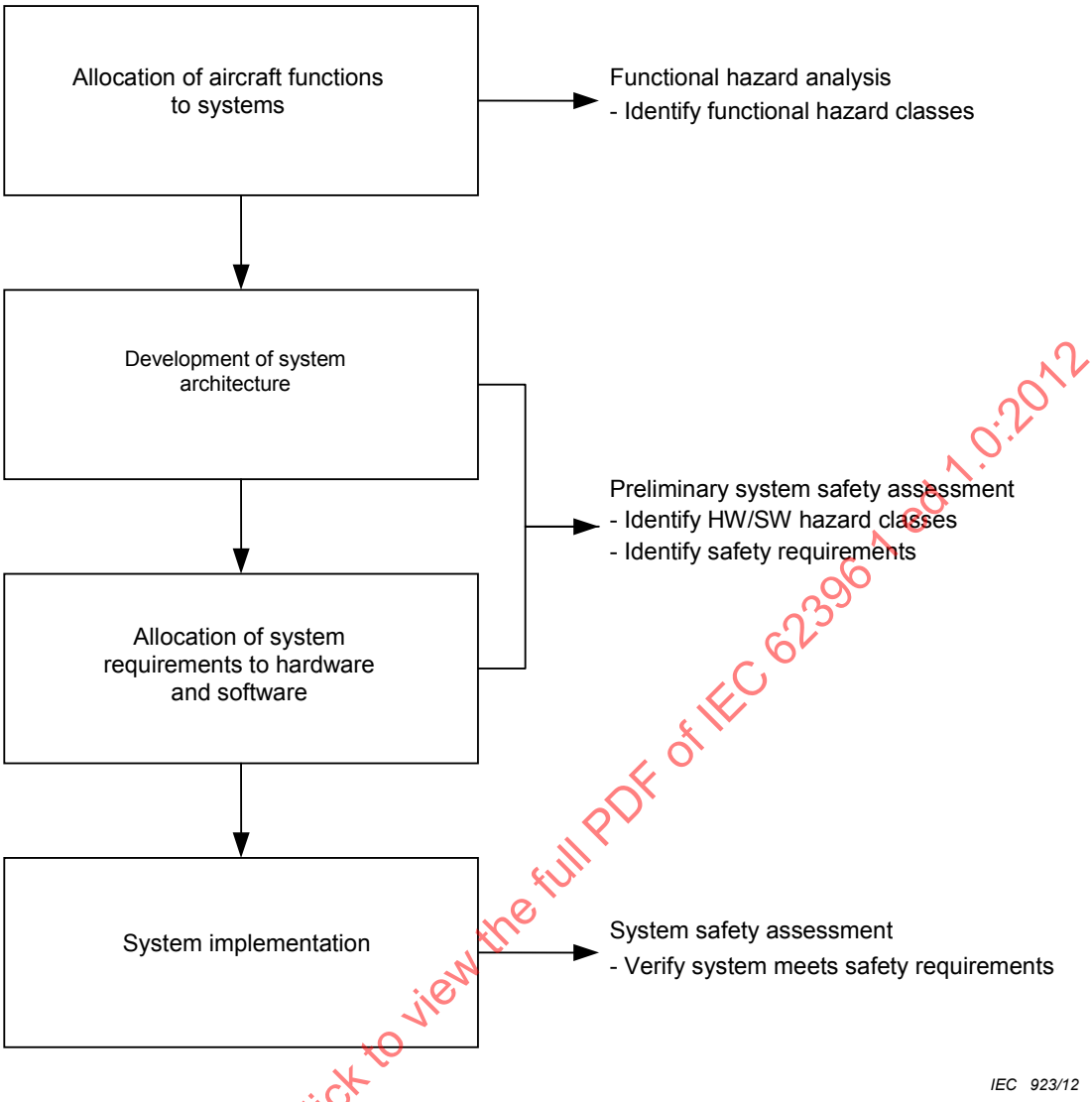

Figure 6 – System safety assessment process

The first step in the development process is to allocate the aircraft level functions to systems which will implement these functions. As part of this development phase, each of the systems is assessed relatively to potential hazards, which could impact aircraft safety, by use of a functional hazard analysis (FHA). The FHA assesses all hazards against a set of hazard classes similar to the classes shown in Table 1. In addition to identification of top-level system hazards the FHA identifies required hazard classifications for each function. This classification is set equal to the highest criticality hazards associated with each function. SEE does not generally cause unique function level failure effects as other hardware failure modes can cause the same effects. As a result SEE does not need to be included as a separate hazard within the FHA.

System development assurance levels refer to processes used during system development (design, implementation, verification/certification, production, etc.). It was deemed necessary to focus on the development processes for systems based upon "highly-integrated" or "complex" (whose safety cannot be shown solely by test and whose logic is difficult to comprehend without the aid of analytical tools) elements (primarily digital electronic components and software).

Development assurance activities support system development processes. Systems and items are assigned "development assurance levels" based on failure condition classifications associated with aircraft-level functions implemented in the systems and items. The rigor and

discipline needed in performing the activities supporting development processes will vary corresponding to the assigned development assurance level and should be tailored accordingly.

Systems that implement aircraft functions are classified by the failure effects of the functions they implement. Table 1 provides a cross-reference between functional failure effects and the classification of systems that implement the corresponding function.

Table 1 – Nomenclature cross reference

Functional failure condition classification (AC 23.1309-1C, AC 25.1309-1A and ARP4754)	System development assurance level (ARP4754)
Catastrophic	Level A
Severe major/hazardous	Level B
Major	Level C
Minor	Level D
No effect	Level E

During the development of the system architecture and allocation of system requirements to hardware and software, a preliminary system safety assessment (PSSA) is performed. The purpose of the PSSA is to evaluate the planned architecture to determine the reasonableness of the architecture to meet the system safety requirements. Unlike the FHA, the PSSA considers the intended system architecture and identifies failure modes, which individually or in combination, can lead to the top-level hazardous events identified in the FHA. Since SEE would not introduce new failure modes, the failure modes considered in the PSSA would include SEE. Depending on the effects of SEE the PSSA will consider those that cause soft versus hard faults separately. The impact of phase of flight typically will need to be considered since the probability of SEE is higher during cruise than during take-off and landing. Since PSSA results will drive architecture mitigation measures, it will identify any architectural mitigation that is required.

During the system implementation phase the design is completed and verified. The system safety assessment (SSA) is performed to verify and document that the system, as designed and built, complies with the safety requirements. Thus, all applicable SEE rates will be included in the SSA.

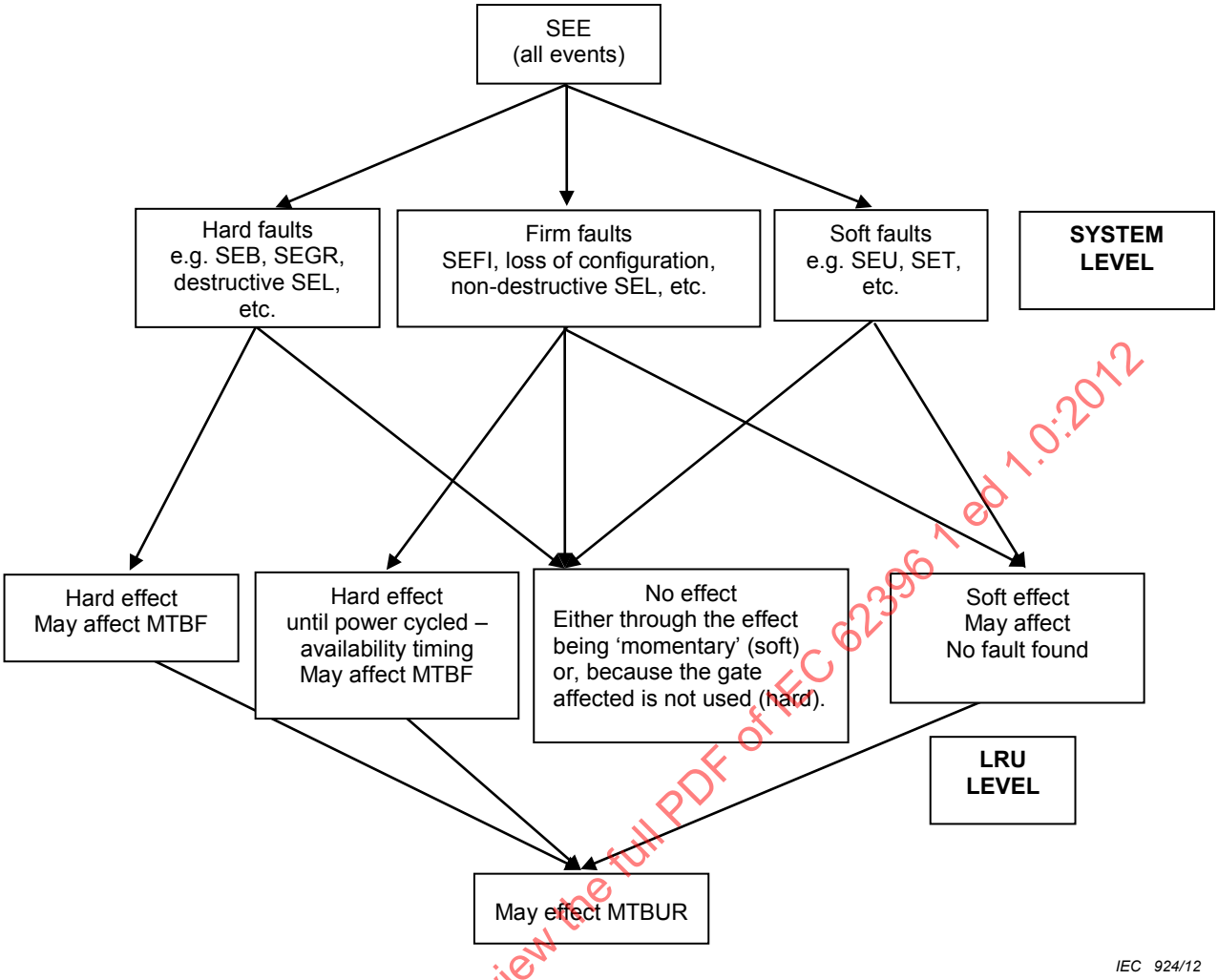

Figure 7 – SEE in relation to system and LRU effect

7.2 System design

Because failure effects may include both malfunction and loss of function, the implementation of some aircraft functions usually requires system architectures with some degree of equipment monitoring and redundancy. The degree of redundancy is dictated by equipment component failure rates that include SEE failure/fault rates. An indication of the impact of SEE is given in Figure 7. Since the neutron interaction events that result in SEE are stochastic and relatively rare, potentially adverse safety effects would be confined to Level A, B or C systems. For Level D and E systems, the impact of SEE would primarily affect economics and customer satisfaction and need not be considered in system safety assessments.

For Level A, B and C systems the SEE rates shall include single event effects that result in both soft errors and hard errors. Soft errors are defined as those that are easily recovered from, usually by a rebooting of the system, or even recycling power. The non-destructive SEE effects that comprise soft errors include SEU, MCU, SET and SEFI (most of the time). Hard errors are those that cannot easily be recovered from by a rebooting of the system. They can be brought about by destructive damage to a device or by a soft error being propagated within a system that results in the standard boot-up not being available. The destructive SEE effects that constitute hard errors include SEL, SHE, SEB, SEGR and on occasion SEFI. In those few devices that are susceptible to destructive SEE effects by high-energy neutrons, such as SHE and SEL, the SEE rates in avionics (see 8.2.3 and 8.2.4) will be much larger than the rates of hard failures in those devices due to mechanical mechanisms, which are generally in the range of 100 to 1 000 FITs (1×10^{-6} to 1×10^{-7} failure/device·hour, [67] for avionics).

The SEU rates for individual devices may be obtained from a variety of data sources, and the two main approaches that can be utilized for these are discussed in B.3 and B.4. The approach described in B.2, exposing an LRU or circuit board to a proton or neutron beam, provides more information as to how potential SEEs in devices affect the subsystem, but few such tests have been carried out. Very few devices have been documented to be susceptible to destructive SEE effects, primarily SEL, by high-energy neutrons or protons, but only a limited number of devices have been tested in such beams in the first place. However, actual in-flight experience of devices used in avionics boxes could be utilized to demonstrate the lack of susceptibility to destructive SEE mechanisms, although this has not been done formally to date.

Equipment redundancy along with other mitigating architecture measures would in turn translate to requirements for acceptable SEE rates. For a single system implementation of a particular aircraft function, objectives should revolve around acceptable equipment failure rates that include SEE rates. Architectural considerations, equipment design or component selection mitigates the impact of failure rates (including SEE rates) on a product. The discipline and rigor required in the system design for and verification of mitigation of fault effects is dependent on the system development assurance level.

Separate error rates are required for soft errors and hard errors (faults) depending on the overall equipment impact of these errors/faults. For example, soft errors may not constitute an equipment fault if an automatic or crew initiated reset is able to return the equipment to full operation. The discipline and rigor associated with SEE rate determination could range from characterisation of the actual SEE rate for a specific device to a determination of similarity to a class of devices with a known SEE rate. A device SEE rate impacting a Level A (function failure effect of Catastrophic) system should be quantified with greater rigor (see 7.4.2) than that impacting a Level B (function failure effect of Severe Major/Hazardous) system. Likewise, a SEE rate impacting a Level B system should be quantified with greater rigor (see 7.4.3) than those impacting Level C (Major) systems (see 7.4.4) or Level D (Minor) and Level E (No Effect) systems (see 7.4.5).

For the purpose of this document, soft errors result in error or loss of function but recoverable for example by reset or power cycle. Hard errors result in equipment failure that is permanent and only recoverable by repair activity.

7.3 Hardware considerations

SEU rates are a particular issue with digital electronic hardware. Such effects refer to the characteristic of invalid state changes; for example, those that occur in latch circuits (memories, registers, etc.) that are fundamental building blocks of digital hardware.

Extreme solar flare events produce additional neutrons within the atmosphere that increase the overall atmospheric neutron flux without direct warning. Therefore for Levels A, B and C systems a scaling factor for solar enhancement of the high-energy neutron flux should be applied (see 5.6).

Using the safety assessment process and given a failure/fault rate, for each type of SEE, the system architectures can be provided to achieve robust operation in a potentially fault producing environment. System architectural features, such as redundancy, monitoring, error correction, or partitioning, can be useful in mitigating the effects of an equipment fault on the system operation and reducing the probability of a system hazard. Redundancy is a technique for providing multiple implementations of a function – either as multiple items, or multiple lanes within an item. It assumes that a hard error/fault (SEE induced, etc.) impacting one element of the system implementing a function is independent of such a fault impacting the redundant system element. Monitoring for and accommodation of an equipment fault effect is a useful technique to minimise the impact of any such effects.

If various functions are provided by the integrated modular avionics (IMA) technology, the determination of the development assurance level shall include the effects of the simultaneous loss and/or malfunction of all of the functions that the IMA system provides. The rigor and discipline associated with the highest system development assurance level would typically be applied to the hardware associated with the IMA computing platform.

7.4 Parts characterisation and control

7.4.1 Rigour and discipline

The rigour and discipline needed in characterising parts SEE rates and in parts control will vary according to the development assurance level and should be tailored accordingly.

7.4.2 Level A systems

7.4.2.1 Characterisation

Level A systems are categorised into two groups. One group involves functions for which the pilot will not be part of the operational loop. These are classified as Level A Type I systems, for example, FBW, etc.

The second group involves functions for which the pilot will be within the loop through pilot/system information exchange. These are defined as Level A Type II systems, for example, EFIS, etc.

Level A Type I system failures and malfunctions can more directly and abruptly contribute to a catastrophic event than Level A Type II system failures and malfunctions. It is, therefore, appropriate to require a more rigorous compliance method for Type I systems than for Type II systems.

7.4.2.2 Level A Type I

This assurance level will require the most rigorous/disciplined (testing/analysis) approach (including SEE rate characterisation) for showing compliance to requirements for acceptable function performance in the radiation environment. One of the following methods should be employed:

a) SEE rates in electronic components may be derived from neutron testing on the specific parts used in the design by exposure to a suitable simulation facility. An example of a high fidelity atmospheric neutron environment simulation is the Los Alamos WNR (see 8.3.3 and Annex C). Accuracy of this method is approximately a factor of 2 on the event rate.

b) SEE rates in electronic components may also be derived from proton testing on the specific parts used in the design by exposure to high energy (greater than 100 MeV) proton beams (see 8.3.3, B.2 and Annex C). Accuracy of this method is approximately a factor of 3 on the event rate.

c) At system level, “in-the-loop” type of SEE testing of avionics equipment or systems may be used as described in B.1. Accuracy of this method is approximately a factor of 2 to 3 on the event rate dependent on particle beam used.

d) Where such data is not available or testing is impractical then the methods of 7.4.2.3 may be used to derive event rates, however a suitable minimum factor in event rates over values calculated by these methods shall be applied.

These types of systems require the most robust parts performance and device technology controls. Technology controls shall be in place to monitor device supplier changes that could impact SEE failure/fault rates.

7.4.2.3 Level A Type II

SEE rates should be based on either:

a) Level A Type I rigour/discipline or

b) less rigorous/disciplined approach using one of the following methods:

   1) The use of proprietary information and data applicable to SEE for example silicon on insulator and established thin radiation tolerant epitaxial layer to prevent latch up, and non-contiguous memory to avoid MBU (Accuracy approximately factor of 2 on event rate).

   2) Irradiation of individual avionics equipment items containing a variety of potentially susceptible parts as described in B.2.

   3) Any of the following SEE engineering tools that shall be applied by SEE radiation effects experts:

      i) Use of heavy ion SEE data processed using an analytical approach to obtain neutron SEE data (see B.3). Accuracy is approximately a factor of 10 on the event rate.

      ii) Use of neutron/proton SEE data on specific part types (see B.3). Accuracy is approximately a factor of 10 on event rate.

      iii) Use of generic SEE data based on component basic technology and type (for example CMOS SRAM) (see B.4); it is used where there is no relevant SEE data for the parts. Accuracy is approximately a factor of 10 on the event rate because this is an inherently conservative method.

      iv) Use of component SEE testing by laser simulation using a laser that has been calibrated using a reference device of the same functional type (for example SRAM) and similar technology and feature size (see B.5). Accuracy using calibration devices is approximately a factor of 10 on the event rate.

These types of systems require the most robust parts performance and device technology controls. Technology controls shall be in place to monitor device supplier changes that could impact SEE failure/fault rates.

7.4.3 Level B

SEE rates should be based on either:

a) Level A rigour/discipline; or

b) SEE failure/fault rates traceable to SEE tests on similar parts using test results from non-neutron testing facilities see B.3, B.4 and B.5.

These types of systems require moderate parts and technology control with periodic assurances that no supplier changes could impact SEE failure/fault rates.

7.4.4 Level C

SEE rates should be based on either:

a) Level B rigour / discipline; or

b) SEE failure/fault rates traceable to testing results via a SEE failure/fault rate model (use of an average SEE error rate for all potentially sensitive components – in these instances, the SEE error rate may be high for some components and low for others but the overall equipment error rate can be expected to be acceptable – see B.4).

These types of systems use normal parts control and change notification practices. Changes shall be reviewed for potential impact on SEE failure/fault rates. The impact of a part change will be tracked by product (identify trends indicating major increases in failure/fault rates).

7.4.5 Levels D and E

These types of systems use of normal parts control and change notification practices. No additional screening for the effects of atmospheric radiation is required unless specifically requested by the customer.

8 Determination of avionics single event effects rates

8.1 Main single event effects

Many microelectronic devices are susceptible to SEEs in avionics at aircraft altitudes, and there are many different ways of dealing with the phenomena. First, it shall be recognised that even though Clause 6 lists many different kinds of single event effects, in almost all cases for devices available at the beginning of the 21st century, the main effects that need to be dealt with are SEU, MBU, MCU and SEFI. This may not hold true in the future, as fabrication methods and output requirements of newer electronic devices are further advanced through developments in device technology. The event rate for the other single event effects are generally low enough that they can be ignored in most cases. However, SEL presents a difficulty because while the majority of CMOS parts are not susceptible to SEL due to the atmospheric neutrons, a few parts are susceptible, and the atmospheric neutron SEL rate for some of these may not be considered small enough to ignore. The potential for SEL may change as a result of die revision of existing parts.

The key to being able to deal with single event effects in avionics is to quantify the SEE rate of an LRU, which usually is taken as the combined SEE rate of all of the devices that are used in the LRU. The SEE rate per device-hour is calculated by the following equation:

$$\text{SEE rate} = \text{atmospheric neutron flux } (\text{n/cm}^2\cdot\text{h}^{-1}) \times \text{SEE cross-section } (\text{cm}^2 \text{ per device}) \quad (2)$$

A number of different approaches can be used for this, from testing an LRU or the electronic boards within it while exposed to a beam of neutrons or protons (dynamic test), to calculating rates based on data for the static SEE response of individual parts. The subject of single event testing of avionic systems is covered in more detail in IEC/TS 62396-2.

The SEE response of a device to a beam of particles is characterised as the SEE cross-section, which is the number of events divided by the fluence of particles (p/cm^2; the particle flux integrated over the exposure time) to which the device was exposed. Thus the cross-section is given in units of cm^2/device or cm^2/bit.

8.2 Single event effects with lower event rates

8.2.1 Single event burnout (SEB) and single event gate rupture (SEGR)

Single event burnout (SEB) and single event gate rupture (SEGR) apply only to devices such as power MOSFETs and IGBTs. As discussed in Clause 6, energetic neutrons in the atmosphere can induce SEB and SEGR in power MOSFETs, but there is an additional important device parameter involved, V_{DS}, the drain-source voltage (V_{GS}, the gate source voltage plays a minor role). Power MOSFETs are generally operated at a derated condition, i.e., operated at a V_{DS} that is lower than the rated V_{DS} of the device. A large number of power MOSFETs have undergone laboratory testing with beams of heavy ions for SEB and/or SEGR, and these have identified the value of V_{DS} (passing V_{DS}) at which no SEB or SEGR occurs. Similarly, a smaller number of power MOSFETs have been tested with beams of protons and energetic neutrons for SEB, and the results of these, the passing V_{DS} values, have been tabulated [68, 69, 70]. The proton/neutron passing V_{DS} is higher than the heavy ion passing V_{DS}. From these results we can generalise that, based on those devices that were tested, atmospheric neutrons can induce SEB in power MOSFETs rated at 400 V and above. However, if the devices are operated at a V_{DS} of < 300 V, the probability of an SEB will be low enough that SEB should not be a concern. For voltages > 300 V, the SEB cross-section is

needed in order to calculate the SEB rate, and this cross-section can be obtained only from high energy proton/neutron SEB tests, such as those in [71, 72, 73].

There is evidence that high voltage electronics has been affected by secondary neutrons at sea level. As indicated in [61, 68], the instances in which high power electronics have failed on the ground are all attributable to the cosmic ray neutrons.

8.2.2 Single event transient (SET)

Single event transient (SET) responses have been measured in a number of devices with heavy ions, but in only three different types of devices using proton beams, a comparator [51], analogue to digital converter [74] and a pulse width modulator (PWM) [50]. The ability of a circuit to tolerate a SET is highly dependent on the specific application. Nevertheless, the calculated SET rates for these three types of devices at aircraft altitudes considering the nominal neutron flux (see 5.3.2) can be helpful for purposes of assessing the kind of effects that could be induced, and providing an upper bound on their probability of occurrence. For the PWM, SETs led to changes in the waveform output of the device, which is usually at constant frequency and duty cycle [50]. Phase shift errors in the output were considered small events, and they have an upper bound rate of 4×10^{-6} event/device·hour at aircraft altitudes, while period mismatch errors (larger events), have an upper bound rate of 1×10^{-6} event/device·hour. With the comparator, the recorded transients were about 1 μs in duration, and the probability of such events depended on the voltage input. For a –25 mV input, the proton results lead to an upper bound SET rate 1×10^{-6} event/device-hour at aircraft altitudes, and with a –12,5 mV input, the proton results lead to an upper bound SET rate 2×10^{-5} event/device-hour at aircraft altitudes.

8.2.3 Single event hard error (SHE)

For single event hard error (SHE), a 64 Mbit SDRAM was recently tested with high-energy protons and stuck bits, SHEs, were recorded [62]. This is the most useful data for estimating the SHE rate at aircraft altitudes. SHE is a microdose effect, and it is not at all clear that other large SDRAMs will also have the same susceptibility to this effect as the SDRAM that was tested. Nevertheless, the calculated SHE rate for this SDRAM at aircraft altitudes is helpful in providing an upper bound on the probability of occurrence of hard errors. Using this proton data [62] an upper bound rate of 4×10^{-6} SHE event/device·hour is obtained at aircraft altitudes due to the atmospheric neutrons. This rate is based on the assumption that each bit of the 64 Mbit SDRAM is equally susceptible.

8.2.4 Single event latch-up (SEL)

Many CMOS devices are susceptible to SEL from heavy ions. A small number of these have also been tested with beams of energetic protons and neutrons, and have been shown to be susceptible to SEL from the protons and neutrons. References [75, 76] contain a few of these devices that can have SEL induced by protons and neutrons and their SEL cross-sections, but each year or two one or more new devices are identified by SEE researchers as susceptible to proton SEL [77].

One approach that may be useful is to provide an upper bound rate based on the device with the highest probability of having SEL [75, 76] induced by atmospheric neutrons at aircraft altitudes. References [75, 76] list a total of seven devices with proton SEL cross-sections, and the two highest have SEL cross-sections of $4{,}5 \times 10^{-9}$ cm^2 (DSP) and $6{,}6 \times 10^{-9}$ cm^2 (microcontroller). Unfortunately, two very recent proton-induced latch-up cross-sections have been published for SRAMs [47, 78] and these proton-induced SEL cross-sections, 7×10^{-9} cm^2 and 4×10^{-8} cm^2; both exceed the largest previous proton SEL value. Another study [79] exposed SRAMs to the WNR neutron beam and SRAMs from three different vendors latched up, two also with high SEL cross-sections. Thus an upper bound SEL rate for avionics based on the largest measured SEL cross-section to date of 4×10^{-8} cm^2 and the neutron flux of 6×10^3 n/cm^2 per hour is $2{,}4 \times 10^{-4}$ latch-up/device per hour, or once in about 4 000 h. Since this rate appears to be high enough to be of concern, the best certain alternative would be to expose all devices in a LRU to a beam of high-energy

protons or neutrons, and monitor for latch-up (increase in current). For latch-up screening, the pulsed laser approach constitutes also an efficient solution. The laser is used only to determine whether or not a device will latch up following an ionization event [80]. This testing provides a relevant and reproducible answer for device assessment during design phase but also to control die changes influence on SEL susceptibility.

Devices that are susceptible to neutron-induced SEL could thereby be identified and alternative actions considered. This is the approach taken by a number of NASA centres and programs due to concerns of SEL by the trapped protons in space.

8.3 Single event effects with higher event rates – Single event upset data

8.3.1 General

The key to being able to deal with single event effects in avionics is to quantify the single event effect rate for an avionics box. Once an estimate can be made of the event rate, appropriate measures can be considered to accommodate the event. If the event rate is low enough, a decision might be made to tolerate it. If it is too high, a variety of fault tolerant measures can be considered for incorporation, such as error detection and correction (EDAC) or redundancy. These fault tolerant measures involve architecture and systems approaches that are beyond the scope of this document.

As indicated in Clause 6, SEU, MCU and SEFI are the three single event effects that present the largest potential threat to aircraft avionics, and they are listed in order of decreasing occurrence. In addition, as discussed in 8.2.4, for a few CMOS parts, the single event latch-up rate could be a concern. At a simplified level, the SEU rate depends on the number of bits in a device, and in most cases the bits serve as either memories, registers or latches. The kinds of devices that contain the largest number of volatile bits are memories, microprocessors, ASICs and field programmable gate arrays (FPGAs). When the SEU rate at aircraft altitudes is considered on a per bit basis, the SEU rate is similar for these various kinds of devices to within a range of 1 to 2 orders of magnitude.

8.3.2 SEU cross-section

The SEU response of a device to a beam of particles is characterised as the SEU cross-section, which is the number of upsets divided by the fluence of particles (p/cm^2, particle flux integrated over the exposure time) to which the device was exposed. Thus the cross-section is given in units of cm^2/device or cm^2/bit. Various scientific and engineering organisations around the world carry out such SEU tests in order to characterise the SEU response of devices to the different particles. The vast majority of these tests are performed for electronics that are being considered for use in space. Therefore, most of the tests are with heavy ion particle beams, and some are with proton beams. A smaller number are performed using neutron beams.

Thus, in the radiation effects literature, there are three different types of SEU cross-sections that are reported, heavy ion SEU cross-sections, proton SEU cross-sections and neutron SEU cross-sections. For immediate purposes, the heavy ion SEU cross-sections, which are used for electronics intended for space applications, are not directly relevant for avionics applications; however the utilisation of heavy ion SEU data for avionics purposes is further discussed in B.3.

8.3.3 Proton and neutron beams for measuring SEU cross-sections

For particle energies above 50 MeV, SEU cross-sections measured with protons and neutrons can be taken to be essentially the same, but at lower energies this is not true due to the coulomb barrier for the proton that is not present for the uncharged neutron. However, there is a problem in making comparisons between neutron and proton data in that the proton SEU cross-sections are measured using a monoenergetic proton beam, whereas it is difficult to achieve a beam of neutrons of a single energy except under special circumstances. Proton beams are available at a number of high energy accelerators around the world, for example

the Indiana University Cyclotron Facility (IUCF) in the US, the Paul Scherrer Institute (PSI) in Switzerland, the Tri-University Meson Facility (TRIUMF) in Canada, etc. Each accelerator has an upper energy, but testing is often done at several energies and the SEU cross-sections are reported as a function of the proton energy. Therefore SEU cross-section from proton beams greater than 100 MeV can be used to give the equivalent cross-section from WNR.

At aircraft altitudes, the spectrum of the atmospheric neutrons covers the energy range to greater than 1 000 MeV. One type of neutron source is available that simulates the atmospheric neutron environment and is set up to allow experimenters to expose electronics to the beam and measure the induced single event effects. This is the spallation neutron source examples of which are given in Annex C; these sources can be designed so that their spectrum simulates the atmospheric radiation environment (white neutron source) up to the maximum energy of the accelerator. Such sources can produce neutron fluxes that are orders of magnitude greater than that of the atmospheric radiation environment and enable highly accelerated testing of electronics.

The other neutron sources that are available are monoenergetic neutron generators and quasi-monoenergetic neutron beams. The neutron generators rely on the D-T reaction to produce monoenergetic beams of 14 MeV neutrons and occasionally on the D-D reaction to produce beams of ~3 MeV neutrons. The quasi-monoenergetic beams rely on a proton beam striking a lithium 7 target producing a peak of neutrons at nearly the energy of the protons, and a lower flux of neutrons with energies over the entire energy range from the peak energy down to thermal energies. This low energy “tail” constitutes a significant fraction of all of the neutrons produced. There is some uncertainty as to how to remove the SEU contribution from the neutrons in the lower energy tail in a consistent manner to yield monoenergetic neutron SEU cross-sections.

However, there is another source of neutrons within an aircraft that can cause SEEs that requires an entirely different kind of neutron source for purposes of laboratory testing. These are the thermal neutrons discussed in 5.3.5. The average energy of these neutrons is 0,025 eV, but they are more generally considered to be below 1 eV; thus they are 6 to 9 orders of magnitude in energy lower than that of the high energy neutrons of primary concern, those in the 1 MeV to 1 000 MeV range. The thermal neutrons cause single event effects by their interaction with the boron-10 isotope within the IC (glassivation layer over silicon), rather than with the silicon atoms. The reaction that is responsible for the increased SEU rate due to thermal neutrons is:

$$^{10}B + \text{neutron} \rightarrow {}^{7}Li + {}^{4}He \text{ (alpha)} \quad (3)$$

Research nuclear reactors and other facilities (see Annex C) provide convenient sources of thermal neutrons with relatively high neutron fluxes for accelerated testing. However there have been few studies in which devices have been exposed to thermal neutrons and the resulting SEU cross-section measured. Of these only a small number have exposed SRAMs to both thermal neutron and high-energy neutron beams and compared the SEU cross-sections. In one study [47], both the thermal and high energy neutron SEU cross-sections in SRAMs from four different vendors were measured. For SRAMs from two vendors the thermal neutron cross-section was higher than the high energy SEU cross-section by a factor of between 1,5 and 3 for one vendor’s device the ratio of the SEU cross-section from thermal and high energy neutrons was about 1 and for the fourth vendor, there were no SEUs from thermal neutrons. In a second study [81], for one SRAM the thermal neutron SEU cross-section was lower than that due to the high energy neutrons by about a factor of 10, but for a second SRAM, the thermal neutron SEU cross-section was higher by a factor of 2,5. The most compelling study [82] exposed SRAMs to naturally occurring neutrons at a high altitude location, with some devices receiving the full spectrum and others having the thermal neutrons shielded out. The SEU rate due to thermal neutrons was about three times that due to the high-energy neutrons, and when account is taken of the relative magnitude of the neutrons fluxes, the SEU cross-section from thermals is about four times that due to high energy neutrons. Additional comparison between high energy and thermal neutron cross-sections for SRAMs is made in [22]. Thus the additional SEU rate from thermal neutrons is an

issue for avionics. There is further discussion of thermal neutron SEE in Annex A and in IEC/TS 62396-5.

Thus the neutron SEU cross-section obtained from a specific test depends on the neutron source that was used. For avionics applications, cross-sections measured with the WNR beam are best because these neutrons have the same energy spectrum as the atmospheric neutrons. These WNR SEU cross-sections can be applied directly to the atmospheric neutrons at aircraft altitudes [76].

The relationship between the WNR SEU cross-section and proton and neutron SEU cross-sections at specific energies is shown in Figure 8 for three older SRAMs. For the two devices with the SEU cross-section measured in the WNR beam, it appears the WNR SEU cross-section is approximately equal to the proton SEU cross-section for energy > 100 MeV and to the monoenergetic neutron SEU cross-section at 100 MeV. Therefore SEU cross-section from proton beams greater than 100 MeV can be used to give the equivalent cross-section from WNR. The monoenergetic neutron SEU cross-section data were derived from measurements made with a pseudo-monoenergetic beam and corrected for the contribution from the tail of lower energy neutrons [83]. Further, based on more recent testing [21], SEU cross-sections obtained from testing with monoenergetic proton beams (> 100 MeV) in SRAMs, FPGAs and microprocessors are expected to be within less than a factor of 2 of those that would be obtained from testing with the WNR neutron beam.

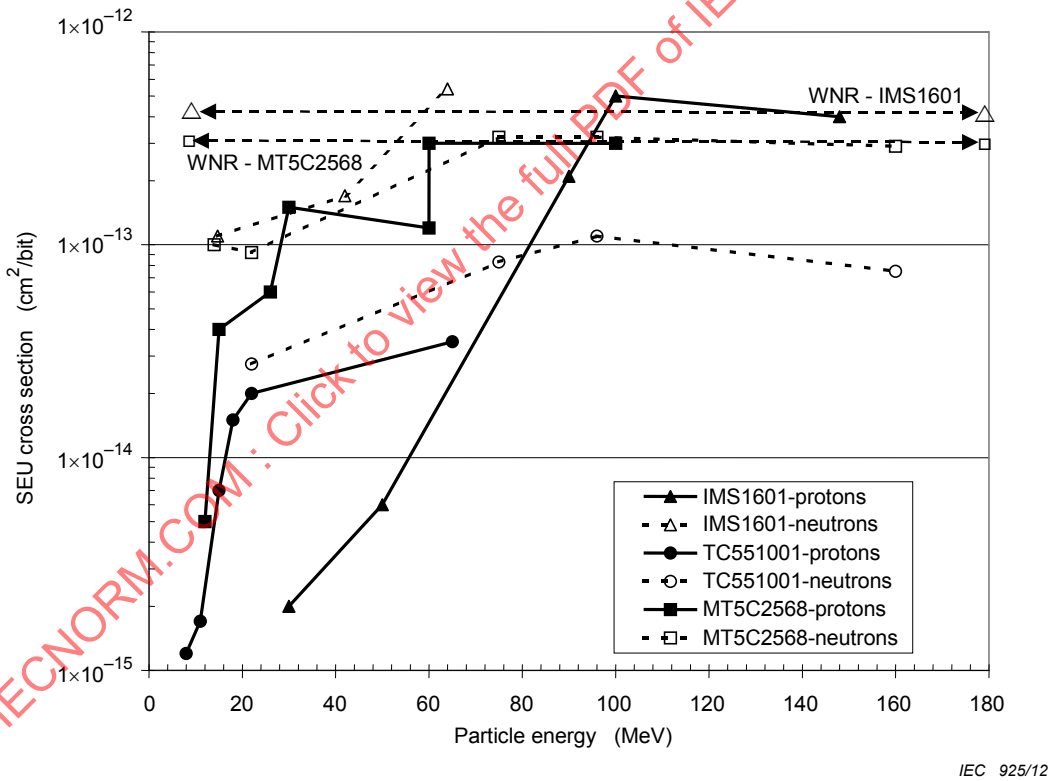

Figure 8 – Variation of RAM SEU cross-section as function of neutron/proton energy

For the comparison of neutron and proton measurements and the significance of low energy neutrons two examples are presented in Figure 9 with data on 4 Mbit SRAMs [21, 47]. The feature size of these devices was 0,4 μm and this figure gives data for the most and least sensitive devices from this sample. For the results obtained from neutron energies of 21 MeV to 174 MeV at TSL, the neutron upper and lower limits are derived by dividing by neutrons in the peak and total neutrons respectively. Proton results at 13 MeV to 490 MeV from TRIUMF are truly monoenergetic and fall in between. The neutron point at 14 MeV was obtained from monoenergetic neutron sources (D-T) and is higher than the lowest energy TSL point. The cross-sections obtained at the TRIUMF spallation neutron source are averaged over the

spectrum > 10 MeV and are shown as the dotted lines. These are in good agreement with the plateau cross-sections obtained from monoenergetic proton and quasi-monoenergetic neutron testing. Further data points at 3 MeV and 4 MeV were obtained from ASP (D-D) and IUCF facilities (3 MeV to -5 MeV) and are one to two orders of magnitude below the high energy plateau. Additional data comparing 3 MeV to 5 MeV data with spallation neutron sources are available in [21] and indicate the former to be less by factors ranging from 5 to 600.

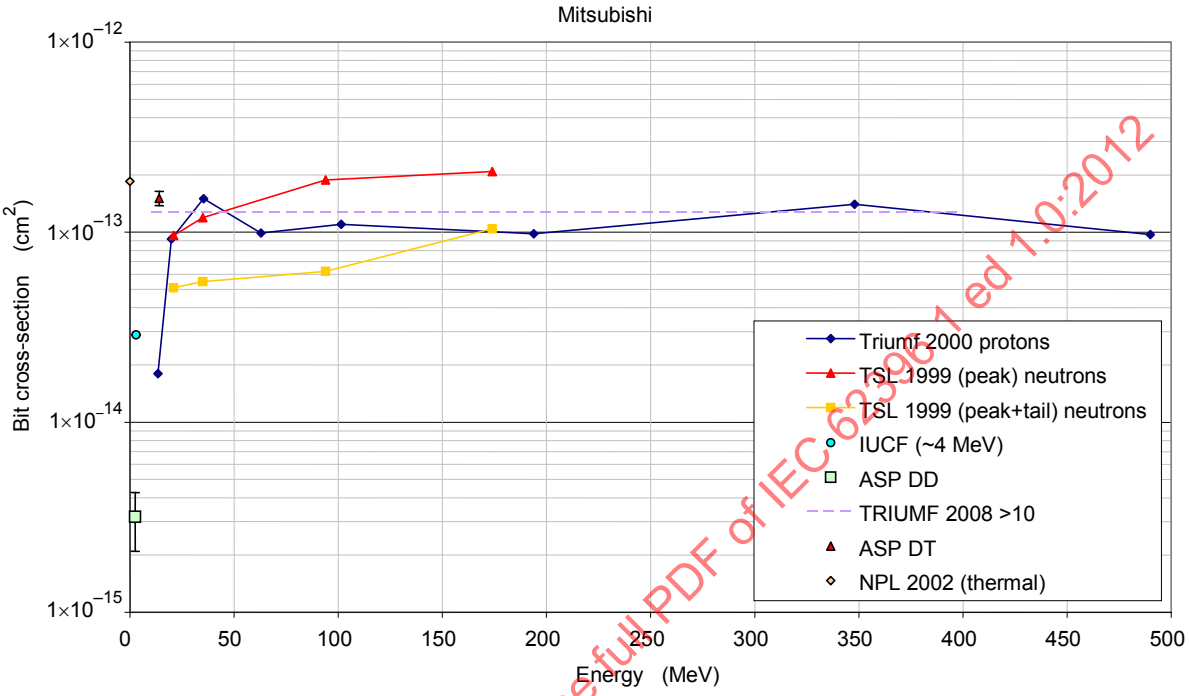

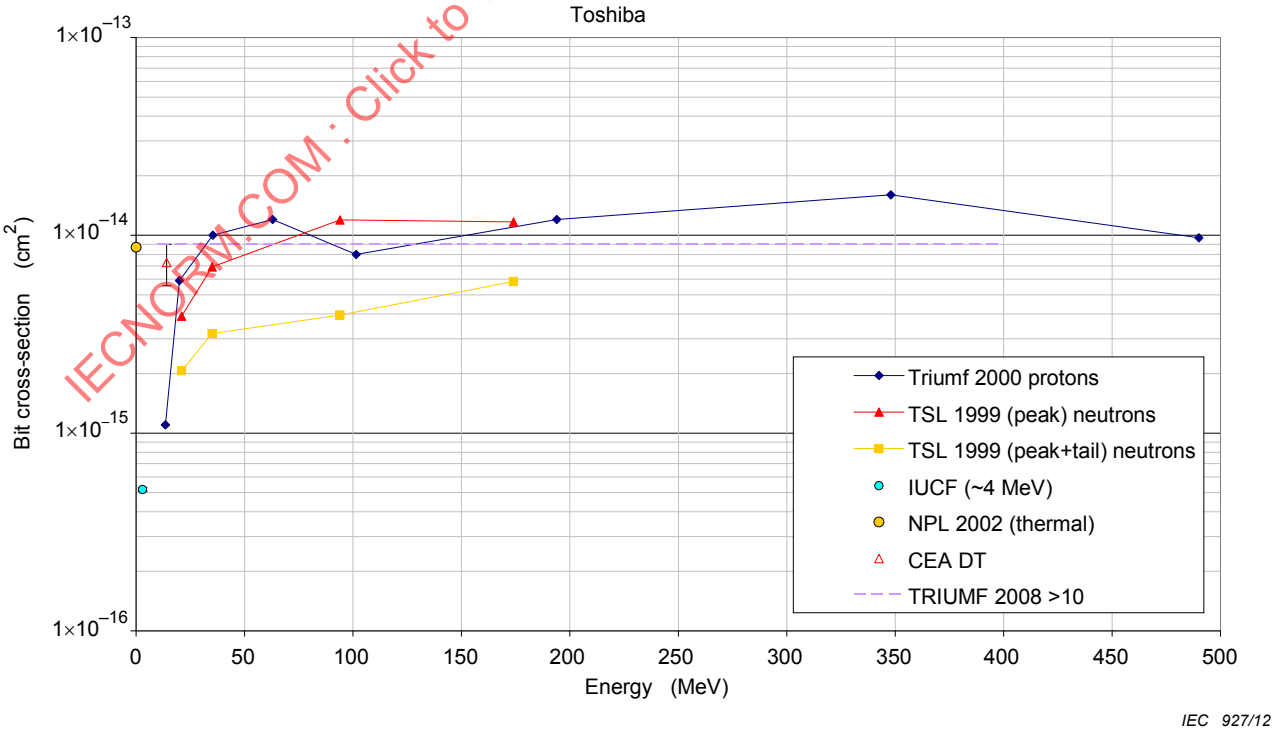

Figure 9 – Neutron and proton SEU bit cross-section data

Figure 9 also has the SEU cross-section from thermal neutrons (less than 1 eV) obtained at the NPL facility. For one device this is about a factor 1,5 to 3 higher than the SEU cross-section from high energy neutrons and for the other it is comparable. Further examples of test data on thermal neutron sensitivity are given in references [21, 22] and these show that for some devices, thermal neutrons could dominate the SEU rate in avionics while for others the contribution could be minor. Full discussion on how to deal with the thermal neutron problem is given in IEC/TS 62396-5.

8.3.4 SEU per bit cross-section trends in SRAMs

Thus, as a practical matter, even though the best SEU data is from measurements in the WNR beam, the largest source of SEU data that can be used as a substitute for the WNR SEU cross-sections are proton SEU cross-sections at energy > 100 MeV. Recognising this, tabulations were compiled in 1997 of SEU cross-sections, cm^2/bit, applicable to avionics, that were derived from WNR and proton (energy > 200 MeV) measurements for both SRAMs and DRAMs [84]. The conclusion reached in reference [84] is that based on the original data that had been compiled, the average SEU susceptibility of both SRAMs and DRAMs was decreasing over time. However, for SRAMs the SEU sensitivity per bit was decreasing slowly, while for DRAMs the SEU sensitivity was decreasing much more rapidly.

Because this compilation of SEU cross-section data as a function of the date of the device is very useful for purposes of understanding trends in the SEU susceptibility of electronics, we have updated the two curves for SRAMs and DRAMs [85, 86]. The updating was done by plotting all of the original data, and then adding data from more recent sources to expand years covered and the breadth of parts included. The SRAM data is shown in Figure 10, (Figure 11 shows corresponding data for DRAMs). However, since the SEE cross-section data changes so rapidly with changes in IC technology, as better characterized by feature size rather than device date, Annex G has been added. It contains the latest SEE response data (for feature sizes down to < 50 nm) and guidance (SEU, MCU, SEFI, SEL, SET and SEB).

Figure 10 shows a reduction in the SEU cross-section over time, but with a gradual slope. In looking at Figure 10 that includes the newer data, it is difficult to justify a continuing trend in the reduction of the SEU cross-section, i.e., for most parts it appears to be approaching an asymptotic value. Much of the data appears to be centred around a SEU cross-section of 1×10^{-13} cm^2/bit, but more broadly within a band of a factor of 3 to 0,33 of this value.

The conclusion regarding the approximate asymptotic behaviour of SRAMs over time with respect to their SEU susceptibility from atmospheric neutrons should be treated with caution. It is derived primarily from the data in Figure 10, and there is no way to determine how representative the parts used in Figure 10 are for all SRAMs that may be used in avionics. The SRAMs used in Figure 10 are those that had been tested for SEU with either the WNR beam or high-energy protons. As seen in Figure 10, a few SRAMs have even lower SEU cross-sections than the apparent asymptotic bands that can be derived, either 1×10^{-14} to 1×10^{-13} cm^2/bit or 3×10^{-14} to 3×10^{-13} cm^2/bit.

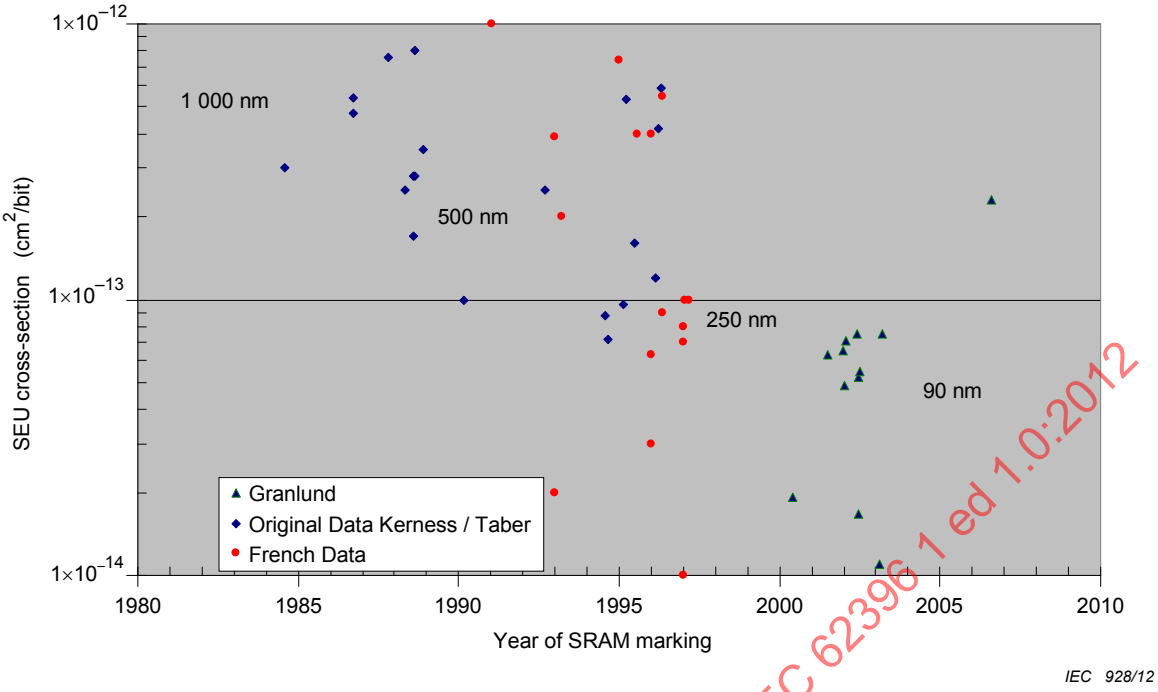

Figure 10 – SEU cross-section in SRAMs as function of manufacture date

The SRAM SEU data in Figure 10 includes SRAMs that had feature sizes of > 500 nm and others down to below 100 nm the approximate technology feature sizes have been added in nanometre. Compilations of SEU cross-sections from more recent devices, down to feature sizes of 180 nm [87, 88, 89] have shown a gradual decline in the cross-sections, with most of the cross-sections falling into the range of 1×10^{-13} to 1×10^{-14} cm^2/bit but a few, mostly those for < 200 nm, lying between 1×10^{-14} to 1×10^{-15} cm^2/bit. As the feature sizes have continued to decline, a few SRAMs have exhibited an increased sensitivity at low neutron energies, i.e., $E < 10$ MeV, compared to most previous devices. While the rule of thumb that the SEU contribution in the atmospheric neutron environment from neutrons with $1 < E < 10$ MeV is less than 10 % of the total rate [7] generally applies, for these few devices the ratio of [SEU cross-section ($E > 10$ MeV)] / [SEU cross-section (E between 3 MeV to 5 MeV)] has been ~1,0. Thus for such devices the SEU contribution from neutrons with $E < 10$ MeV will be greater than 10 % [21].

A related but different effect is being seen in SRAMs with feature sizes of < 90 nm and this relates to upsets being caused by direct ionization from low energy protons (E ~0,1 MeV) [63]. Neutrons of all energies can produce secondary protons with such low energies. Thus, SEUs from such low energy secondary protons is a new mechanism through which neutrons can cause SEUs in SRAMs [90] (see 6.2.10 for further discussion). Low energy protons are part of the environment.

8.3.5 SEU per bit cross-section trends and other SEE in DRAMs

With DRAMs the situation is different. The steep decline of the SEU cross-section with year of DRAM production seen in the original data [84] is enhanced by including more recent data. In this case, as microelectronic technologies are being modified to enable individual devices to hold an increasing larger number of bits, the net result for SEU susceptibility is a continuing decline in that susceptibility on a per bit basis. This is seen in Figure 11 which shows the original data [84] along with SEU results from more recent tests. For more detailed information and more recent data, see Annex G. The original data were based mainly on 4 Mbit and 16 Mbit DRAMs, but the more recent tests, with much reduced SEU cross-sections per bit, are based mainly on devices in the range of 64 Mbit to 256 Mbit. In addition, [8, 40] DRAMs were tested that were designed using different DRAM technologies, trench internal capacitance (TIC, utilised only by IBM and one or two other vendors) and stacked capacitance (SC, utilised by all other DRAM vendors). TIC DRAMs have a lower SEU susceptibility.

However due to the large variations between devices of differing technology and feature size, designers are recommended to seek relevant data or to test the selected device.

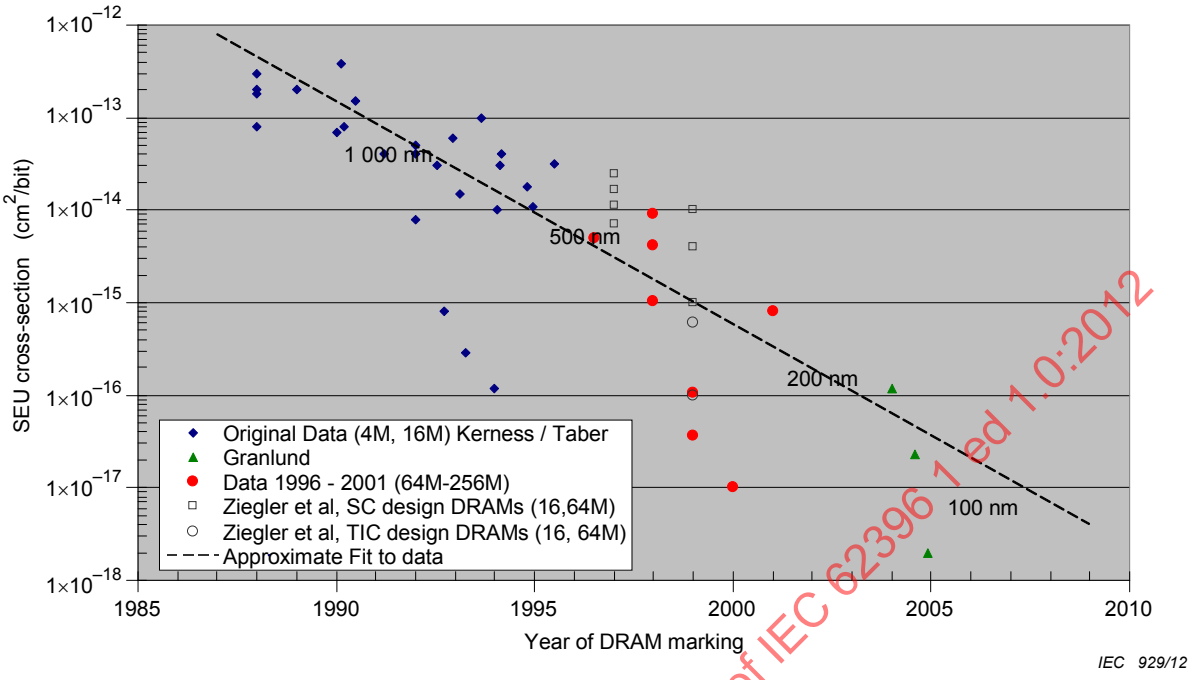

Figure 11 – SEU cross-section in DRAMs as function of manufacture date

An approximate trend line is shown in the Figure 11, together with approximate generic technology feature size. The data on DRAM was obtained from several sources, including data for SC DRAMs [86, 91, 92]. This data was modified to fit the format of the figure since the original Baumann curves were based on the size of the DRAM and not the year of manufacture. The main point to be derived from the trend line is that the SEU per bit cross-section has continued to decrease as the size of the DRAM has increased, which appears to be related to the new DRAM technology that has been developed to achieve the higher density memories.

In most applications, the occurrence of SEU in the DRAMs that constitute main memory is protected by EDAC. With EDAC additional bits are attached to each word to enable the EDAC scheme to detect a flipped bit and correct it. However, there are also other SEE effects in DRAMs that should be considered, namely their susceptibility to multiple cell upset (MCU), stuck bits (single hard errors) and single event functional interrupt (SEFI). The new larger DRAMs (Gbit size arrays) may be susceptible to all of these effects [48, 49]. Regarding MCU, two different kinds of effects are possible, standard MCU in which two or three errors are induced per neutron strike in the memory array, and a burst type of effect in which thousands of errors are induced due to a neutron strike in the logic portion of the DRAM (see 6.2.3). The susceptibility of new DRAMs to burst errors varies significantly with DRAM vendor and so this effect needs to be considered for future developments in usage of DRAM designs. Thus, these effects should be considered for future developments in DRAM designs.

Probably the major effect is MCU, which had been about 1 % to 3 % of the SEU rate for older devices, but for more recent devices with feature sizes below 180 nm MCUs increase and, burst errors affecting > 1 000 bits may be important (see 6.2.3). However, the MCU fraction relative to the SEU rate can vary significantly from one DRAM to the next, and the impact that a MCU in a DRAM has on the operation of a board can also vary significantly due to the distribution of the bits per word in the DRAM. The method by which bits per word are physically distributed within the DRAM varies among the DRAM vendors. Stuck bits can be a concern because once such bits are stuck, the SECDED EDAC technique protecting words containing these bits no longer works for those words. The MCU fraction variation can be much higher and there is value in laser screening to give physical location of bits and relative

sensitivity to MCU. If there is physical separation between the bits per word then this reduces the susceptibility to MBU in a given word.

8.4 Calculating SEE rates in avionics

Based on the SEE data shown and discussed in Clause 8, it is clear that SEEs can be induced in electronics used in avionics. Clause 8 discussed a variety of SEE tests that have been carried out in the laboratory, using both neutron and proton beams, during which SEE cross-sections in microelectronics have been measured. In addition, a limited amount of data has been published of actual SEE rates recorded during flight [5, 8, 39, 40, 41]. The objective is to establish a methodology for obtaining the SEE rate in the microelectronics used in the avionics due to the atmospheric neutrons, and to addressing the impact of the SEE on the actual avionics.

The simplified method of calculating the SEE rate for a particular effect as defined in this standard is to multiply the SEE cross-section for that effect (units of cm^2) by the integrated neutron flux of 6 000 n/cm^2 (energy > 10 MeV). This 6 000 n/cm^2 flux is a nominal value for 40 000 feet (12,2 km) altitude and 45° latitude, and may be adjusted for different altitudes and latitudes (see Annex D), and the enhancement from a solar flare, as discussed in 5.6. Using the environment described above the SEE rate may be calculated from:

$$\text{SEE rate per device-hour} = 6\,000\ (n/cm^2 \cdot h^{-1}) \times \text{SEE cross-section}\ (cm^2 \text{ per device}) \quad (4)$$

The greater than 10 MeV neutrons will be the dominant cause of SEE on sensitive devices with geometric feature size above 150 nm, however for devices with feature size at and below 150 nm the contribution of neutrons with energy between 1 MeV and 10 MeV may be significant. Although, for such devices, based on [7] the contribution from the $1 < E < 10$ MeV neutrons to the overall SEE rate is 10 %. Therefore when calculating the SEE contribution from parts having geometric feature size 150 nm and below to 90 nm the SEE rate from $E > 1$ MeV shall be calculated as 1,1 SEE rate $E > 10$ MeV. This neutron conversion factor has been derived using geometries between 150 nm and 90 nm and needs to be kept under review as further low energy neutron test data on small feature size devices (below 150 nm) become available. A greater than 1 MeV nominal neutron flux of 9 200 n/cm^2 per hour at 40 000 feet (12,2 km) and 45° latitude shall be used. This value can be scaled to other altitudes and latitudes (see Tables D.1 and D.2).

The other method of calculating the SEE rate is by integrating the SEE cross-section as a function of energy (e.g. as in Figure 8) with the neutron spectrum (as in Figure 1) over all E. However, in the vast majority of cases the measured spallation neutron, e.g., WNR SEE cross-section is available for devices but the cross-section as a function of energy is not. In comparing calculated SEU rates in six SRAMs (0,5 μm < feature size < 0,35 μm) based on the integration method using the QARM neutron spectrum [15], the rates from the simplified method of this standard are in good agreement with the integration method rates, but higher by about 50 %, but may not be applicable for smaller geometries.

The multiple cell upset (MCU) rate should be calculated for the EDAC protected memory that had been identified earlier, and had been deleted from consideration for the SEU rate. Because the MCU/SEU fraction has been changing so rapidly with decreasing feature size and RAM type, as described in 6.2.3, the MCU rate should be calculated only after considering the guidance provided in 6.2.3. On a simplified level, this MCU rate in the protected memory is assumed to evade the EDAC scheme and lead to an error that can affect the LRU.

A four level hierarchical procedure is proposed for answering these questions regarding SEE rates and the impact of the SEE rates on the avionics, proceeding from a rigorous assessment to a conservative upper bound assessment. The primary levels involve testing of specific microelectronics devices or boards, whereas the lowest level involves utilising existing SEE cross-section data to the extent possible, and applying it in a conservative

manner, which therefore entails the highest level of risk. The methods are detailed in B.1 to B.6.

8.5 Calculation of availability of full redundancy

8.5.1 General

Most modern avionics equipment utilizes state-of-the-art electronic components that have submicron feature size integrated circuits within the design. Such components may be SEE sensitive due to the avionics atmospheric radiation. The result of such SEE is to generate errors or faults within the equipment that could have an impact on the functionality of the equipment. Mitigation features can be incorporated as necessary in order to satisfy the avionics system requirements for the higher design categories A to C (see Clause 7). The equipment may contain some method of detecting the error or fault and utilise some level of redundancy to avoid any impact on the function. However, the affected element will not recover until some form of correction is applied for the original SEE; during this time, the time to recover the full redundancy is not available [93]. The correction can be made by a regular process like "scrubbing" (memory refresh from uncorrupted data at fixed intervals) or rely on correction when an error or fault is discovered. As an example, consider the availability, A, of a block of memory. If the mean time to recover is t_{rec}, the mean rate of recovery $\mu = 1/t_{rec}$, and if the mean time between SEE error generation is t_{SEE}, the mean SEE rate $\lambda = 1/t_{SEE}$. The availability of full redundancy is then given by the equation:

$$A = \mu / (\lambda + \mu) \quad (5)$$

When the recovery rate is very much higher than the SEE rate the availability tends towards 1, i.e. full availability. System availability is considered for three different types of SEE event:

a) Transient errors and upset (e.g. SEU, MCU) with correction applied quickly after the event or as the data is required.

b) Firm errors and faults (e.g. SEFI, non-destructive latch), which persist until the power to the device is cycled. If there is no facility during normal equipment operation for power cycling, the condition will persist until the end of the operational period.

c) Hard faults (e.g. stuck bits and destructive latch up) which are permanent and require maintenance activity on the unit. These events are considered in the same manner any other component failure see Clause 7.

The first two of these SEE types do not require maintenance activity since they recover for the next operational use without any external intervention. Examples of full redundancy availability for the first two types of SEE event are given below.

8.5.2 SEU with mitigation and SET

Consider SEU in SRAM, with applied mitigation such as EDAC, ECC or multiple strings (redundancy) along with voting. In such cases, the recovery time for ECC or redundancy with voting can be very fast; if 1 ms is assumed, then the recovery rate is 1/1 000 = 1 000 s^{-1}, which is 3,6 million per hour. For SRAM with 5Mbits of used locations, and with SEU cross-section between 10^{-13} cm^2/bit and 10^{-14} cm^2/bit (see Figure 10), the corresponding SEU rates vary from 3×10^{-3} to 3×10^{-4} upset/dev-hr. In this example, the recovery rate is orders of magnitude larger than the SEU rate, and therefore the availability is very close to 1. There would be no significant impact on the equipment availability, but could be significantly impacted if the memory were very large and the scrubbing operation not carried out at a sufficiently low periodicity.

Single event transients (SET) can persist for up to 10 μs, after which the device recovers to normal operation. For a typical recovery time of 10 μsec, the recovery rate would be $1/10^{-5}$ = 100 000 s^{-1} or 3 600 million h^{-1}. The SET rate during flight for a comparator or a pulse width modulator ranges from 10^{-7} to 2×10^{-5} event/device-h (see 8.2.2). In this example, the

recovery rate is again orders of magnitude greater than the SET rate and the availability is very close to 1.

8.5.3 Firm errors and faults

Consider SEFI, where device functionality is recovered by cycling power or rebooting. If the avionics equipment is not able to cycle power or reboot automatically, the fault will persist for the remaining flight duration (10 h or more) and full redundancy will be unavailable for this period. For triple modular redundant systems, the recovery time from the first event is immediate, but the occurrence of another event during the recovery time will cause that element of the system to fail. For a typical SDRAM device (in READ mode, taken from [43] with a SEFI cross-section of 3×10^{-11} cm^2/device, the SEFI rate will be 2×10^{-7} event/device·h, and again the recovery rate would be orders of magnitude greater than the SEFI rate, and the availability near 1.

As indicated in the Figure 7, events such as SEFI may impact the MTBUR and MTBF if they are identified as failures by any built-in test system.

9 Considerations for SEE compliance

9.1 Compliance

The following steps are a means to compliance and should be documented; however alternative methods may be used where such methods can be justified.

9.2 Confirm the radiation environment for the avionics application

General guidance is given in 5.3. The degree of solar flare enhancement accommodation should be defined by the user (see 5.6).

9.3 Identify system development assurance level

The development assurance level will determine the rigour and discipline associated with the SEE accommodation (see Clause 7).

9.4 Assess preliminary electronic equipment design for SEE

9.4.1 Identify SEE-sensitive electronic components

As part of the equipment manufacturer Electronic Component Management Plan (ECMP), there is a requirement for the equipment to be able to function in the application avionics environment – see 4.2.6 of IEC/TS 62239:2008. Guidance for the identification of SEE-sensitive electronic components is given in Clauses 6 and 8 of this standard.

9.4.2 Quantify SEE rates

Quantify SEE rates based on the rigour required by 7.4 and the calculation approach defined in 8.4.

9.5 Verify that the system development assurance level requirements are met for SEE

9.5.1 Combine SEE rates for entire system

The accumulation of SEE-induced hard faults may impact on the MTBF of the system. Unaccommodated soft faults may impact the MTBUR and also the MTBF. The soft SEE-induced faults may be accommodated by hardware and/or software measures refer to Clause 7.

Whilst the equipment recovers from radiation induced soft errors some redundancy elements are not available, and the recovery time shall be demonstrated acceptable at system level.

9.5.2 Management of parts control and dependability

Refer to 4.5 of IEC/TS 62239:2008, and to 8.4 of the present standard. Changes by the semiconductor vendor to electronic components may affect their SEE rates.

9.6 Corrective actions

Take corrective actions if necessary.

Annex A
(informative)

Thermal neutron assessment

It is important to assess the contribution that thermal neutrons make to the overall SEU rate. The thermal neutrons can play a major role for two main reasons:

a) it appears that the thermal neutron flux inside an airliner is 1 to 2 times the high energy (> 10 MeV) neutron flux; and

b) for many devices the SEU cross-section due to thermal neutrons is higher (by a factor of 1,5 to 3) than the SEU cross-section due to > 10 MeV neutrons.

There are confounding issues that make this assessment difficult and uncertain for both of the factors. Regarding the thermal neutron flux, it varies significantly within a commercial airliner, due to the proximity of hydrogenous materials which produce them, but the magnitude of the variation has yet to be quantified through rigorous measurements. The high energy (> 10 MeV) neutron flux within the aircraft is essentially the same as the flux in the atmosphere right outside the aircraft structure. This is not true for the thermal neutrons. The thermal neutron flux within the aircraft is approximately 10 times higher than it is outside the aircraft because as the atmospheric high energy neutrons interact with the materials of the aircraft, the flux of thermal neutrons builds up inside the aircraft. Anecdotal information regarding measurements in a stripped down military 707 indicates variations of up to a factor of 3 in a thermal neutron detector as it was moved inside the aircraft, but this aircraft contained far less hydrogenous material compared to modern airliners. Based on the one detailed calculation that has been carried out for a crudely modelled 747, it can be estimated that within an aircraft, the thermal neutron flux may be a factor of 1 to 2 times the high energy neutron flux. By comparison, within the atmosphere, the thermal neutron flux may be a factor of 0,15 to 0,25 times the high energy neutron flux.

Regarding thermal neutron SEU cross-sections, from the limited number of devices in which this has been measured [47, 81, 82], most have a thermal neutron SEU cross-section comparable or larger than the high energy SEU cross-section, but a few devices are not susceptible to SEU from thermal neutrons. These latter devices should not contain any BPSG, the major source of boron-10 which leads to the SEU by the thermal neutrons. However, these devices do contain boron in lower concentrations through other constituents in the die (for example p dopant). Thus in older parts without BPSG, the thermal neutron SEU cross-section from these other boron sources would be reduced by 2 to 3 orders compared to that in BPSG and hence can be ignored, but in more recent SRAMs [18, 108] without BPSG, the SEU contribution from thermal neutrons is somewhat reduced compared to BPSG, but may not be ignored. At present, it appears that SRAMs are the only devices which have been tested with thermal neutrons and found to have a thermal neutron SEU cross-section. However it is very likely that other devices such as DRAMS, microprocessors and FPGAs are also susceptible to SEU from thermal neutrons, but that has not yet been verified by measurements.

In the SRAMs in which thermal neutron SEU has been measured, for most devices, the ratio of the thermal neutron SEU cross-section to the high energy SEU cross-section is > 1, generally in the range of 1,5 to 3. However, for devices from some vendors there is notable part-to-part variation in the ratio, which is generally higher than the part-to-part variation of the individual SEU cross-sections. For the highest ratio measured to date, the thermal neutron SEU cross-section to high energy SEU cross-section ratio is approximately 7. Thus when combined with the fact that the thermal neutron flux in an airliner may be 1 to 2 times higher than the high energy neutron flux, the SEU rate due to thermal neutrons could be as high as a factor of 10 or more greater than the SEU rate due to high energy neutrons. This appears to be a bounding value, but is nevertheless important since the remainder of this international standard is devoted to SEU from the high energy neutrons. The effects of thermal neutrons on electronics are covered in more detail in IEC/TS 62396-5.

Annex B
(informative)

Methods of calculating SEE rates in avionics electronics

B.1 Proposed in-the-loop system test – Irradiating avionics LRU in neutron/proton beam, with output fed into aircraft simulation computer

This is the highest level of testing and is expected to give the most accurate answer and lowest risk for how the SEEs induced by the atmospheric neutrons will affect actual avionics. It involves an in-the-loop test in which an avionics LRU is exposed to a beam of high energy neutrons or protons, and the signals from the LRU are interfaced into a host computer containing a simulation of the aerodynamic responses for the aircraft of interest. No such test system exists today, however an experimental "proof of principle" is being proposed that would utilise the WNR neutron beam and the expertise of the Systems and Airframe Failure Emulation Testing and Integration (SAFETI) Laboratory at NASA-LaRC. At the present time this should be viewed as a future and unique testing capability involving the combining of specialised facilities at two laboratories.

At the present time, one hour in the WNR beam (2002 calibration) is equivalent to approximately 1×10^6 h at 40 000 feet (12,2 km). With this normalisation factor, the number of upsets that affect the avionics system in one hour of exposure in the WNR beam can be adjusted to obtain the rate at aircraft altitudes.

Alternatively, the typical high energy neutron flux being suggested for use in avionics single event effects evaluations (see 5.3) is the integrated neutron flux of 6 000 n/cm^2 per hour (energy > 10 MeV). Thus, for a lifetime of 100 000 flight hours, the lifetime fluence is 6×10^8 n/cm^2. The contribution to the SEE rate by neutrons of energies < 10 MeV is small enough, as seen in Figure 8, that it can be neglected. This does not, however, consider SEU induced by thermal neutrons.

B.2 Irradiating avionics LRU in neutron/proton beam

This approach also involves radiation testing of an avionics LRU, but in this case, the operability of the LRU is the basis for how the neutron-induced SEE effects are manifested. The output of the LRU is not fed into a simulation computer. This test is similar to those that have been conducted for space applications, in which an LRU was exposed to a beam of high-energy protons. If the proton or neutron beam is not large enough to encompass the whole LRU then a number of different exposures will be required.

NASA-JSC has used this kind of testing to identify parts that are prone to proton (or neutron) induced single event latch-up; these parts have generally been deleted from consideration, irrespective of the SEL rate. The tests have also involved many SEUs in a variety of devices; in all cases the effects of the SEU have propagated in such a way that the LRU indicates that normal operation has been interrupted. Thus, this is a dynamic type of testing, in which the original SEU in one device may propagate to an error in another device which causes the LRU to malfunction and reboot. Compared to the B.1 testing approach, this methodology requires the test/analysis team to project how the non-normal operation of the LRU will impact the avionics system. The architecture of the avionics subsystem may have built-in fault tolerance measures, such as various types of redundancy, which could over-ride an unexpected or erroneous signal from the LRU due to a SEU or other cause. However, without rigorous testing of the entire system, or a specified procedure for how the fault tolerance is to be implemented, it will generally be necessary to be conservative and assume that the SEE rate in the LRU will be directly propagated to the avionics system.

If this kind of testing is carried out, it will be advantageous to expose the LRU to fluences much greater than the expected lifetime fluence for avionics (100 000 flight hours) of 6×10^8 n/cm^2. As an example, if a LRU were exposed to a proton fluence of 1×10^{10} p/cm^2 and 5 events were recorded in which the LRU malfunctioned, the LRU upset cross-section would be 5×10^{-10} cm^2 (5 events/1 $\times 10^{10}$ p/cm^2). For avionics purposes, the LRU rate per hour would be 5×10^{-10} cm^2 $\times$ 6 000 n/cm^2 or 3×10^{-6} event/LRU per hour.

B.3 Utilising existing SEE data for specific parts on LRU

B.3.1 Neutron proton data

This approach is much simpler than B.2 because it attempts to rely on existing neutron or proton SEE data for the few main parts on the LRU that will be susceptible to SEE. An extension of this approach could be to carry out SEE testing of individual parts utilising a neutron or proton beam. In both cases, this approach relies on the static SEE response of a device to neutrons or protons, and ignores dynamic effects in the LRU, such as propagated errors.

The disadvantage of this approach is that the number of parts which have been tested for SEE response to high energy protons or neutrons in all of the databases is relatively small. A list of some of the more useful sources of such proton/neutron SEE data is given in Table B.1, and it includes both web sites and journal compilations. In addition, commercially available parts are continuously changing, so by the time that some of the data is incorporated into a database, the part may no longer be available, or a next generation part has replaced it.

As seen in Figure 8, proton SEE data at high energies, i.e., energy > 100 MeV, may be used to represent the SEE response due to the atmospheric neutron spectrum. Further, based on more recent testing [21, 52], SEU and SEFI cross-sections obtained from testing with monoenergetic proton beams (> 100 MeV) in SRAMs, FPGAs and microprocessors are expected to result in SEU/SEFI cross-sections that are within less than a factor of 2 of those that would be obtained from testing with the WNR neutron beam. However, in testing for SEL, only high energy beams ($E \geq 100$ MeV) of either neutrons or monoenergetic protons should be used to obtain SEL cross-sections expected to be within a factor of 2 of those that would be obtained from the WNR neutron beam (for $E_{\text{proton}} > 200$ MeV, the SEL cross-section may be conservatively higher, [21]). Further, for other SEE effects in other kinds of devices, only high energy beams ($E \geq 100$ MeV) of either neutrons or monoenergetic protons should be used in place of a spallation neutron source to obtain the relevant SEE cross-sections.

Table B.1 – Sources of high energy proton or neutron SEU cross-section data

Organisation	Publications	Internet site
NASA – Goddard Space Flight Center (Rad Effects & Analysis Section)	Yearly publication of SEE results (w/ protons and heavy ions) in IEEE Radiation Effects Data Workshop	Http://radhome.gsfc.nasa.gov/radhome/parts.htm
NASA – Jet Propulsion Laboratory (JPL)	Biannual publication of SEE results in (w/ protons and heavy ions) in IEEE Radiation Effects Data Workshop	Http://radnet.jpl.nasa.gov/SEE.htm Http://radnet.jpl.nasa.gov/Compendia/P/ProtonSeeCompendium.htm
European Space Agency	"Proton SEE Results – A Summary of ESA's Ground Test Data", R. Harboe-Sorensen, 1997 RADECS Conference Data Workshop, p. 89.	Http://www.escies.org/public/radiation/database.html

B.3.2 Heavy ion data

A less accurate approach is to utilise the available SEE cross-sections on parts that were exposed to heavy ions, and transform this data into proton/neutron SEE cross-sections. This

is not straightforward and should only be carried out by engineers and scientists who are experienced in utilising this kind of single event effects data. A number of models have been developed that allow for this heavy ion SEU data to be used to calculate the corresponding proton SEU cross-sections or rates. However, care should be taken in correctly utilising the data and employing the models, since there are ample opportunities for the heavy ion SEE data to be erroneously applied. References to some of these models are included in Table B.2. Almost all of this SEE data (heavy ion or proton) are for parts that were or are being considered for use in space applications; very little are for parts specifically being targeted for aircraft avionics.

Table B.2 – Some models for the use of heavy ion SEE data to calculate proton SEE data

Model	Author	Reference
PROFIT	P. Calvel	"An Empirical Model for Predicting Proton Induced Upset," IEEE Trans. Nucl. Sci, 43, 2827, 1996
FOM (Figure of Merit)	E. L. Petersen	"The SEU Figure of Merit and Proton Upset Rate Calculations," IEEE Trans. Nucl. Sci., 45, 2550, 1998; also J. Barak *et al.*, "On the Figure of Merit Model …," IEEE Trans. Nucl. Sci., 46, 1504, 1999
	J. M. Palau	"A New Approach for the Prediction of the Neutron-Induced SEU Rate," IEEE Trans. Nucl. Sci., 45, 2915, 1998
	L. D. Edmonds	"Proton SEU Cross-sections Derived from Heavy-Ion Test Data," IEEE Trans. Nucl. Sci., 47, 1713, 2000
	J. Barak	"A Simple Model for Calculating Proton Induced SEU," IEEE Trans. Nucl. Sci., 43, 979, 1996; also "A Akkerman *et al.*, "A Practical Model for Calculation of the Proton Induced SEU …," Proceedings 1991 RADECS, p. 509
BGR	E. Normand	"Extensions of the Burst Generation Rate Method for Wider Application to Proton/Neutron-Induced Single Event Effects," IEEE Trans. Nucl. Sci., 45, 2904, 1998
SEUSIM	C. Inguimbert	"Proton Upset Rate Simulation by a Monte Carlo Method: the Importance of Elastic Scattering Mechanism," IEEE Trans. Nucl. Sci., 44, 2243, 1997
IMDC	C.S.Dyer	"Microdosimetry Code Simulation of Charge-Deposition Spectra, Single Event Upsets and Multiple-Bit Upsets," IEEE Trans Nucl. Sci., 46, 1486, 1999
CUPID	P. McNulty	"Proton Induced Spallation Reactions," Radiat. Phys. Chem., 43, 139, 1994

In general, proton/neutron SEE response data needs to be found for just a few of the devices on an LRU, those part types that are judged to be susceptible to SEE. This consists primarily of RAMs, microprocessors and FPGAs, devices that contain a large number of bits, which can upset. However, only those bits that are used are susceptible to SEUs that can be recognised as errors, and often only a fraction of all of the bits on a device are utilised in the way it operates on the LRU. Therefore, without specific knowledge of the fraction of bits that are actually used in a device on the LRU, the conservative approach is to assume that 1) all of the bits are used and therefore susceptible to SEU, and 2) all of these SEUs will cause the LRU to malfunction.

Any memory that is protected by EDAC should be deleted from consideration for single event upset, because these upsets are corrected by the EDAC. The combined neutron SEU cross-section for the LRU is obtained by adding the SEU cross-sections for each of the LRU parts types that were identified (RAMs, microprocessors and FPGAs), multiplied by the number of each part type on the board.

B.4 Applying generic SEE data to all parts on LRU

In this case the LRU has a number of parts that are likely to be susceptible to SEE by the atmospheric neutrons, but there is no SEE data available for one or more of these parts. Calculating the SEU rate for such parts by this approach has the least technical basis in terms of specific data and therefore has to be, of necessity, the most conservative. Like the approach in B.3, it evaluates only the static SEE response of a device to neutrons or protons, and ignores dynamic effects in the LRU, such as propagated errors.

Overall, the procedure is quite similar to the approach in B.3. Susceptible devices are divided into two categories, DRAMs, and all others (SRAMs, microprocessors and FPGAs). For a DRAM with no available proton or neutron SEU cross-section data, we look at Figure 11 to obtain the per bit SEU cross-section. The figure clearly shows that there are large differences in the per bit SEU cross-section, but this is strongly influenced by the size of the DRAM. As indicated, most DRAMs in LRUs are protected by EDAC, but this has to be verified for each LRU. Even if the DRAM is protected by EDAC so that the SEU rate can be deleted as a matter for concern, the MBU and MCU rates need to be calculated, and the MCU rate is conservatively taken to be 3 % of the SEU rate at feature sizes 350 nm and above.

For all of the other devices, the per bit SEU cross-section will be based on the data for SRAMs shown in Figure 10. The number of bits in all of the SRAMs, microprocessors and FPGAs needs to be added together. From Figure 10, we choose a conservative SEU cross-section of 5×10^{-13} cm^2/bit, and with the integral flux of 6×10^3 n/cm^2 per hour, a SEU rate of 3×10^{-9} upset/bit-hour. This rate is multiplied by the total number of bits in all of the devices to obtain the SEU rate for the LRU due to SEUs in all of the devices except DRAMs. If, for example, there were a total of 10 Mega bits on the LRU, the SEU rate would be 3×10^{-2} upset/LRU-hour, or one upset every 30 hours. In looking at Figure 10 we see that this is clearly a conservative approach, SEU cross-sections at least an order of magnitude lower are available, but this approach is being used because no SEE data is available for the specific parts on the LRU. Thus a trade-off could be made between a high SEU rate for the LRU with no specific SEU data, resulting in a high error rate for the LRU, or efforts to more accurately quantify the SEU response of the devices on the LRU by testing or analysis of relevant parts data. This approach also ignores the architecture of the avionics subsystem and any built in fault tolerance measures it may have that would over-ride unexpected or erroneous signals from the LRU due to a SEU or other cause.

B.5 Component level laser simulation of single event effects

It is feasible to use focussed picosecond-pulsed laser facilities to measure microchip SEU cross-sections (as a function of LET) by delivering large arrays of laser pulses at a range of pulse energies [94]. Methodologies and codes have also been devised for converting LET cross-section curves to neutron SEU upset rates [95]. However, these methodologies further require an estimate of the sensitive volume of the microchip cells. For crude calculations, the sensitive volume may be estimated; but it has also recently been shown that it is possible to use a laser facility directly to measure the sensitive volume by testing microchips at a range of different wavelengths [96]. It should be noted that the empirical techniques reported in references [94, 96] were demonstrated using three commercial 4 Mbit SRAM types.

These methodologies provide a basis for employing laser facilities to measure the neutron and proton SEU sensitivity of devices. The use of such facilities potentially circumvents the apparent high costs and occasional long lead times, which can arise from the use of neutron and proton beam facilities to assess components. Laser simulation is suitable not only for initial test of SEU sensitive components but also the ongoing monitoring of the effects on SEU of proposed die changes to such components as notified by PCN, product change notifications (see IEC/TS 62239).

Laser systems are potentially effective for identifying excessively susceptible and selecting relatively insensitive device types, where a range of equivalent parts from alternative manufacturers is under consideration for inclusion in an avionics system. Nevertheless, laser assessment is not a fully mature technology and will normally be less accurate and reliable than neutron beam testing, so the latter should be preferred where relatively precise results are justified by the cost-benefit analysis. Furthermore laser testing is indirect, in that it relies on integrating the results of several assessment steps. However as more experience is accumulated the relative accuracy and efficiency of laser testing would be expected to improve.

Parts need to be delidded for laser testing (also necessary for ion beam testing, but not for neutron or proton beam testing). The laser technique may therefore be relatively more beneficial in cases where the bare die within the component is readily accessible.

Laser beams are also effective to characterize the sensitivity of power devices like power MOSFET or IGBT to Single-Event Burnout. Even if cross-correlation between laser and proton or neutron data remains limited, laser testing has been demonstrated as efficient to determine the safe operating area (SOA) of a power device [97]. This additional input could be very useful for designers to select the most appropriate device for dedicated applications and establish with the full knowledge of the SOA the adequate mitigations technique notably on the voltage de-rating.

It should also be noted that the availability of cross-correlation data between laser and neutron testing is currently very limited. The laser simulation testing for a component may be calibrated using the cross-correlation data results (neutron/proton test to laser simulation) of components from the same functional type (for example SRAM) having similar semiconductor technology and feature size. However, some studies have shown distinct differences in the SEU response among parts of the same functional type [47], and in how poorly proton and heavy ion SEU data sometimes correlate [78]. Therefore the user should be very cautious when applying this laser simulation method for obtaining the high energy neutron SEU response of devices.

B.6 Determination of SEU rate from service monitoring

This procedure can provide a measure of the SEU rate of monitored electronics in operational service for these systems where error detection and correction (EDAC) or another kind of error checking scheme is used to identify erroneous bits which are then recorded. The errors should be stored in non-volatile memory (similar to fault code store) and can subsequently be used to identify the errors that have occurred due to SEU from the atmospheric neutrons. This can generally be done by obtaining a bit error rate from the service monitoring, and assuring by comparison with rates that can be calculated from 8.3 and 8.4, that it is consistent with a SEU bit error rate from the atmospheric neutrons.

There are several issues that should be addressed when considering this method.

a) The system will record that an error has taken place. The recorder/monitor will only be effective if it reliably identifies and stores error data.

b) The extent of the system that is monitored and recorded for errors should be clearly identified and some elements of the system will not be addressed by the monitor. Those participating in the post-removal analysis should understand how other effects not related to the atmospheric neutrons (power transients, vibration transients, software problems, etc.) may contribute to the errors.

c) The information obtained will always be historical, i.e. the system will be in operation.

d) Where the errors are corrected (not a hard fault) the errors will be recorded in the errors non-volatile memory area but how this is enunciated to the aircraft system should be determined on a case by case basis and any action as a result. The data may be regularly recorded and cleared during scheduled maintenance, or as the memory fills.

e) The recovery of the data from such store memories during maintenance requires the co-operation of the fleet operators and equipment manufacturer customer support facilities.

f) The procedure for processing of such data should be clearly defined. This should be done by a person experienced in analysing SEU data. Since the bit upset rate is so important in verifying that the errors are indeed due to the atmospheric neutrons, the number of bits potentially susceptible to SEU by the neutrons in the particular system being monitored should be known or reliably estimated. An understanding of the normal SEU rates may indicate potential response during periods of high SEP activity.

g) The coverage of the store and the route to data and analysis of results for SEU should be auditable by customer and third party (including atmospheric radiation experts).

h) It would be extremely helpful if additional information would be recorded that is related to the location and altitude when a SEU takes place this will assist correlation of the SEU data. Following a SEU the altitude and location data would need to be requested from the flight control computer.

Annex C
(informative)

Review of test facility availability

Note: This list of test facilities is given for the convenience of the users of this standard and does not constitute an endorsement by the IEC.

C.1 Facilities in USA and Canada

C.1.1 Neutron facilities

Facility	Description	Availability/Cost
Los Alamos Neutron Science Center – LANSCE (alt. WNR (Weapons Neutron Research) facility or ICE (Irradiation of Chip and Electronics) House, Located in Los Alamos, NM	Facility with neutron beam having energy spectrum (neutrons with energies up to 700 MeV) providing most accurate simulation of the atmospheric neutrons. Eight beam lines, with 30 Left the beam line used for SEE testing (the ICE House). Facility upgraded in 2003, making it very convenient to use for SEE tests. Since 2000, 1 h in beam is equivalent to ~1 × 10^6 h at 39 000 feet (11 860 m). The neutron spectrum is recorded accurately each run using a fission ionization chamber. LANL staff provide fluence for each run (E>E_{thresh}, with E_{thresh} specified by user; per this international standard E_{thresh} should be 10 MeV). Spot size typically 2,5 cm to 8 cm diameter with other options possible.	Cost ~$ 8 250/day. Facility is open for ~8 months/year. Numerous users want to use this beam, so LANSCE personnel schedule outside users for one session/year. See "The Los Alamos National Laboratory Spallation Neutron Sources," P. Lisowski *et al.*, Nucl. Sci. Eng. v. 106, p. 208, 1990 and http://wnr.lanl.gov. Facility contact: Steve Wender wender@lanl.gov, 505-667-1344)
TRIUMF Neutron Facility (TNF) of the Tri-University Meson Facility (TRIUMF) located on University of British Columbia (Vancouver, Canada) campus	Facility has neutron flux with similar spectrum to that of atmospheric neutron (highest energy ~400 MeV). Unique facility because beam also contains thermal neutron component (approximately 30 % of the >10 MeV neutron flux). For >10 MeV neutron flux is ~1E6 times the atmospheric neutron flux at 39 000 feet. Neutron SEU cross-sections due to >10 MeV and thermal neutrons can be determined from two successive SEE tests (with and without cadmium plate over the IC). Not too convenient to use since test card has to be lowered 5 m down a channel on a mounting plate connected to a pulley system. Fluxes are determined for each run based on neutron monitor that has been calibrated against activation foil measurements and calculations with FLUKA code In 2005, a "flood" beam of neutrons, beam size 50 cm to 100 cm in diameter at the test point has been developed at the proton test facility. Neutrons are produced by stopping either 115 MeV or 500 MeV protons in a lead target. The >10 MeV neutron flux is variable from 1 000 n/cm^2/s to 50 000 n/cm^2/s and is designed for testing large electronic systems.	The TNF cost is $ 150/h. This facility is available about 8 months per year and is presently scheduled about 30 % of the time. The flood beam cost is $ 450/hr, the same as for the monoenergetic proton testing, and is heavily utilized. Contact Ewart Blackmore ewb@triumf.ca to schedule. See "Improved Capabilities for Proton and Neutron Irradiations at TRIUMF," E. Blackmore et al, Workshop Record, 2003 IEEE Radiation Effects Data Workshop, p. 149 and http://www.triumf.ca/pif
Boeing Radiation Effects Laboratory (BREL), Seattle, WA	This is a 14 MeV neutron generator, capable of producing fluxes as high as 1 × 10^8 to 5 × 10^8 n/cm^2·s at close proximity (3 cm to 6 cm) to the generator head, emitted in 4 π geometry. It was upgraded with a new source and control electronics in 2009. For recent SRAMs (> 2 000) testing has shown that the SEU cross-section from 14 MeV neutrons is very close to that from the high energy neutrons. Fluence is determined using an electronic neutron dosimeter. After an exposure, a 20 minute cool-down time is required to re-enter the neutron chamber.	Cost is approximately $ 600/h of beam time; availability is ~10 months per year (contact D. Russell at dennis.a.russell@boeing.com); See http://www.boeing.com/assocproducts/radiationlab/equip/neutron.htm

Facility	Description	Availability/Cost
NCNR (NIST Center for Neutron Research), National Institute of Standards and Technology, Gaithersburg, MD	Two different types of facilities are available at the NCNR to provide thermal neutrons, the thermal column and a cold neutron facility. The thermal column provides a collimated beam of thermal neutrons with a diameter of 1" to 2" (2,54 cm to 5,1 cm), and a flux of 1×10^8 n/cm^2·s. Epithermal neutrons and gamma rays are also in the beam at much lower levels, but they do not cause any SEUs. Occasionally another facility, the neutron beam imaging area, having a much larger thermal neutron beam spot, may be available. The second type of source is that of cold neutrons, having energies well below 0,025 eV. At present the cold neutron facility that had been used for electronics testing is about to be retired. A new cold neutron beam area, the "bench top facility" should be available in late 2005 for electronics testing. The cold neutron beams are pure, having no other particles, and have a higher effective thermal flux since the B-10 neutron cross-section increases with decreasing energy.	The thermal column is currently (2010) out of service, with a return to service of, at the earliest, sometime during 2012. The neutron imaging facility is available, though the price has increased to approximately $ 4 500/day (FY2009)
Nuclear Science Center, Texas Engineering Experiment Station, Texas A&M University, College Station, TX	The TRIGA research reactor operates at 1 $MW_{thermal}$ and has beam ports available that can be used for exposing electronics to thermal neutrons. One beam port can provide a neutron beam of thermal neutrons (0,025 eV) with an average flux of 1×10^6 n/cm^{2}s. The reactor has a dry irradiation cell that can be used for irradiating electronics and the average thermal flux can be close to 1×10^{10} n /cm^2 s. The reactor also supports isotope production and there are irradiation locations in the core where the neutron flux on the order of 10^{13} n/cm^{2}s can be expected.	The cost of usage of beam port, the dry cell as well as core irradiation locations vary with time and usage. Unknown at this point. http://nuclear.tamu.edu/facilities/lab08/

C.1.2 Proton facilities

Facility	Description	Availability/Cost
Los Alamos Neutron Science Center –LANSCE (alt. WNR (Weapons Neutron Research) facility or Target-2 or Blue Room) Located in Los Alamos, NM	Facility with 800 MeV proton beam with 10^8 protons/ pulse. Beam spot size typically 1 cm diameter with other options possible. Proton currents up to approximately 80 nA or 5×10^{11} protons/ sec.	For cost and availability contact Leo Bitteker (lbj@lanl.gov 505-667-0333)
Indiana University Cyclotron Facility (IUCF), Indiana University, Bloomington, IN	Within the RERP (Radiation Effects Research Program) of the IUCF, two separate beam lines, radiation effects research stations, are available to provide protons, RERS-1 and RERS-2. At RERS-1, which has been operational for about 10 years, protons are available with energies in the range of 30 MeV to 200 MeV. The lower energies are achieved by the use of Cu degraders. The diameter of the beam spot can be 2 to 20 cm, but the usual diameter is 7 cm, with a uniformity of >70 %. During normal operation the maximum beam flux is ~1×10^9 p/cm^2 s, but at night and on weekends it can be higher. Typical particle fluences of 1×10^{10} to 1×10^{11} p/cm^2 are usually obtained in a few minutes. Dosimetry is by means of secondary electron monitor. Although the RERS-2 beam line (operational Dec. 2003) is similar to RESR-1, exposures with proton energies <200 MeV will be mainly performed at this station using Be degraders. Devices to be tested are mounted on an adjustable x,y,z table which can be moved remotely, and alignment with the beam is assured by means of a laser.	Cost ~ $627/h with a 12-hour daily minimum. The facility is open most of the time but beam time has to be scheduled. Fluxes >1×10^9 p/cm^{2}s can be obtained only at night and on weekends. See "Opportunities for Single Event and Other Radiation Effects Testing and Research at the IUCF," C. C. Foster *et al.*, Workshop Record, 1996 IEEE Radiation Effects Data Workshop, p. 84 and http://www.iucf.indiana.edu/

Facility	Description	Availability/Cost
Francis H. Burr Proton Therapy Center (formerly Northeast Proton Therapy Center) (FHBPTC), Massachusetts General Hospital, Boston, MA	As of 2002, the FHBPTC has replaced the Harvard Cyclotron Laboratory as the facility used for exposing both patients and electronics to proton beams. The FHBPTC beam can provide energies in the range of 90 MeV to 230 MeV via a magnetic energy selection system, and beams down to 20 MeV using degraders. The diameter of the beam spot can be <1 cm and up to 30 cm, but the usual diameter is 5 cm to 10 cm, with uniformity variation of <10 %. Beam flux is available from 10^2 p/cm^2·s to ~2 ×10^{11} p/cm^2·s. Dosimetry to a device under test (DUT) is by means of a thin foil transmission ion chamber calibrated to the Faraday cup or thimble chamber. A scintillator/phototube system is available for low flux runs. A laser alignment system is used to centre the DUT in the beam.	Cost is $ 650/h (experimenter present). Because main customers are cancer patients, the beam is available for radiation effects testing only on weekends. See "The Proton Irradiation Program at the Northeast Proton Therapy Center," E. Cascio *et al.*," Workshop Record, 2003 IEEE Radiation Effects Data Workshop, p. 141
Tri-University Meson Facility, (TRIUMF) located on University of British Columbia (Vancouver, Canada) campus	Since 1995 the Proton Irradiation Facility (PIF) has been providing two separate beams of monoenergetic protons, covering the range of 65 to 500 MeV. Beam line BL2C provides protons with energies up to 120 MeV, and beam line BL1B provides protons with energies in the range of 180 MeV to 500 MeV. The facility has been optimized to provide fluxes of ~1 × 10^8 p/cm^2 s, with uniform beam diameters of up to 7,5 cm. However, by reducing the beam spot, fluxes of 1 × 10^{10} p/cm^2 s can be achieved. Beam dosimetry is achieved using a miniature ion chamber and also a Faraday cup for high flux beams. Absorbers are used in conjunction with collimators to lower the beam energy, and scattering foils to broaden the beam. A beam profile monitor is employed upstream and lasers are used to align positioning of the DUT within the beam.	Cost is approximately $ 450/h. The facility is available about 8 to 10 months per year during which time BL2C is available for week-long periods approximately once per month, but 8 to 16 h test periods can be scheduled at other times on BL2C with several week's advance notice. BL1B is available during one or two 3-week periods per year, see "Improved Capabilities for Proton and Neutron Irradiations at TRIUMF," E. Blackmore *et al.*, Workshop Record, 2003 IEEE Radiation Effects Data Workshop, p. 149 and Workshop Record, 2000 p.1 http://www.triumf.ca .
University of California at Davis, Crocker Nuclear Laboratory (CNL), Davis, CA	Since 1970s CNL has been providing industry and government agencies access to the variable energy 76" isochronous cyclotron. The cyclotron can accelerate protons from 1 MeV to 68 MeV. In the Radiation Effects Facility (REF) the maximum proton energy to the DUT is 66 MeV. The spatial spreading of the beam is accomplished by passing the beam through a Ta diffuser foil. Lower energies can also be obtained by choosing a cyclotron proton energy combined with a proper diffuser foil to give an acceptable beam energy spread. Typical the beam energy spread is kept below 600 KeV. In the REF the flux can be in the range of 1 to 1 × 10^{10} p/cm^2 s, although typical beam fluxes for exposing electronics are 1 × 10^4 to 1 × 10^9 p/cm^2 s. For this beam line the diameter of the beam spot can be up to 6 cm, with a uniformity of 92 %. A second beam line, 1C, has recently become available for higher flux beams, up to 1 × 10^{12} p/cm^2·s, but with a beam spot of 2 cm in diameter. A compound x-y table is provided for locating the DUT, the range on translation is 7,37" and 19,59" in the X and Y direction respectively (this table can also be remotely controlled); two laser beams are used to align positioning of the DUT within the beam. A vacuum box 16,5" × 16,5" and 25" tall can be attached at the end of the REF beam line to use cyclotron proton beams lower than 7MeV without subjecting them to the energy spreading due to the exit foil or the air path. Beam dosimetry is accomplished by means of a secondary electron emission monitor (SEEM) combined with a removable Faraday Cup. Beam uniformity is monitored with a segmented secondary electron emission monitor (SSEEM).	Cost is approximately $ 746/h. The facility is available ~10 months/year, but needs an agreement w/U of Cal. Contact: Carlos Castaneda (530) 752-4228, see "Crocker Nuclear Laboratory (CNL) Radiation Effects Measurement and Test Facility," C. Castaneda et at, Workshop Record, 2001 IEEE Radiation Effects Data Workshop, p. 77; http://media.cnl.ucdavis.edu/ Crocker/Website/b_Information/ index.php.

C.1.3 Laser facilities

Facility	Description	Availability/Cost
Pulsed Laser Test Facility at the Naval Research Laboratory, Washington DC.	The NRL test facility contains two separate pulsed laser systems, one for doing single-photon absorption (SPA) experiments at a wavelength of typically 590 nm and tunable from 570 nm to 620 nm and the other for doing two-photon absorption (TPS) experiments at a nominal wavelength of 1260 nm that allows through-wafer testing. The device under test is mounted on an XYZ stage that is computer controlled for doing three-dimensional scanning to determine sensitive volumes. In both cases, the light is focused onto the device using long-working distance microscope objective lens that produces a focused beam with a spot size of just over 1 μm in diameter. Pulse rate is adjustable from single shot to 40 MHz for the SPA laser, and from single shot to 1 KHz for the TPA laser. Both setups contain illumination optics for viewing the DUT as well as the focused laser spot. Maximum laser pulse energies are equivalent to LETs >>100 MeV.cm^2/mg.	Rate is $ 5K per day including staff support. Contact Dale McMorrow for scheduling at mcmorrow@ccs.nrl.navy.mil Tel: (202) 767-5469

C.2 Facilities in Europe

C.2.1 Neutron facilities

Facility	Description	Availability/Cost
The Svedberg Laboratory (TSL) at Uppsala University, Uppsala, Sweden	Two neutron beam facilities are available at TSL: (1) Atmospheric-like Neutrons from thIck TArget (ANITA), (2) Quasi-Monoenergetic Neutrons (QMN). (1) The ANITA facility, built in 2007, provides neutrons with atmospheric-like spectrum up to the highest energy of ~180 MeV. The neutron flux above 10 MeV is ~10^6 times the atmospheric one at 39 000 feet. Any beam size between 1 and 120 cm can be selected by the user and variated during the campaign. The flux is promptly variable within a factor of at least 150. (Variation within a factor up to 5 000 may require re-trimming that takes up to 1 h). The thermal neutron flux is ~1 % of the flux above 10 MeV. (2) The QMN facility, upgraded in 2003, provides neutrons with energy controllable in the range 20 MeV to180 MeV, with roughly half the neutrons in the high-energy peak and the rest in the low-energy tail. The peak neutron flux is 3×10^4 – $1{,}5\times 10^5$ cm^{-2} $s^{-1,}$ dependent on energy. Any beam size between 1 cm and 80 cm can be selected by the user and variated during the campaign. The ANITA and QMN facilities share the same area with ~30 m^2 floor space available for users. At both the facilities, the neutron flux is continuously recorded by calibrated monitors based on neutron fission (FIC, TFBC) and on integration of the primary proton beam current.	Cost (2010): ANITA: EUR 460/h, QMN: EUR 460-500/h dep. on energy. See pricing policy: http://www.tsl.uu.se/documents/Pricing_policy.pdf The facilities are available ~9 months/year. Lead time at ANITA 2-8 weeks. Beam time request: http://www.tsl.uu.se/documents/Beam-time-request-form.txt Facility descriptions: A.V. Prokofiev et al., "Characterization of the ANITA Neutron Source for Accelerated SEE Testing at TSL", 2009 IEEE REDW, pp. 166-173, http://ieeexplore.ieee.org/stamp/stamp.jsp?arnumber=05336295, doi:10.1109/REDW.2009.5336295.; "The TSL Neutron Beam Facility", Rad. Prot. Dosim. v. 126, pp. 18-22 (2007); doi: 10.1093/rpd/ncm006. Contact: aprokofiev@tsl.uu.se , beams@tsl.uu.se , or http://www.tsl.uu.se/radiation_testing .
ISIS Pulsed Neutron and Muon Source, Rutherford Appleton Laboratory, Harwell Science and Innovation Campus, Didcot, OX11 0QX, UK	ISIS is a facility that is primarily used for condensed matter physics, operating two separate target stations that can provide neutrons with an energy spectrum up to 800 MeV and which contain epithermal, thermal and cold neutrons. The VESUVIO beamline on Target Station One is immediately available for SEE testing having been characterised through Monte Carlo (MCNPX) simulation and activation foil analysis. The fast neutron content of the beam is $5{,}8\times10^4$ n/cm^2/s (> 10 MeV) with a strong well characterised cold/thermal and epithermal component. This beam is highly collimated with a diameter of 2 cm to 5 cm and has dosimetry based on fission counters, scintillation counters and the proton current. A new development on Target Station Two is in the design and construction phase and should provide both a collimated (~10 cm ×16 cm) and flood area (~100 cm diameter) beam matching atmospheric spectrum up to 800 MeV both with variable collimation. Design fluxes are 1×10^6-1×10^7 n/cm^2/s (>10MeV) for the collimated beam and 1×10^4-1×10^5 n/cm^2/s for the flood beam. A highly flexible large experimental area is envisaged with remote sample positioning and the ability for in-situ dosimetry being developed.	Academic (and therefore published) access is via peer review. Currently non-academic access and proprietary research is negotiated. Contact: Christopher Frost christopher.frost@stfc.ac.uk
CYClotron of LOuvain-la-NEuve, Cyclotron Research Centre (CRC) at Catholic University of Louvain-La-Neuve (UCL), Belgium	CYCLONE has a monoenergetic neutron beam line that provides quasi-monoenergetic neutrons at energies in the range of 25 MeV to 70 MeV. The neutrons are generated by accelerating a monoenergetic proton beam into a lithium target, with roughly half the resulting neutrons having a pseudo peak within 1 MeV to 2 MeV of the proton energy, and the remaining neutrons approximately evenly distributed over energy down to a few MeV (the low energy "tail"). The peak neutron flux is 1 × 10^6 n/ cm^2s (3 mm thick target) over a beam spot of 4 cm in diameter.	Cost is unknown. Beam time has to be scheduled. See "CYCLONE – A Multipurpose Heavy Ion, Proton and Neutron SEE Test Site," Workshop Record, 1997 RADECS Conference Data Workshop, p. 51, 4th European Conference, Palm Beach, Cannes, France; see http://www.cyc.ucl.ac.be

Facility	Description	Availability/Cost
National Physical Laboratory, Teddington, UK	Can provide well-characterized mono-energetic neutron fields covering the energy range 70 keV to 5 MeV and at 17 MeV via a variety of nuclear reactions using beams of protons or deuterons from a 3,5 MV Van de Graaff accelerator. A thermal neutron irradiation facility is also available with a beam fluence of up to 10^4 cm^{-2} s^{-1} over an area of 30 cm diameter or an isotropic field with fluences up to 10^7 cm^{-2} s^{-1} in an access hole of diameter 12 cm.	There are no fixed costs. Prices are estimated primarily in terms of staff time to perform the irradiations. http://www.npl.co.uk/commercial-services/measurement-services/neutron-measurements/
Atomic Weapons Establishment (AWE) Aldermaston, Berkshire, UK	The ASP Accelerator produces 14 MeV neutrons via the d+t reaction. The maximum14 MeV neutron flux is 2×10^{10} $n/cm^2 \cdot s$ at 1 cm from the target. In addition, deuterium loaded targets can be used to produce 3 MeV neutrons using the d+d reaction, giving a maximum flux of 2×10^8. The Accelerator has the capability of being operated in either continuous or pulsed mode. The minimum pulse width is 5 μs.	Cost is ~ £ 2 000 per day. Beam time must be scheduled in advance. For further information contact Shaun Hughes on 01189 824122 or email aspaccelerator@awe.co.uk

C.2.2 Proton facilities

Facility	Description	Availability/Cost
Proton Irradiation Facility (PIF) at the Paul Scherrer Institute (PSI) Villigen, PSI, Switzerland	Within PSI there are now two proton irradiation facilities, the high energy (HE) PIF and the low energy (LE) PIF. The design of the two PIF areas is very similar with regard to set-up and operation (beam dosimetry, flux calibration, energy degrader and data acquisition). At the high energy PIF (also called the NA3 PIF) the initial proton beam has an energy of 590 MeV, but at the irradiation area the energy is reduced to 254 MeV (range of 30 MeV to 254 MeV). At 254 MeV, the maximum flux is 2,5 × 10^8 p/ cm^2s and the maximum diameter of the beam spot is 9 cm. Degraders are used to achieve lower energies, but the uniformity of the beam is reduced, which varies with the distance from the degrader. Because part of the beam line is used for biomedical therapy, electronics are exposed only during weekends. The LE PIF (also called NEB PIF) is located near another biomedical beam line called OPTIS, however the operation of the two beams is more directly coordinated. The energy range for the LE PIF is 6 MeV to 71 MeV), the maximum proton flux is 5 × 10^8 p/ cm^2s, the largest beam spot is 5 cm diameter, and the beam uniformity is >90 %. Electronic components are exposed at the LE PIF mainly at night and during weekends. These exposures are performed during OPTIS treatment weeks (once/month) beginning at 17:00 after patient therapy has ended, and also on "free weekends".	Cost is unknown. Beam time has to be scheduled in order to coordinate with the biomedical treatment operation. See "Radiation Effects Testing Facilities in PSI during Implementation of the Proscan Project," W. Hajdas *et al.*, Workshop Record, 2002 IEEE Radiation Effects Data Workshop, p. 160 and "Radiation Effects Testing Facility in PSI Low Energy OPTIS Area," W. Hajdas *et al.*, Workshop Record, 1998 IEEE Radiation Effects Data Workshop, p. 152.
The Svedberg Laboratory (TSL) at Uppsala University, Uppsala, Sweden	The TSL proton irradiation facility, upgraded in 2003, provides monoenergetic protons with energy controllable in the range 20 MeV to 180 MeV. Two modes of operation are available: (1) Scattered beams have the spot diameter between 0,5 cm and 20 cm, selectable by the user. The highest flux amounts to 7×10^8 – 5×10^9 cm^{-2} s^{-1}, for the highest and the lowest energy, respectively. The lowest achievable flux is ~10^2 cm^{-2} s^{-1}. The flux within the beam spot is uniform to ±10 %. The flux is monitored by TFBCs and by scintillator telescopes. (2) Unscattered beams have the highest intensity of 3×10^{11} – 2×10^{12} s^{-1} for the highest and the lowest energy, respectively. The lowest achievable intensity is ~10^2 s^{-1}. The typical beam spot shape is a circle with the diameter of 0,7 cm to 2 cm. The beam profile shape is approximately Gaussian. The intensity is measured with a Faraday cup and monitored by scintillator telescopes.	Cost (2010): EUR 460-500/h dep. on energy. See pricing policy: http://www.tsl.uu.se/documents/Pricing_policy.pdf The facility is available ~9 months/year. Beam time request: http://www.tsl.uu.se/documents/Beam-time-request-form.txt Facility description: http://www.tsl.uu.se/radiation_testing Contact: aprokofiev@tsl.uu.se , beams@tsl.uu.se , or http://www.tsl.uu.se/radiation_testing .
CYClotron of LOuvain-la-NEuve, Cyclotron Research Centre (CRC) at Catholic University of Louvain-La-Neuve (UCL), Belgium	One of the CYCLONE proton beam lines called the Light Ion irradiation Facility (LIF) has been modified for testing electronics. The proton energy can be varied between 10 MeV to 70 MeV, by adjusting the cyclotron or using plastic degraders. The beam spot is 10 cm in diameter. Beam flux can be modified between a few p/s cm^2 and 5 × 10^8 p/s cm^2.	Cost is unknown. Beam time has to be scheduled. See "CYCLONE – A Multipurpose Heavy Ion, Proton and Neutron SEE Test Site," Workshop Record, 1997 RADECS Conference Data Workshop, p. 51, 4th European Conference, Palm Beach, Cannes, France; see http://www.cyc.ucl.ac.be

C.2.3 Laser facilities

Facility	Description	Availability/Cost
Single Event Radiation Effects in Electronics Laser (SEREEL2) at MBDA in Bristol, UK	SEREEL incorporates a 1 picosecond pulsed laser with a computer controlled parametric amplifier system for generating wavelengths in the range 450 nm to 2 600 nm (covering the entire laser SEE range including both Single Photon Absorption and Two Photon Absorption). Pulse energies up to 1,5 mJ (dependent upon wavelength). Standard magnification of the focussing objective is ×100 with a 10 mm working distance relative to the microchip under test. Features: InGaAs camera technology for viewing chips through their polished backsides; piezo-electric scanning and positioning technology for fast delivery of large arrays of laser pulses (e.g. 3D SEE sensitivity mapping); selectable laser pulse repetition rate from single shot to 1 kHz. Standard types of memories can be interrogated during testing using MBDA's FPGA-based STREAM system (pin assignment in software for rapid adaptation to many pinout configurations).	Standard rates are ~£ 800 per day including staff support (normally contracts need to be for >£ 2k)
Radiation Analysis Laser Facility at EADS IW, Suresnes, France	EADS IW Radiation Analysis Laser Facility is designed for industrial purpose. It is based on a pulsed (600 ps) laser source operating at a wavelength of 1 064 nm, optimized to perform tests from the device backside with no need for substrate thinning. The laser source is highly stable and the energy can be varied over a wide range. Working distance between the focusing objective and the device under test is 1 cm. The whole laser facility is fully automated thanks to motorized actuators on X Y and Z directions (50 nm minimum step resolution), an automated system for the laser energy adjustment and a camera allowing to view the front side of the chip through the device substrate. Power supply and various acquisition systems may be connected and synchronized to the system as well, which makes parameterized tests easier.	2010 standard rate are around 1k€ per/day including calibration and mandatory staff support
ATLAS (Analysis and Test with Lasers) platform at IMS Laboratory, University of Bordeaux, in Talence, France	ATLAS is an academic laser facility offering SEE test services using three pulsed laser sources, giving access to pulse durations of 150 fs, 1 ps or 30 ps with wavelength tunable from 400 nm to 2 500 nm, pulse repetition rate from single-shot to 10 MHz, and pulse energies higher than 1 μJ on the full range of wavelengths (up to 1 mJ at 800 nm). Standard wavelengths for Single-Photon Absorption SEE testing include 800 nm, 980 nm and 1064 nm. Two-Photon Absorption at 1 300 nm is used for 3D SEE mapping. Laser focusing and real-time imaging of the laser impact location is achieved by 100X front-side or backside infrared microscopes. Other features: standard scanning resolution of 100 nm, down to 10 nm using piezo-electric stages; sample preparation (package opening and substrate thinning) available on-site; flexible mechanical fixture compatible with most PCB geometries; wafer probing station with inverted microscope compatible with naked dies or wafer-level laser testing; software controlled scanning, triggering, data acquisition and analysis; customizable IC tester/software interface; digital tester with customizable daughter-board; standard electronic instruments (oscilloscopes, precision power supplies, delay and pattern generators, spectrum analyzer, lock-in amplifier); remote (internet based) testing capability.	Rates start at ~1 500€ per day (dependent on test details and laser parameters) including the support of an ATLAS engineer. Availability: 4 weeks minimum notice. Contact: atlas@ims-bordeaux.fr

Annex D
(informative)

Tabular description of variation of atmospheric neutron flux with altitude and latitude

Source is the Simplified Boeing Model in [9], Normand and Baker in which the 1 MeV to 10 MeV neutron flux is normalized to a value of 0,85 n/cm^{2}s at 39 000 feet (11 860 m) altitude and 45° latitude. Even though the fluxes in Tables D.1 and D.2 are for neutrons with energies between 1-10 MeV, [9] has shown that the same altitude and latitude variation applies to neutrons for all E > 1 MeV.

Table D.1 – Variation of 1 MeV to 10 MeV neutron flux in the atmosphere with altitude

Altitude feet (m)	1 MeV to 10 MeV neutron flux, n/cm^{2}s
5 000 (1 520)	0,01
10 000 (3 050)	0,04
15 000 (4 570)	0,08
20 000 (6 100)	0,13
25 000 (7 620)	0,24
30 000 (9 140)	0,38
35 000 (10 670)	0,60
40 000 (12 190)	0,88
45 000 (13 720)	1,02
50 000 (15 240)	1,16
55 000 (16 760)	1,24
60 000 (18 290)	1,25
65 000 (19 810)	1,24
70 000 (21 340)	1,22
75 000 (22 860)	1,20
80 000 (24 380)	1,18

Table D.2 – Variation of 1 MeV to 10 MeV neutron flux in the atmosphere with latitude

Latitude °	1 MeV to 10 MeV neutron flux, n/cm^2 s
90	1,26
76	1,25
69	1,23
62,5	1,21
55	1,13
49	0,99
45	0,85
42	0,74
39	0,63
33	0,46
27	0,35
21	0,29
12	0,23
0	0,23

Annex E
(informative)

Consideration of effects at higher altitudes

As altitude increases both protons and heavy ions provide increasingly important contributions to SEE rates and these must certainly be included for applications above about 60 000 feet. For protons the main interaction is non-elastic nuclear interactions and these are similar to neutron interactions at high energies (> 20 MeV). However small feature size components (65 nm and below) are becoming susceptible to direct ionization effects from protons as they reach maximum linear energy transfer (LET) towards the end of their track (the Bragg peak effect). General techniques for dealing with stopping protons have yet to be developed and proper Monte Carlo simulations will be required. However, SEU from direct proton ionization has only been seen in laboratory experiments with collimated beams. For electronic devices used in large fielded systems such as aircraft, the greater the mass surrounding the electronics, the less likely it is that the electronics within will be susceptible to SEU from direct ionization. This is because the "end of track" distance within which the highest proton LET is achieved in silicon (required to produce a SEU) is 1 μm to 2 μm (~4-8 $\times 10^{-5}$ inches), compared to the inches of material that surround the IC devices, making energy deposition from the protons within the 1 μm to 2 μm very unlikely.

Significant heavy ion fragments penetrate down to about 60 000 feet and their higher charge means that many devices are susceptible to SEE by direct ionization.

Direct ionization by energetic heavy ions, for which the range is much greater than device dimensions so that LET is constant across the device, can be dealt with using the integral linear energy transfer spectra as applied to space systems in Creme96 [36] and other codes. However it is necessary to generate such spectra as a function of depth within the atmosphere. This has been done for an updated version of the QARM model (QARM2) using the cosmic ray heavy ion spectra from the Badhwar-ONeill model [98] and the FLUKA radiation transport code [38, 99]. This model propagates all secondary ion fragments and updates the early methods of Tsao, Silberberg and Letaw [28], who employed semi-empirical spallation cross-sections and followed only the larger spalled nuclei and not the other secondary products. Example integral LET spectra in silicon are given in Figures E.1 to E.3 for solar maximum while Figures E.4 and E.5 show the influence of solar modulation.

Readers not involved in aerospace vehicles operating at greater than 60 000 feet (18,3 km) can skip to Figures E.6 and E.7 and can ignore Annex F. Figures E.6 and E.7 show the SEU contribution from three particles within the atmosphere, neutrons, secondary protons and the heavy ions within the primary cosmic rays, all as a function of altitude. These are for two different rigidity cut-offs (see Figure 3), R = 0 (in Polar Regions) and R = 8 (~20° to 40° N. latitude). Figures E.6 and E.7 show that at altitudes of up to 60 000 feet, the neutron contribution to the SEU rate dominates, at ~70 %, but at higher altitudes the neutron SEU rate diminishes and at 100 000 feet, it is less than 50 %. The SEU rates in Figures E.6 and E.7 are based on three separate sets of SEU cross-section data (neutrons, protons and heavy ions) on one specific SRAM, but very similar behaviour has also been seen for a second SRAM [100], thus the overall behaviour in these figures can be considered as typical of how other devices respond to SEU from these three particles as a function of altitude.

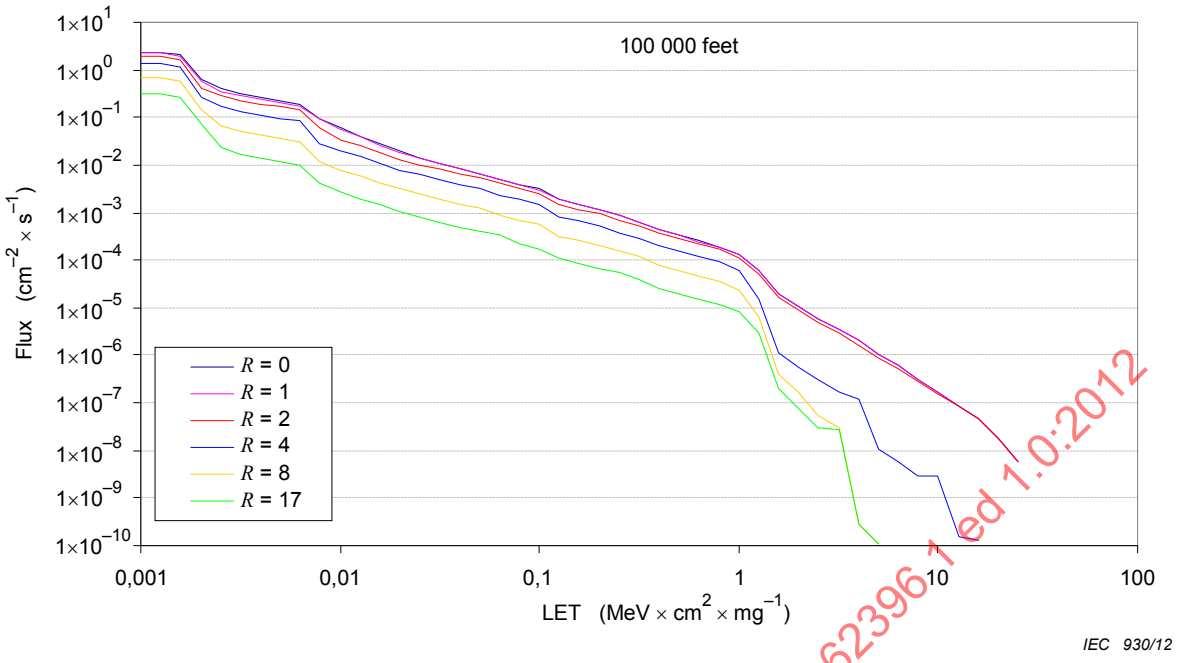

Figure E.1 – Integral linear energy transfer spectra in silicon at 100 000 feet (30 480 m) for cut-off rigidities (R) from 0 GV to 17 GV

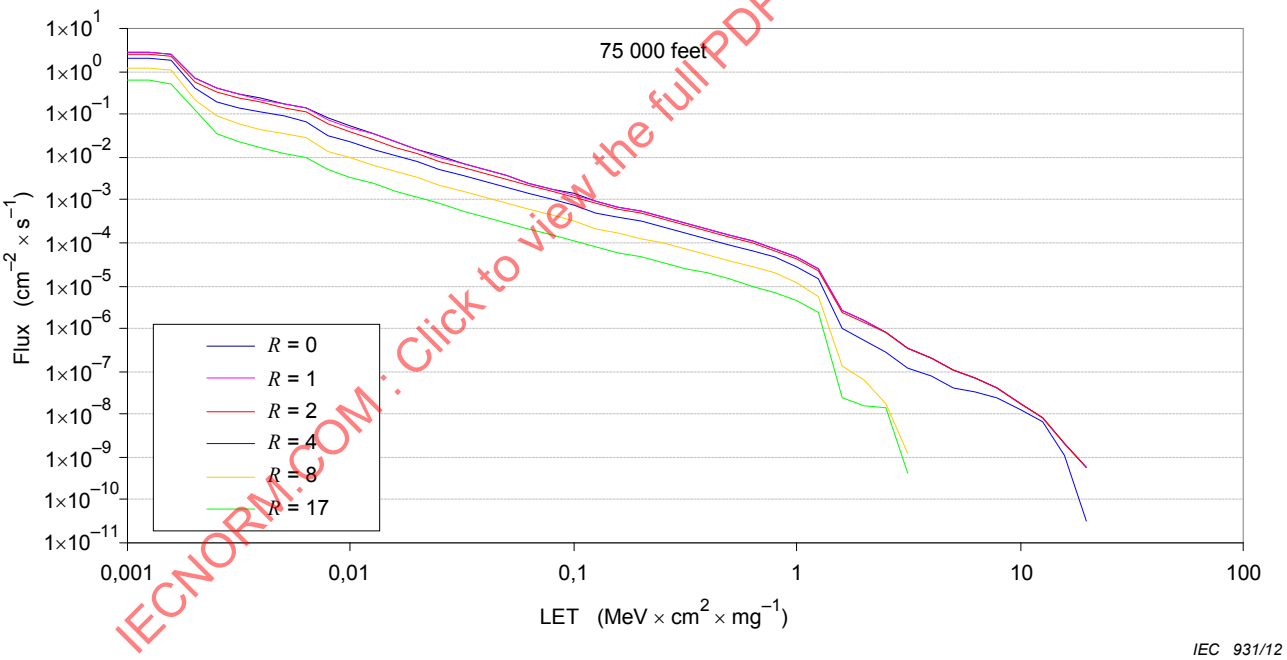

Figure E.2 – Integral linear energy transfer spectra in silicon at 75 000 feet (22 860 m) for cut-off rigidities (R) from 0 to 17 GV

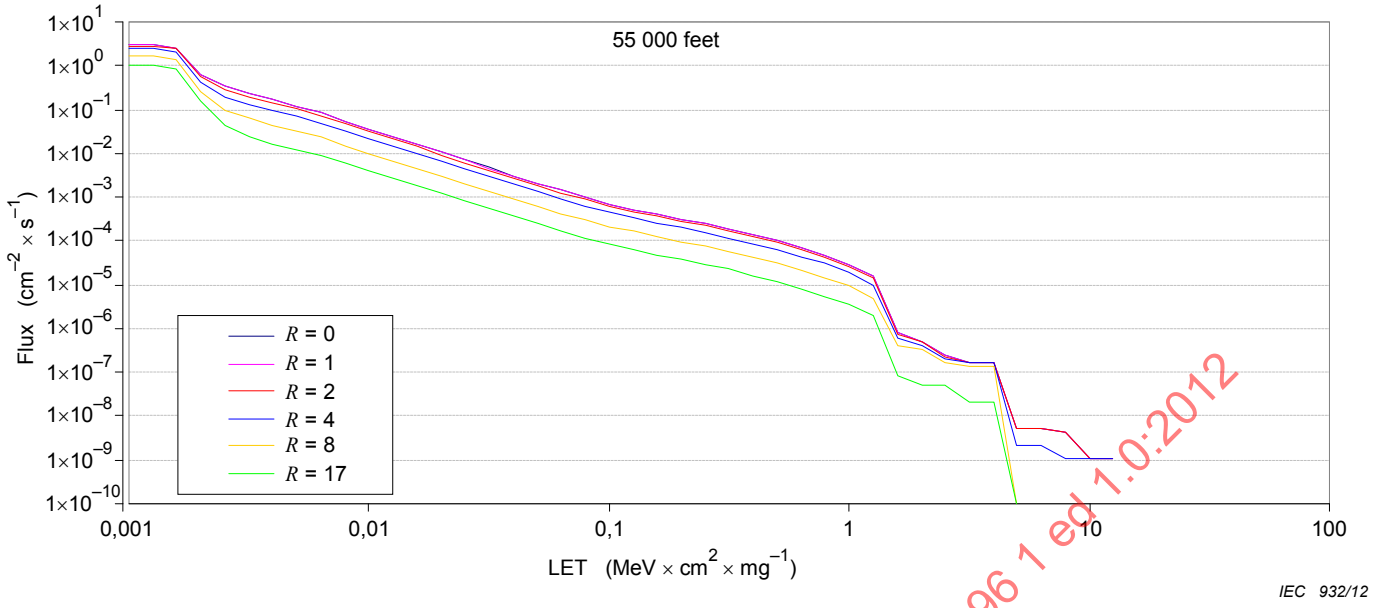

Figure E.3 – Integral linear energy transfer spectra in silicon at 55 000 feet (16 760 m) for cut-off rigidities (R) from 0 GV to 17 GV

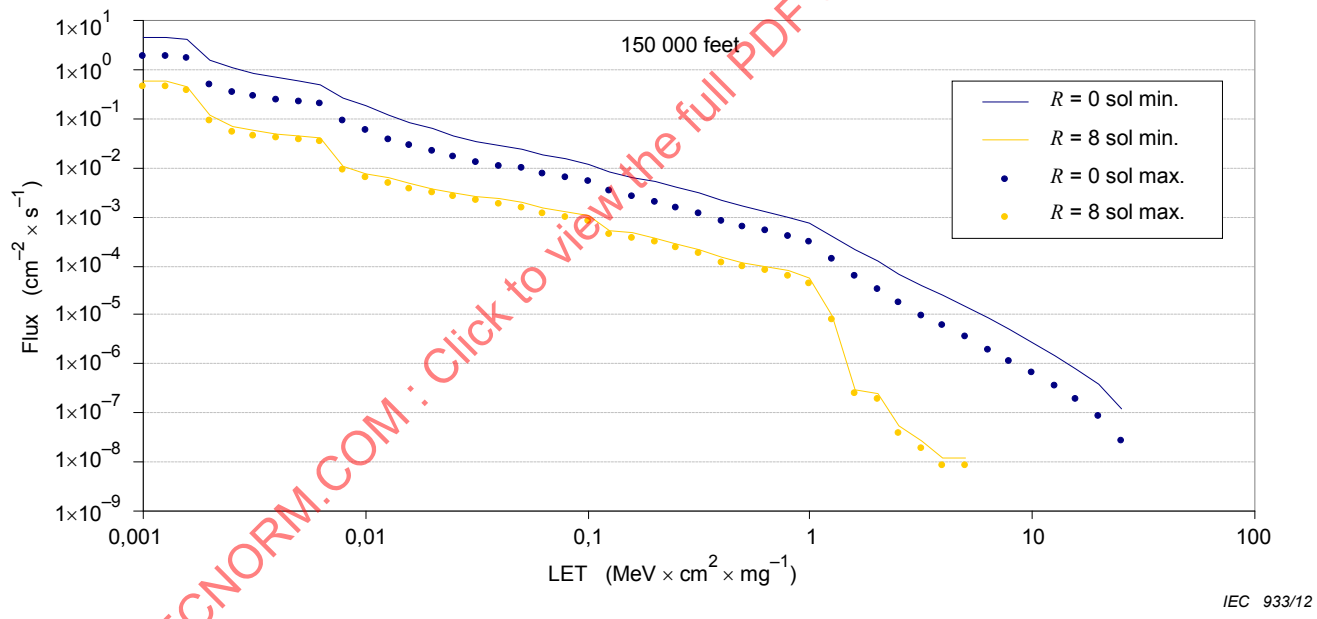

Figure E.4 – The influence of solar modulation on integral linear energy transfer spectra in silicon at 150 000 feet (45 720 m) for cut-off rigidities (R) of 0 GV and 8 GV

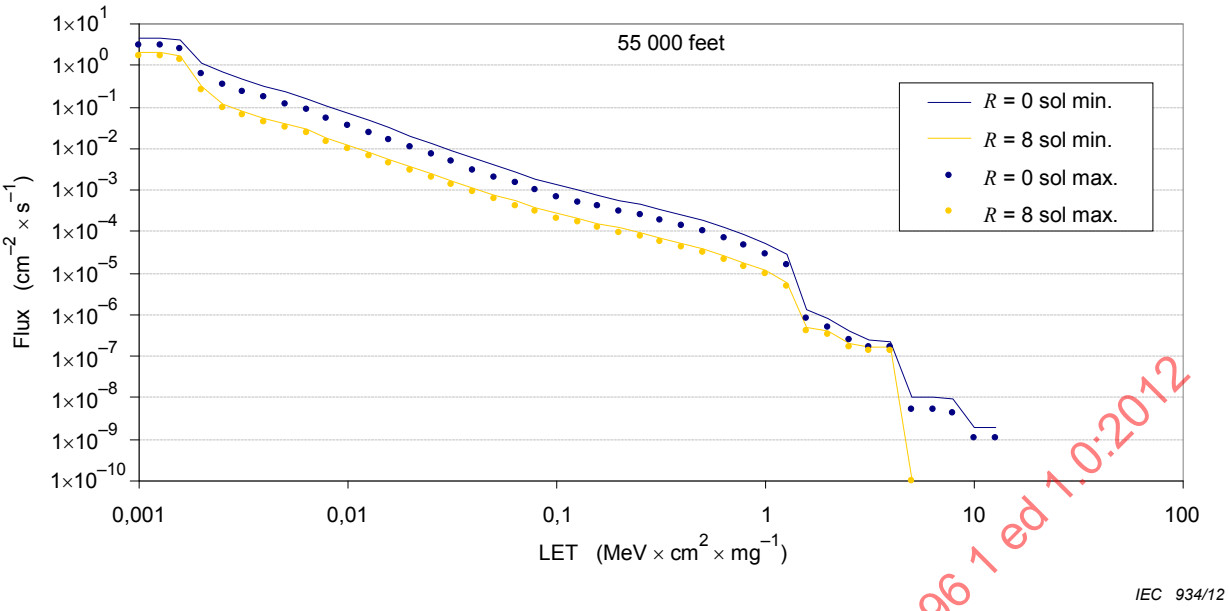

Figure E.5 – The influence of solar modulation on integral linear energy transfer spectra in silicon at 55 000 feet (16 760 m) for cut-off rigidities (R) of 0 GV and 8 GV

The integral LET spectra are combined with a path length distribution through a parallelepiped representation of a device sensitive volume to give SEE rates. A commonly used method is the Integral Rectangular Parallelepiped (IRPP) approach as discussed in Petersen et al. [101, 102]. The methods and equations used for the prediction of SEE rates for ions are fully discussed in the ECSS standard ECSS-E-10-12 [103] and the appropriate section is reproduced below. An essential input is the SEE cross-section as a function of LET measured at ion accelerators and this is often fitted using a Weibull function. Such data are required for space applications and are widely published; e.g. in the IEEE Radiation Effects Data Workshop.

Using this technique, example SEU rates as a function of altitude are given for the Hitachi-A 4-Mbit SRAM in Figures E.6 and E.7 for two different cut-off rigidities at solar maximum. This device has been fully characterised using heavy ion, proton and neutron beams [21, 47, 104]. SEU rates are normalised to 1 Gbit of memory. It can be seen that while the neutron contribution peaks at around 60 000 feet, the contributions of protons and ions both increase with altitude. For this particular device the SEU rates are enhanced by factors of about 1,4, 2,0 and 3,0 at 40 kft, 85 kft and 100 kft respectively when considering all radiation compared with considering neutrons alone. Investigations are being made into other components to ascertain how typical such factors are.

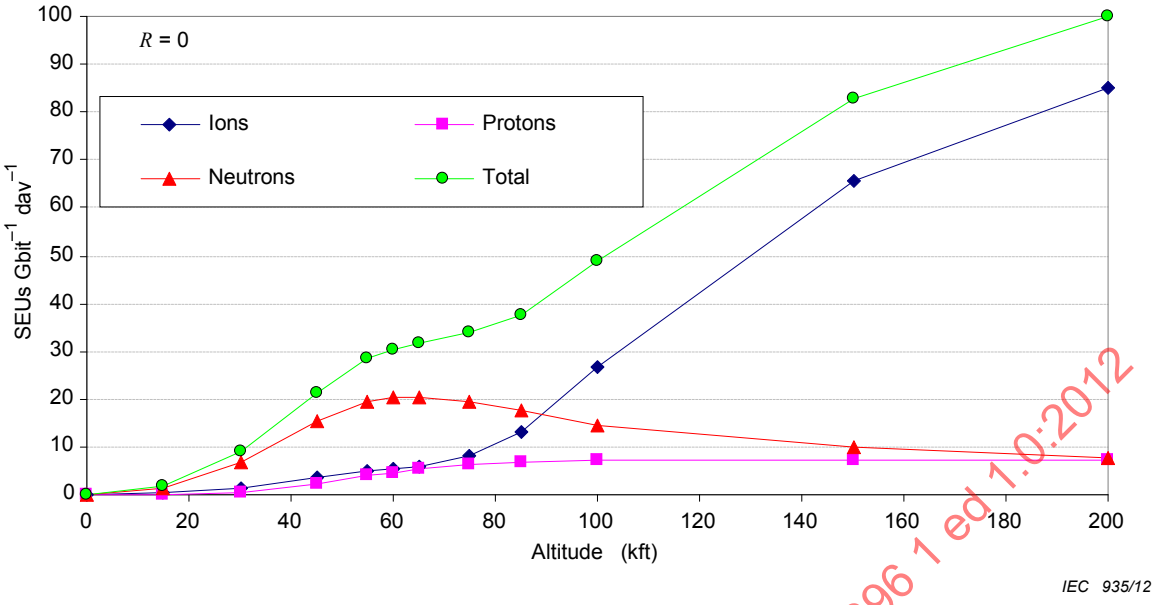

Figure E.6 – Calculated contributions from neutrons, protons and heavy ions to the SEU rates of the Hitachi-A 4 Mbit SRAM as a function of altitude at a cut-off –rigidity (R) of 0 GV

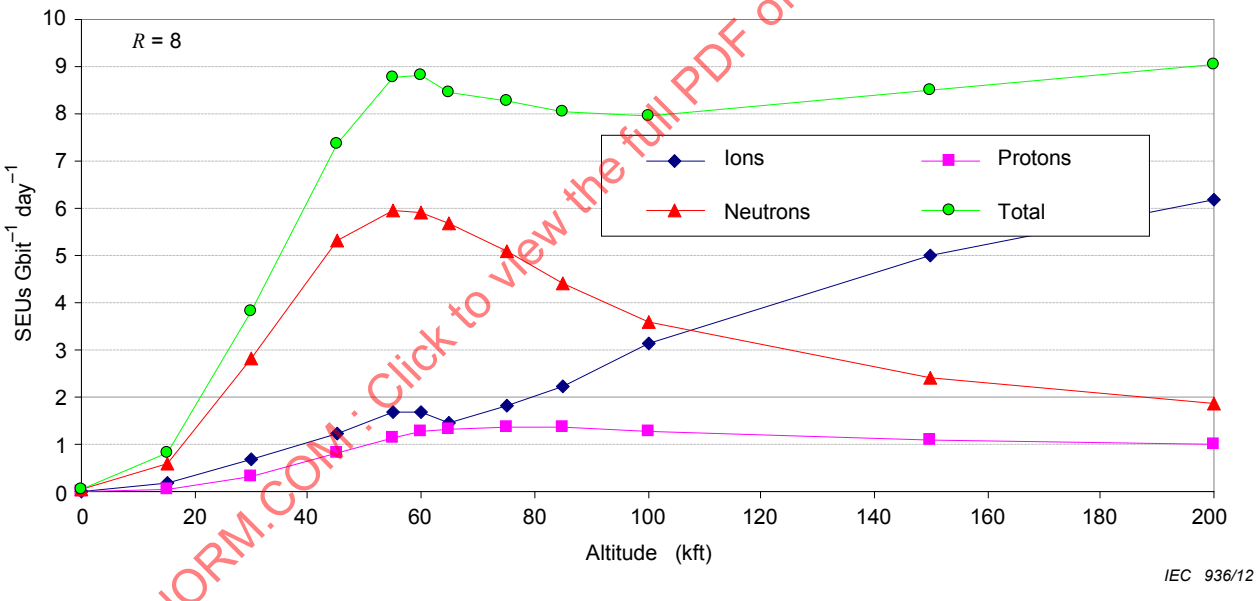

Figure E.7 – Calculated contributions from neutrons, protons and heavy ions to the SEU rates of the Hitachi-A 4 Mbit SRAM as a function of altitude at a cut-off rigidity (R) of 8 GV

Annex F
(informative)

Prediction of SEE rates for ions

Reproduced[2] with permission from ECSS-E-10-12.

When an ion crosses a device, it leaves a dense plasma of electron hole pairs along its path. When the charges are generated close to a sensitive node of a circuit, a p-n junction of a transistor for example, these charges are collected and, if of sufficient magnitude, are able to generate soft errors.

The upset rate calculation depends on the paths available in the charge collection region (the sensitive volume). Ordinarily, this region is assumed to be a rectangular parallelepiped (RPP). It leads to two different SEE rate calculations: the RPP model and IRPP model.

The principle for the RPP model is very simple: the energy deposited (E_{dep}) by an incident ion in the sensitive volume is estimated and if E_{dep} is greater than the threshold energy, the upset occurs. As incident ions are very energetic, they have very long ranges compared with typical device feature sizes and one can assume that their slowing down is continuous and linear. In that case, the deposited energy E_{dep}, can be expressed simply as:

$$E_{dep} = \rho \cdot LET \cdot d \tag{F.1}$$

The ion is characterised by its LET. An upset occurs when the incident ion has a LET greater than the threshold LET (LET_{th}). To calculate the upset rate, one needs to evaluate the LET spectrum of the incident particles. It leads to a very simple formula due to Bradford where the upset rate is expressed as a function of the incident LET spectrum and the path length distribution (such as the examples shown in Figures F.1 and F.2):

$$N = \frac{A}{4}\int_{LET_{Min}}^{LET_{Max}} \frac{d\Phi}{d(LET)}(LET) \cdot P_{CL}(> D(LET)) \cdot d(LET)$$

Bradford formula for RPP (F.2)

$$A = 2 \cdot (lw + lh + hw) \tag{F.3}$$

where

A is the total surface area of the SV;

l, w and h are the length, width and height of the SV;

$d\Phi/d(LET)$ is the differential ion flux spectrum expressed as a function of LET (shortened to “differential LET spectrum”);

$P_{CL}(>D(LET))$ is the integral chord length distribution, *i.e.* the probability of particles travelling through the sensitive region with a path length greater than D;

LET_{Min} is the minimum LET to upset the cell (also referred to as the LET threshold);

LET_{Max} is the maximum LET of the incident distribution (~10^5 MeV·cm^2/g).

2 This annex is taken from ECSS-E-HB-10-12A, 17 December 2010.

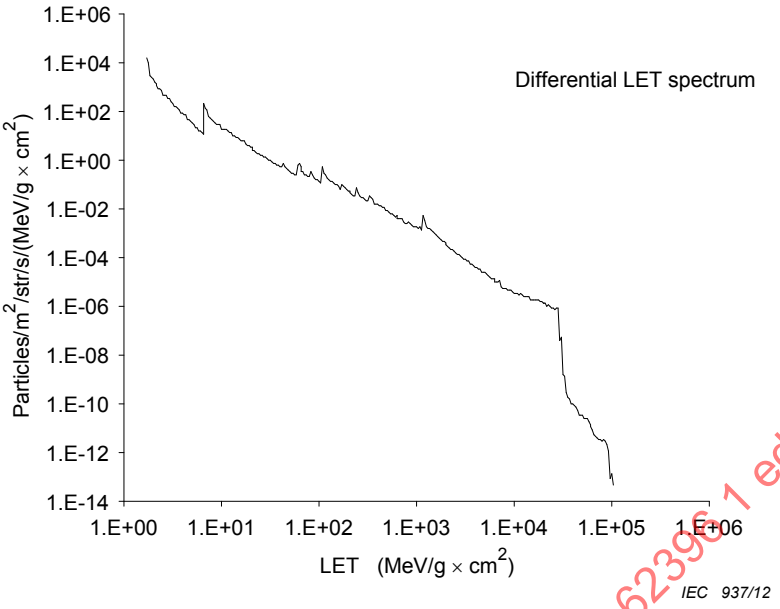

NOTE This graph is from the reference and uses the scientific notation for numbers e.g. 1.E+02 is 10^2.

Figure F.1 – Example differential LET spectrum

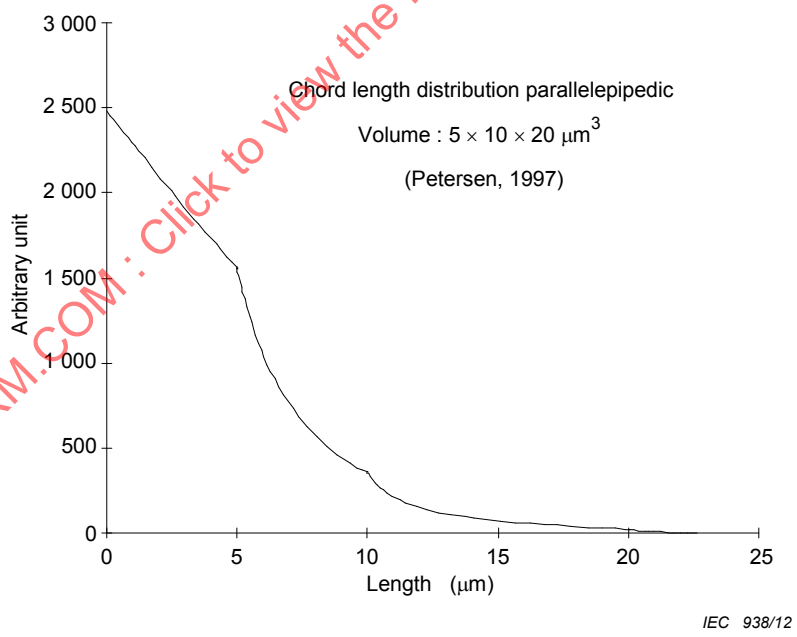

Figure F.2 – Example integral chord length distribution for isotropic particle environment

Equation (F.2) is the Bradford formula [105] used in the CREME model [36]. Some other similar expressions exist that use the differential chord length distribution and the integral LET spectrum as in Equation (F.4) and Equation (F.5) respectively due to Pickel and Blandford and Adams [106, 107].

$$N = \frac{A}{4}\int_{D_{\mathrm{Min}}}^{D_{\mathrm{Max}}} \Phi(> LET(D)) \cdot \frac{dP_{\mathrm{CL}}}{dD}(D) \cdot dD \tag{F.4}$$

$$N = \frac{A}{4}\frac{E_C}{\rho}\int_{LET_{\mathrm{Min}}}^{LET_{\mathrm{Max}}} \frac{1}{LET^2} \cdot \Phi(> LET) \cdot \frac{dP_{\mathrm{CL}}}{d(D(LET))} \cdot D(LET) \cdot d(LET) \tag{F.5}$$

But all these RPP model expressions make the same assumption. The LET threshold of each SV is considered equal to a unique value. Petersen pointed out that it is necessary to fold the LET spectrum with the experimental cross-section curves to properly account for sensitivity variations across the device [101].

In reality the critical LETs of the sensitive nodes are not the same but form a distribution that can be fitted by a Weibull function. To take into account the variation of sensitivity by integrating over a distribution of upset rates corresponding to the variation of cross-section versus LET, the Integral RPP approach (IRPP) is used.

$$N = \frac{A}{4S}\int_{LET_{i,\mathrm{Min}}}^{LET_{i,\mathrm{Max}}} \left\{ \frac{d\sigma_{ion}}{d(LET)}(LET_i) \int_{\frac{h}{D_{\mathrm{Max}}} LET_i}^{LET_{\mathrm{Max}}} \frac{d\Phi}{d(LET)}(LET) \cdot P_{\mathrm{CL}}(> D(LET)) d(LET) \right\} d(LET_i)$$

Integral Rectangular Parallelepiped (IRPP) equation (F.6)

$$S = l \cdot w \tag{F.7}$$

where

$d\Phi/d(LET)$ is the differential LET spectrum;

$P_{\mathrm{CL}}(>D(LET)$ is the integral chord length distribution;

$d\sigma_{\mathrm{ion}}/d(LET)$ is the differential upset cross-section;

A s the total surface area of the sensitive volume;

S is the surface area of the sensitive volume in the plane of the semiconductor die;

l, w and h are the length, width and height of the sensitive volume;

D_{Max} is the maximum length that can be encountered in the SV;

LET_{Max} is the maximum LET of the LET spectrum;

$LET_{\mathrm{i,Min}}$ is the lower bin limit in the differential upset cross-section $d\sigma_{\mathrm{ion}}/d(LET)$;

$LET_{\mathrm{i,Max}}$ is the upper bin limit in the differential upset cross-section $d\sigma_{\mathrm{ion}}/d(LET)$.